Separation Science and Technology
Publication details, including instructions for authors and subscription information:
http://www.informaworld.com/smpp/title~content=t713708471

CARBON ISOTOPE EFFECTS ($^{13}C/^{12}C$) IN BIOLOGICAL SYSTEMS

Alexander A. Ivlev[a]
[a] Department of Inorganic and Analytical Chemistry, Moscow Agricultural Academy, Moscow, Russia

Online publication date: 30 July 2001

To cite this Article Ivlev, Alexander A.(2001) 'CARBON ISOTOPE EFFECTS ($^{13}C/^{12}C$) IN BIOLOGICAL SYSTEMS', Separation Science and Technology, 36: 8, 1819 — 1914
To link to this Article: DOI: 10.1081/SS-100104762
URL: http://dx.doi.org/10.1081/SS-100104762

SEPARATION SCIENCE AND TECHNOLOGY, 36(8&9), 1819–1914 (2001)

CARBON ISOTOPE EFFECTS ($^{13}C/^{12}C$) IN BIOLOGICAL SYSTEMS

Alexander A. Ivlev

Department of Inorganic and Analytical Chemistry,
Moscow Agricultural Academy, Moscow, Russia

ABSTRACT

Carbon isotope ($^{13}C/^{12}C$) fractionation (CIF) occurring in cells of organisms of different types is considered. Three metabolic points are shown to have an exceptional significance for the observed carbon isotope distribution in a living matter: 1) ribulose bisphosphate carboxylation in CO_2 photoassimilation; 2) glycine decarboxylation in photorespiration; and 3) pyruvate decarboxylation in respiration metabolism. Carbon isotope effects (CIE) in ribulose bisphosphate (RuBP) carboxylation is characteristic of photosynthesizing organisms. It is responsible for the observed ^{12}C enrichment of photosynthesizing organism biomass relative to environmental CO_2. According to proposed mechanism of CIF, CO_2 assimilation is a discrete process, which can be described as a flow of CO_2 batches into a cell. Discreteness of the flow arises due to ability of Rubisco (the key enzyme of photosynthesis) periodically operate both as carboxylase and oxygenase depending on CO_2/O_2 ratio in a cell. It provides periodic filling/depletion of cytoplasmic pool of CO_2 in the cell and determines the appearance of isotope Releigh effect following the pool depletion. The degree of pool depletion determines the extent of ^{12}C enrichment of biomass. A full consumption of CO_2 batches entering the cell means the complete depletion of CO_2 cytoplasmic pool and is considered to be the main

reason for the observed ^{13}C enrichment of C_4 plants compared with C_3 and CAM plants. CIE in glycine decarboxylation is the key element of CIF in photorespiration. The effect of the reaction is also amplified by the Releigh effect of photorespiratory pool depletion. The removal of CO_2 enriched in ^{12}C results in ^{13}C enrichment of photorespiratory substrates and biomass itself. Thus the sign of CIE of photorespiration is opposite that of CO_2 photoassimilation. Some factors inducing intense photorespiration can even cause ^{13}C enrichment of biomass in respect to ambient CO_2 when CIE of photorespiration prevails that of CO_2 photoassimilation. Due to the coupling of photorespiration and CO_2 photoassimilation via double function of Rubisco both CIE are in reciprocal relations to each other and generate two isotopically different carbon flows in photosynthesizing cells. CIE effect in pyruvate decarboxylation is responsible for the appearance of carbon isotope heterogeneity in respiration metabolism (isotopic discrepancies of fractions, metabolites and uneven intramolecular ^{13}C distribution of biomolecules). The reaction is a crosspoint of the central metabolic pathways. It is typical of the overwhelming majority of the organisms regardless of their position on the evolutionary stairs. The mechanism of CIE is the combination of the effect in the enzymatic reaction with Releigh effect of pyruvate pool depletion. The reaction provides C_2 and C_3 structural units for biosyntheses of most of the cell components whose carbon isotope ratio changes in parallel with the pool depletion determining the differences in carbon isotope composition of metabolites. At a certain energy state of the organism and the corresponding energy states of the cells, the synthesis of each component in cell cycles occurs synphasically, i.e., within the same interval of pyruvate pool depletion. In such a way a certain isotopic pattern of metabolites and ^{13}C distribution in biomass are provided. Some applications of the technique to study plants, highly organized animals and humans are shown.

INTRODUCTION

Recent achievements in development of the isotope ratio mass-spectrometry and related techniques (1–6) have greatly stimulated the studies of biological isotope fractionation. This phenomenon occurs in metabolic reactions due to the differences in reaction rates of the isotopic species of biomolecules and determines heterogeneous isotope distribution in metabolites, isotopic discrepancies of cell components, of biomass and nutrients, isotopic variations of CO_2 evolved in

MARCEL DEKKER, INC.
270 Madison Avenue, New York, New York 10016

cell processes, and some other characteristics. Regarding these characteristics as manifestations of biological isotope fractionation, we define their shifts as metabolic isotope effects (MIE). During the past 10 years, new and interesting findings and applications of MIE have been made in genetics (7–12), in plant physiology (13–18), in ecology (19–23), in biological evolution (24–29), in paleoreconstruction of ancient atmosphere and climate (30–32), and in organic geochemistry (33–36). The considerable progress has been achieved in molecular biology and biophysics by using isotope effects to study mechanisms, regulation, and temporal organization of cell processes (14,37–39), in microbiology to investigate metabolism of microorganisms and natural gas formation (40–47). So wide application of MIE is explained by their tight link with the molecular mechanisms of the processes and may be used as a delicate tool for their investigation.

MIE of carbon have been predominantly studied because of their essential role in forming skeletons of biogenic molecules. But the role of MIE of other biogenic elements in the study of living matter is also great. They are commonly used separately or in combination to consider important natural processes such as denitrification and N_2 fixation ($^{15}N/^{14}N$) (48–50), microbial sulfate reduction and sulphur oxidation ($^{34}S/^{32}S$) (51–53), plant transpiration (D/H in combination with $^{18}O/^{16}O$) (54–56), plant, animal, and human respiration ($^{18}O/^{16}O$ in combination with $^{13}C/^{12}C$) (57–60), amino acids and carbohydrate formation in cell metabolism ($^{15}N/^{14}N$ in combination with $^{18}O/^{16}O$, D/H and $^{13}C/^{12}C$) (61–64), and many others.

Attempts to apply MIE in solution of agricultural and medical problems gave also very promising results. Heritability of MIE effects of photosynthesis and correlation of some carbon isotopic characteristics of plants with their productivity and water use efficiency made it possible to use them for plant breeding and selection of plants with high productivity and improved drought response (65–70). Oxygen MIE associated with respiration of humans seems to provide a useful way of monitoring certain types of respiratory and blood diseases (60). Metabolic carbon isotope effects (CIE) determined by measuring carbon isotope ratio of CO_2 in the expired air and urea of urine are found to reflect a functional state of human organism (71–73) and may be used to investigate biological rhythms, bioenergetics, and dysmetabolism of pathologic states.

The present work is devoted to biological fractionation of carbon isotopes. In spite of a certain progress in this field, we still do not have complete information about general principles that run carbon isotope distribution in a cell. It is still unknown how many points of carbon isotope fractionation (CIF) are in the cells of different organisms and how it is displayed in their carbon isotope characteristics. To answer these questions, a comprehensive analysis of biochemical and biophysical aspects of cell metabolism is required. To apply the results obtained by studying MIE in a cell to the examination of the whole organism, the physiological consideration of the problem is needed.

MARCEL DEKKER, INC.
270 Madison Avenue, New York, New York 10016

This work mainly treats the first part of the problem and considers some approaches to solve the second. It consists of three parts. The first one is devoted to CIEs in photosynthesis, comprising CIEs in CO_2 photoassimilation and in photorespiration of plants and photosynthesizing microorganisms in the light period. The second part describes CIF in secondary metabolism of photosynthesizing organisms in dark period as well as isotope fractionation in heterotrophic cells both associated with the functioning of glycolytic chain, Krebs cycle and related processes, i.e., the consideration comprises the whole cell metabolism including respiration (dark respiration in photosynthesizing organisms) and turnover. CIF in these processes is essential to the cells of all kinds of organisms from protozoan to humans. A corresponding biophysical mechanism representing the principal features of CIF in a cell is suggested. In the third part, carbon isotopic characteristics of highly organized animals and humans, and their changes in the course of biological rhythms, and in different pathological states, are analyzed in the light of the cell CIF hypothesis. The structure of the work reflects the author's standpoint that the main principles controlling carbon isotope distribution in organisms and their isotopic characteristics are general for most of them regardless of organization level and their position on the evolutionary stairs. This idea is based on a principal similarity of central metabolic pathways and mechanisms in all living cells. It is proved that the main mechanism of isotope fractionation in cells is a combination of kinetic isotope effect in enzymatic reactions with Releigh effect following substrate pools depletion. From this viewpoint, the key points of CIF in a cell should be bound to the central amphibolic pathways. On the other hand, a variety of peculiarities of carbon isotope distribution in different organisms should be closely associated with their metabolic specificity emerged evolution and depending on their adaptivity to the environmental factors.

In the theoretical study of isotope fractionation in living systems considering their complexity, the theoretical model should satisfy the following requirements. It should be based on real biochemistry of cell metabolism and take into account the real cell conditions and biophysical aspects of cell processes. It should contain minimal assumptions sufficing to explain the observed data and should describe not only isotopic data but also all biochemical and biophysical data. Our approach to the study of biological isotope fractionation includes the following steps:

1. Identification of concrete enzymatic reaction, where isotope effect is likely to arise. Data on experimental examination of the reaction in vitro are useful to establish the limits of isotope effect variations.
2. Determination of carbon isotope ratio and ^{13}C distribution of the reaction products, taking into consideration the estimated magnitude of the effects.
3. Estimation of metabolic consequences of the isotope effect in the key point for carbon isotope ratio of other metabolites considering biosyn-

thetic pathways and biophysical mechanisms of cell metabolism. The results of the estimate should be compared with the known facts. This approach is demonstrated in the following parts of the work.

CIF IN PHOTOSYNTHESIS

CIE in CO_2 Photoassimilation

General Background

The ^{12}C enrichment of biomass in plants and other photosynthesizing organisms relative to CO_2 assimilation was discovered right after the appearance of the first isotope ratio mass-spectrometers (74,75). Nevertheless, intensive studies of metabolic CIEs started since Craig (76) worked out the precision technique for isotope measurements. He was the first person who tried to explain the reason of the above phenomenon (77,78) while overestimating the role of CO_2 diffusion and absorption in plant leaves. Park and Epstein (79) demonstrated that the main reason of $^{13}CO_2$ discrimination in photosynthesis is the ribulose bisphosphate (RuBP) carboxylation, which is the key enzymic reaction in photoassimilation process. The interest in investigating CIEs in photosynthesis greatly increased after Smith and Epstein (80) found the great discrepancies between isotope ratios of two large groups of terrestrial plants of the C_3- and C_4-type with different CO_2 assimilation pathways (see Fig. 1). Carbon isotope ratios of

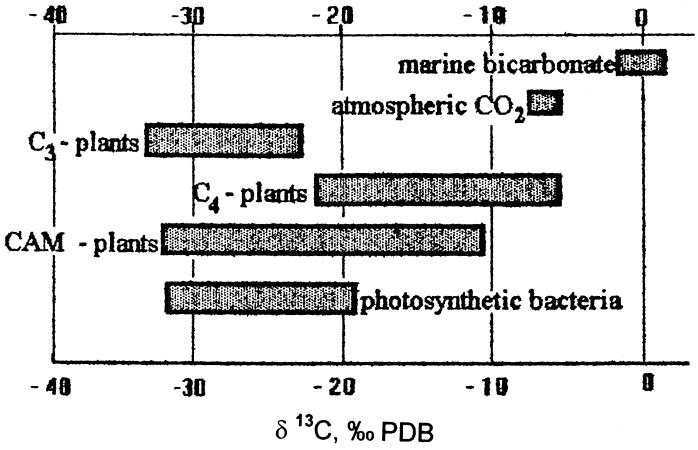

Figure 1. Carbon isotope composition of plants with different pathways of CO_2 photoassimilation (see text).

C_3 plants ranged from -20 to $-35‰$ and those of C_4 plants varied from -9 to $-14‰$.* Another group of terrestrial plants, so-called CAM plants, and aquatic plants have carbon isotope ratio of biomass intermediate between those of C_3 and C_4 plants (81,82). A strong effect of certain environmental factors on $\delta^{13}C$ of plant biomass was reported in many publications (see 83–87). These factors either control (directly or indirectly) the access of CO_2 into the cell or affect the rate of CO_2 fixation in the cell (see Figs. 2–4). For terrestrial plants, the most

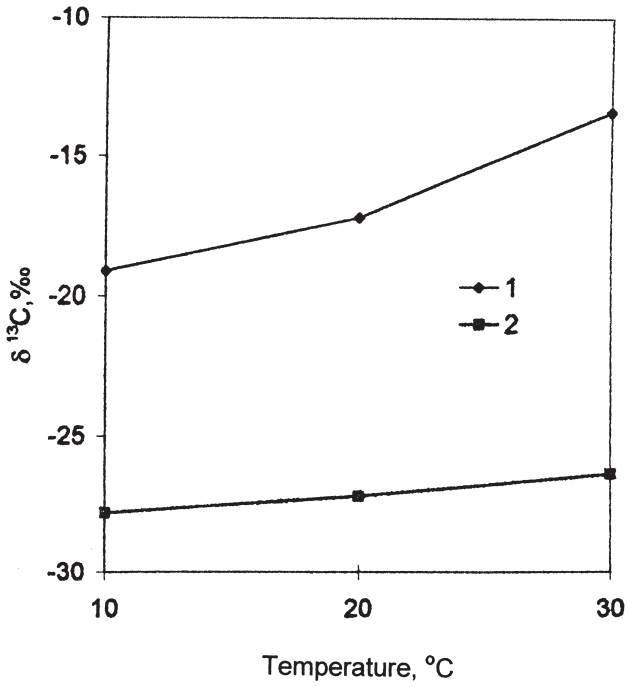

Figure 2. Effect of temperature and CO_2 concentration on carbon isotope composition of biomass marine alga *Cyclotella* (94). 1, 0.03% CO_2; 2, 5% CO_2.

*It is adopted to express isotopic composition of samples via differential notation:

$$\delta^{13}C‰ = [(^{13}C/^{12}C)_{sample}/(^{13}C/^{12}C)_{standard} - 1] \times 1000$$

The ratio of carbon isotopic concentrations in a sample is normalized to that in a standard. The standard is carbon dioxide obtained from limestone from the Pee Dee belemnite (PDB, Pee Dee formation in South Carolina) that has the $^{13}C/^{12}C$ value of 1.1237×10^{-5} (76). Thus, samples enriched in ^{13}C (in comparison with standard) have positive $\delta^{13}C$ values whereas those enriched in ^{12}C will have $\delta^{13}C < 0$.

MARCEL DEKKER, INC.
270 Madison Avenue, New York, New York 10016

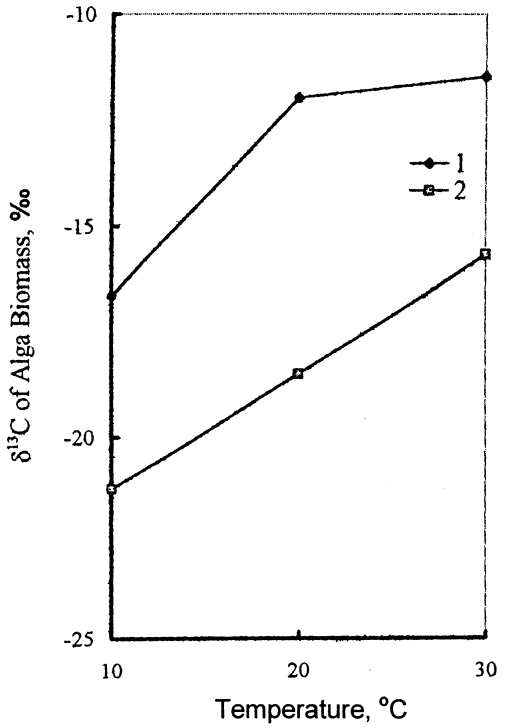

Figure 3. Effect of temperature and water aeration on carbon isotope composition of marine alga *Skeletonema* biomass (94). 1, weak aeration; 2, intense aeration.

important factors are the following: 1) CO_2 content in the air and aeration influencing the diffusion rate of carbon dioxide into photosynthesizing cells; 2) temperature; 3) availability of moisture and salinity of irrigating water regulating the degree of openness of leaf stomatal apertures (88–91). For aquatic plants, the list of parameters includes also pH, water salinity, temperature, water-mixing conditions, and population density of photosynthesizing organisms per unit volume of water (13,92–98). Some additional factors influencing indirectly the rate of CO_2 fixation inside the cell either via enzyme activity, electron transport chain, or through the coupled biochemical reactions must also be mentioned. They include the intensity of impinging light, its wavelength, oxygen concentration in the air, presence of microelements, nitrogen and phosphorous nutrition (14,15,37,84,98–100). The analysis of the facts enables one to conclude that factors strengthening the CO_2 supply to the cells result in enrichment of plant biomass with ^{12}C, whereas the factors increasing the rate of CO_2 fixation in a cell bring about the effect of opposite sign (38,101).

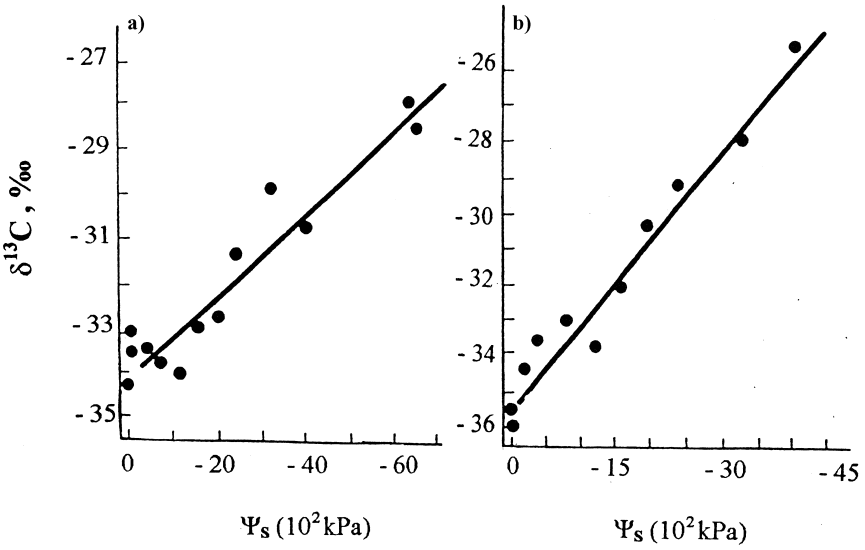

Figure 4. Carbon isotope ratio of alga biomass plotted versus osmotic potential Ψ_s (salinity) of nutrient solution for *Selicornia europeae* subsp. *rubra* (a) and *Paccinelli nuttalliana* (b) (87).

The attempts to understand the mechanism of CIF in photosynthesis and to find the sites where ^{13}C discrimination occurs stimulated numerous studies of isotope fractionation in carboxylating reactions in vitro. The early data reported by Park and Epstein (80) on considerable CIF in RuBP carboxylation responsible for CO_2 fixation in C_3 plants were reproduced by other authors (102–104). At the same time, no significant isotope effects in phosphoenolpyruvate (PEP) carboxylation (the main point of CO_2 fixation in C_4 plants) have been noticed (105–107). It corresponds to the observed differences between these types of plants. But the values of the effects in RuBP carboxylation in vitro appear to be much greater than those in vivo. The former range up to 80‰, whereas the latter are less than 25‰ (102). To explain these facts and to clarify the plausible mechanism of appearance of the isotope effect in the reaction the theoretical treatment of the congruent model reaction has been undertaken (108). Transformation of the linear form of CO_2 molecule to the bent one is the only stage of five stages of the above enzymatic reaction (109) (shown in the scheme below), which might explain the observed ^{12}C enrichment of the fixed carbon relative to the initial CO_2. The maximum value of theoretically estimated effect was about 100‰ thus corresponding closely to the maximum values observed in vitro.

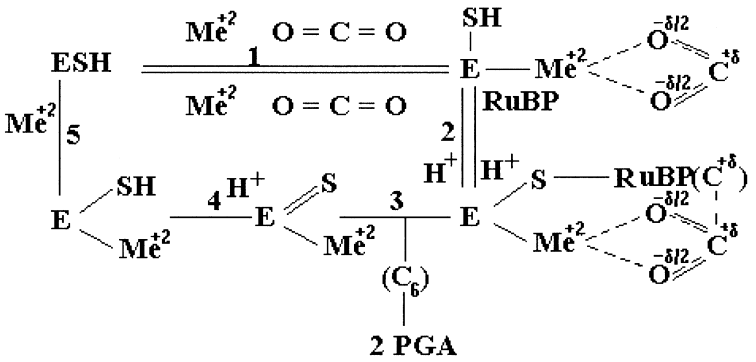

The suggested scheme can explain variations of CIE observed for enzymes isolated from different plants by the differences in binding of CO_2 with the enzyme-bound metal cofactor by which, in turn, depend on the source of enzyme. It can also explain pH dependence of the isotope effect through the H^+ transfer at stage 2. Nevertheless, it cannot explain either the differences between effects observed in vitro and in vivo or the carbon isotope differences of C_3 and C_4 plants (see Fig. 5).

It is essential to note that C_4 plants have RuBP carboxylases, which are able to fractionate carbon isotopes in the same manner as carboxylases from C_3 plants. The above scheme also fails to explain the great dependence of C_3 plants carbon

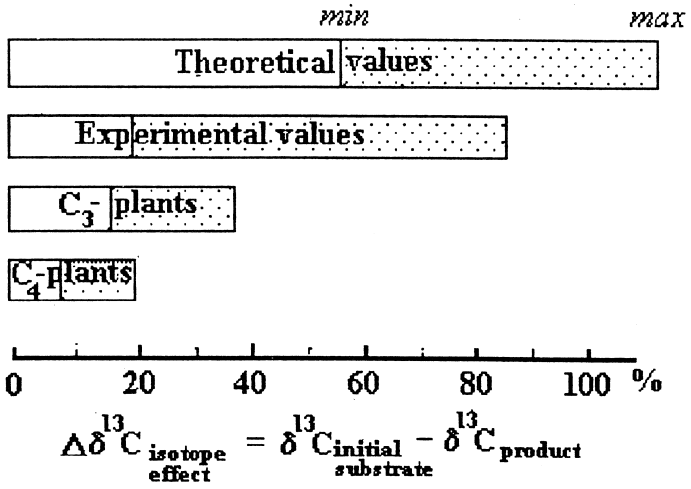

Figure 5. Carbon isotope effects of photosynthesis in C_3 and C_4 plants and isotope effect of RuBP carboxylation (theoretical and experimental) determined in experiments in vitro. Data of in vitro experiments are adapted from Bowman et al. (102).

isotope ratio on some environmental factors mentioned above. This leads us to conclude that to explain the above facts one needs to consider CIF in RuBP carboxylation in connection with other cell reactions and with cell micro-environmental conditions.

Modeling of CIF in Photosynthetic Assimilation of CO_2

Two approaches are known to describe CIE in photosynthesis. The first (and the most widely disseminated) approach (110–113) considers assimilation of CO_2 as a stationary process, in which the decrease of CO_2 concentration in a cell during carboxylation is compensated for by the equal entry of carbon dioxide from the atmosphere. The photorespiration is considered to proceed simultaneously with CO_2 assimilation. The second alternative approach, developed by the author (38,114), assumes that assimilation is a discrete process. Carbon dioxide entering a cell is partially fixed in RuBP carboxylation. The assimilation is interrupted by RuBP oxidation and newly formed CO_2 with the residual one unused in the previous carboxylation phase are ejected from the cell into the atmosphere. According to this model, RuBP carboxylation and oxidation are the alternating cell processes in light period, providing photoassimilation and photorespiration, correspondingly.

Steady-state model. Steady-state models have been developed in two versions. According to one of them, the diffusion stage of assimilation is considered as an ordinary reversible chemical reaction coupled with RuBP carboxylation and some other chemical steps inside a cell (111,113,115). For the analysis, it is convenient to consider a simplified two-step carboxylation sequence that can be written in the following way:

$$\mathbf{A} \underset{k_{-1}}{\overset{k_1}{\rightleftharpoons}} \mathbf{B} \xrightarrow{k_2} \mathbf{C}$$

where the first stage corresponds to diffusion of CO_2 molecules from the atmosphere into the cell and back; the second stage corresponds to carboxylation; k_1, k_{-1}, and k_2 are the rate constants of the corresponding processes. Using $A(A_o)$ and B to designate CO_2 concentration in the atmosphere and the cytoplasm, respectively, and C to designate the amount of fixed carbon, one can easily obtain the following kinetic equations:

$$\frac{dB}{dt} = k_1 A_o - (k_{-1} + k_2)\, B \tag{1}$$

$$\frac{dC}{dt} = k_2 B \tag{2}$$

MARCEL DEKKER, INC.
270 Madison Avenue, New York, New York 10016

Their integration for each of the isotopic species (an asterisk is generally used to denote the molecules containing ^{13}C) gives the relationship between the ratio of isotopic concentrations in carbon dioxide dissolved in the cytoplasm and in fixed carbon (biomass) and the analogous ratio in carbon dioxide of the atmosphere:

$$\frac{B^*}{B} = \frac{k_1^*}{k_1}\frac{k_{-1}+k_2}{k_{-1}^*+k_2^*}\frac{A_0^*}{A_0} \tag{3}$$

$$\frac{C^*}{C} = \frac{k_1^* k_2^*}{k_1 k_2}\frac{k_{-1}+k}{k_{-1}+k_2^*}\frac{A_o^*}{A_o} \tag{4}$$

The following two extreme cases can be theoretically analyzed: 1) when the rate of CO_2 is limited by diffusion, i.e., $k_{-1} << k_2$, and 2) when the rate of CO_2 assimilation is limited by carboxylation of RuBP, i.e., $k_{-1} >> k_2$. In plants and other photosynthesizing organisms, the first case is the most probable because the direct measurements (116) have shown that the activation energy of mesophyll cell conductance to CO_2 ranges from 10.2 to 12.5 kJ/mol at 25°C. This means that the diffusion is the limiting stage of CO_2 assimilation. According to the theory (117), a high concentration of enzyme enhances the diffusional limitation of reaction rate, and concentration of Rubisco in photosynthesizing cells are known to be high (116). For this case, expressions (3) and (4) transform into (5) and (6), respectively:

$$\frac{B^*}{B} = \frac{k_1^*}{k_1}\frac{k_2}{k_2^*}\frac{A_0^*}{A_0} = \frac{\alpha_2}{\alpha_1}\frac{A_o^*}{A_o} \tag{5}$$

$$\frac{C^*}{C} = \frac{k_1^*}{k_1}\frac{A_o^*}{A_o} = \frac{1}{\alpha_1}\frac{A_o^*}{A_o} \tag{6}$$

where $\alpha_1 = k_1/k_1^*$ and $\alpha_2 = k_2/k_2^*$ are the corresponding kinetic coefficients of isotope separation at the reaction stages.

Experimental estimates of α_1 and α_2 give values of 1.004 and 1.020, respectively (92,111,118). By introducing these values in expressions (5) and (6), one can conclude that, according to the model, in cases when CO_2 assimilation rate is limited by diffusion, ^{13}C enrichment of cytoplasmic CO_2 should be as much as 16–26‰ relative to environmental CO_2. Simultaneously, ^{12}C enrichment of the fixed carbon cannot exceed 4‰. These conclusions contradict the following facts: 1) the most widely spread in nature C_3 plants are enriched with ^{12}C by 20‰ and more; 2) the maximal ^{13}C enrichment of cytoplasmic CO_2 does not exceed 6‰ (92,118).

Another version of the steady-state mode, developed by Farquhar et al. (112,119) considers diffusion to be proportional to the difference of CO_2 concentrations in the cell and atmosphere that leads to the following expression:

$$\Delta = a + (b - a)\, p_i/p_a \tag{7}$$

MARCEL DEKKER, INC.
270 Madison Avenue, New York, New York 10016

where Δ denotes the ^{13}C discrimination in photosynthetic assimilation, a and b are equal to

$$a = (\alpha_1 - 1)10^{-3} \tag{8}$$

$$b = (\alpha_2 - 1)10^{-3} \tag{9}$$

Here α_1 and α_2 are the isotope separation factors for diffusion and RuBP carboxylation, respectively, P_a and P_i in Eq. (7) are the partial pressures of CO_2 in the atmosphere and in the leaf.

The advantage of this version is in its ability to explain the link between carbon isotope discrimination and the gas exchange parameters. The effects of water availability, salinity, and some other factors, which directly or indirectly are an influence on intercellular CO_2 concentration and hence, on carbon isotope composition of plants can also be adequately interpreted (15,86,119). The model can explain the differences of isotopic ratios of C_3, C_4, and CAM plants as well, but this requires the introduction of a new parameter ϕ, accounting for the leakage of CO_2 from sheath cells into mesophyll cells:

$$\Delta = a + (\phi b - a)p_i/p_a \tag{10}$$

However ϕ parameter cannot be found by an independent experimental way and its validity is problematic.

The analysis of expression (7) in the case of diffusional limitation of CO_2 assimilation ($P_i << P_a$) gave the same result as before: the theoretical forecast did not coincide with the real CIF in photosynthesis. It seems to be quite clear because expressions (5) and (6) can be reduced to (7) (38). The observed violations of the principal model relationship (7) give more evidence for the obtained result. In some water- and salt-stressed plants the value of carbon isotope discrimination Δ appears to be independent from p_i/p_a ratios (120,121). The same violation was observed in cowpea and its chlorophyll-deficient mutants. It was shown that, in spite of the closeness of the gas-exchange and water-use-efficiency characteristics of the plants, they were quite different in carbon isotope discrimination (7,16,122). Inability of the steady-state model to explain higher values of the isotope discrimination Δ in RuBP carboxylation in vitro relative to ^{12}C enrichment of plants (102–104), observed ^{13}C enrichment of environmental CO_2 around the plants (122,123), what in accordance with the model is impossible since CO_2 pool, which is infinite relative to carbon pool of plants, the influence of nitrogen assimilation (14,15,99,125), and some other facts on carbon isotope discrimination (38,122), which cannot be explained in the frame of the steady-state model without introducing new parameters, prompted attempts to create new models. The discrete model is one of them (38,114).

Discrete model. The model is based on the assumption that the discreteness of CO_2 flow entering a cell arises due to the ability of the enzyme Rubisco

MARCEL DEKKER, INC.
270 Madison Avenue, New York, New York 10016

(RuBP; carboxylase/oxygenase) to function not only as carboxylase but also as oxygenase. Periodically switching the enzyme on and off interrupts the CO_2 flow, which makes it enter the cell by discrete portions. The moments of switching depend on the ratio of CO_2 to O_2 concentrations in the cell, which periodically changes in accordance with RuBP carboxylation or oxygenation function in the cell. In the carboxylase phase of enzyme function, CO_2 fixation is accompanied by CIE, as described before. During the oxygenase phase, RuBP is oxidized to CO_2, which along with the residual CO_2 unused in the previous carboxylase phase is rejected from the cell with photorespiration flow. The periodic exhaustion of CO_2 cytoplasmic pool in combination with the CIE in RuBP carboxylation brings about the Releigh effect and results in dependency of the carbon isotope composition of biomass on the degree of cytoplasmic pool exhaustion, F. It also determines the isotopic difference between the biomass carbon and the carbon of environmental CO_2. This difference is maximal when the degree of CO_2 pool exhaustion in cytoplasm is minimal (essentially when $F < 10\%$), and it decreases when CO_2 pool diminishes. These relationships are described by the following expressions:

$$(\delta^{13}C_{bio}10^{-3} + 1) = (\delta^{13}CO_2\, 10^{-3} + 1)[1 - (1 - F)^{1/\alpha}] \tag{11}$$

$$(\delta^{13}C_{res}\, 10^{-3} + 1) = (\delta^{13}CO_2\, 10^{-3} + 1)(1 - F)^{1/\alpha - 1} \tag{12}$$

where $\delta^{13}C_{bio}$, $\delta^{13}C_{res}$, and $\delta^{13}CO_2$ are the carbon isotope composition of biomass, cytoplasmic CO_2, and carbon dioxide of the atmosphere, respectively; α is the effective coefficient of carbon isotope separation determined as the ratio of the rate constants for isotopic species in RuBP carboxylation, which, in turn, are the function of the rate constants on the elementary steps of reaction.

As follows from Eq. (11), the maximal fractionation is achieved when F is small (i.e., >0.1). In this case, the difference between isotope ratio of biomass and environmental CO_2 can be presented as follows:

$$\delta^{13}C_{bio} - \delta^{13}CO_2 = (\alpha - 1)10^3 \tag{13}$$

At high F values ($F > 1$), the isotope composition of biomass carbon approaches that of environmental CO_2 ($\delta^{13}C_{bio} = \delta^{13}CO_2$). Examples of these cases will be given below.

The crucial point of the model is the biophysical mechanism of CO_2 cell uptake making Rubisco switch on and off and causing the discreteness of CO_2 flow in and out of the cell. Our version of this mechanism is shown schematically in Fig. 6. Let us consider that points 1 and 1′ in Fig. 6 correspond to the moment when carbon dioxide enters the leaf causing an increase of CO_2 concentration in the boundary layer (dashed curve) and cell cytoplasm (solid curve). This process occurs due to the difference between CO_2 concentration in the air, the boundary layer, and the cell. It continues to the moment (points 2 and 2′) when CO_2/O_2 ra-

MARCEL DEKKER, INC.
270 Madison Avenue, New York, New York 10016

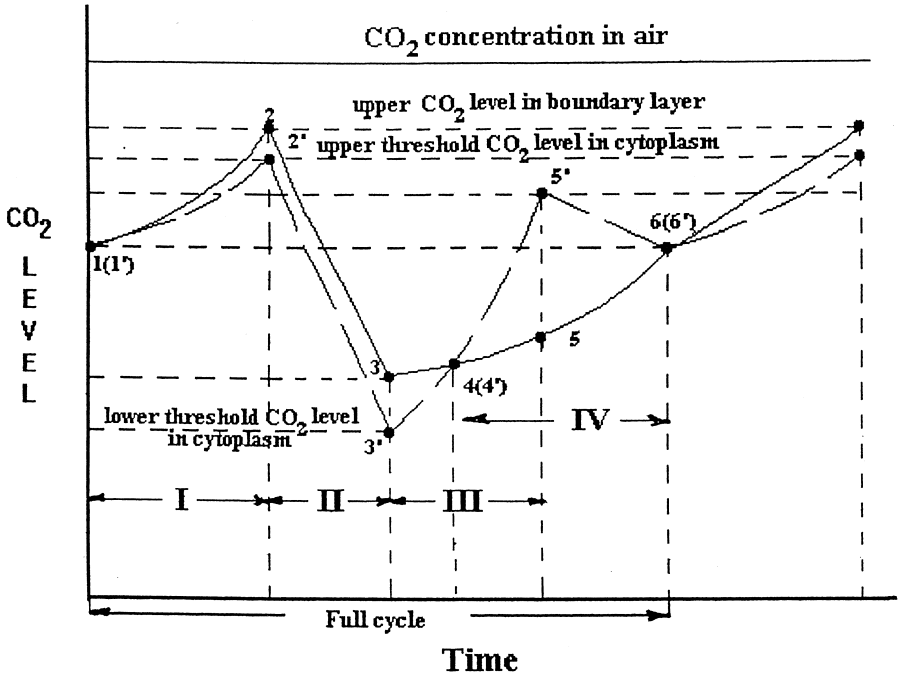

Figure 6. Hypothetical scheme of variations of CO_2 concentration in cell cytoplasm (dashed line, points with apostrophes) and in outer boundary layer (solid line) in course of carboxylase/oxygenase activity of Rubisco. I, diffusion; II, carboxylase Rubisco function; III, oxygenase Rubisco function; IV, photorespiration phase. Points denote time-boundaries of separate phases of CO_2 assimilation process (see text).

tio reaches the upper threshold level corresponding to activation of carboxylase function of Rubisco. In accordance with the data on CO_2 conductivity through the mesophyll cells mentioned above, we have supposed that the rate of RuBP carboxylation is higher than the diffusion rate. Then, the activation of carboxylation activity of Rubisco must cause a drop in CO_2 concentration in cytoplasm (line 2–3) followed by a respective decrease of CO_2 concentration in the boundary layer (line 2′–3′). It proceeds until CO_2/O_2 ratio reaches the lower threshold level (points 3 and 3′) corresponding to reswitching the carboxylase activity of Rubisco to oxygenase function. This results in oxidation of RuBP followed by O_2 uptake and CO_2 formation (lines 3–4–5). The latter is formed in the course of decarboxylating reactions in glycolate pathway. In accordance with the aforementioned reason, now the higher rate of RuBP oxidation (compared with CO_2 diffusion) again results in abrupt increase of CO_2 concentration in the cell. At point 4(4′) in

Marcel Dekker, Inc.
270 Madison Avenue, New York, New York 10016

Fig. 6, CO_2 concentration in the cell becomes equal to that in the boundary layer and then prevails it. At point 5, the rate of CO_2 production reaches its top level and then decreases because of depletion of the RuBP pool. CO_2 concentration in cell drops down until it becomes equal to that of in boundary layer at point 6. A negative gradient of CO_2 concentration arising between the cell and the boundary layer provides rejection of carbon dioxide from the cell. The time interval between crosspoints where CO_2 concentrations in cytoplasm and in the boundary layer are equal to each other corresponds to photorespiration phase. From point 6, the CO_2 concentration both in cytoplasm and in the boundary layer increases up to the upper threshold level (point 7) when the activity of Rubisco changes from carboxylase to oxygenase 1. Note, that point 6(6′) coincides with starting point 1(1′); then all processes repeat.

Hence, the dual carboxylase/oxygenase function of Rubisco appears to be responsible for the splitting of CO_2 flow entering a cell into discrete batches. As follows from the material balance, CO_2 evolved from a cell must be enriched with ^{13}C unlike to CO_2 derived from the oxidation of ^{12}C-enriched RuBP in the photorespiration phase. It occurs due to ^{13}C enrichment of the residual batch of CO_2 unused in the carboxylation phase of Rubisco activity, providing ^{13}C enrichment of total CO_2 after mixing it with CO_2 formed in the oxygenation phase. Although the above processes correspond to the most common case, some exceptions may also occur as it will be demonstrated below.

The rates of the slowest diffusional processes in a cell are estimated to lie between 0.02 and 0.1 s^{-1} (116), and those of chemical reactions are one order of magnitude higher. For this reason it is very difficult to obtain an experimental confirmation of the above theoretical scheme from gas-exchange or in other kinetic data. Nevertheless, some of the gas-exchange experiment results indirectly confirm this scheme. At the outset of illumination of a sunflower leaf exposed to $^{14}CO_2$ in a chamber, the carbon dioxide induction curve regularly declined, which was explained by rejection of CO_2 from the cell (126). Moreover, it was found that a part of this CO_2 represented previously fixed carbon dioxide. A permanent illumination did not allow detection of these induction losses because of the positive effect of carbon dioxide uptake.

Since carboxylase/oxygenase activity of Rubisco and its relation with CO_2/O_2 ratio have been disclosed only in in vitro experiments (116,127,128), the real molecular mechanism of coupled CO_2 photoassimilation/photorespiration in a cell is still unclear. The discrete model permits a reasonable explanation for this property of enzyme regarding it as a necessary element of photosynthetic metabolism.

Some more arguments in favor of the suggested mechanism come from the isotope data. The model permits an explanation of the higher values of carbon isotope discrimination in vitro compared with the real ^{12}C enrichment in plants, including C_3 plants having maximal discrimination effect. The conditions of in vitro

MARCEL DEKKER, INC.
270 Madison Avenue, New York, New York 10016

experiments were chosen in such a way to provide determination of the isotope separation factor α. They correspond to a low degree of CO_2 pool exhaustion ($F < 0.1$) where according to Eq. (13) the isotope discrimination is equal to α. In real plants the conditions are far from those used in experiments and correspond to F values much closer to 1.

The same reasoning can be used to explain the carbon isotopic differences in C_3, CAM, and C_4 plants, which are characterized by different photorespiration intensity. The lower the photorespiration intensity, the higher the F value and vice versa. Then, in accordance with Eqs. 11 and 12, C_3 plants having more intense photorespiration are mostly enriched with ^{12}C whereas C_4 plants with lower photorespiration are enriched with ^{13}C. Accordingly, CAM plants having intermediate intensity of photorespiration are characterized by intermediate carbon isotope ratio of biomass (being in between the above two).

According to the model, both external and internal factors differently effect the carbon isotope ratio of photosynthesizing organisms depending on how they influence the degree of cytoplasmic CO_2 pool exhaustion. From this one can easily understand the effect of the following factors on the carbon isotope ratio of biomass: water and salt stress, CO_2/O_2 ratio, ozone and oxygen concentrations in the air, illumination intensity and impinging light wavelength (15,88,98,121). The first two control the access of CO_2 to the cell whereas the others are responsible for reswitching of Rubisco function from carboxylation to oxygenation and back. Hence, all the above factors influence the carbon isotope composition of biomass.

The interrelation of carbon isotope composition of a photosynthesizing organism with N-assimilation (14,99,125) is also explainable. N-Assimilation determines the rate of malate-aspartate shuttle by exerting the photorespiration intensity (129). It also causes the isotopic changes in biomass carbon via CO_2 assimilation/photorespiration ratio as it has been demonstrated for plants with different CO_2-assimilation pathways.

The genetic correlation between carbon isotope ratio of plants and the inherited properties like productivity and water-use efficiency (65,66,130) are explained by the inheritance of photosynthesis organization of plant, which reproduces the specific mechanism of CIF.

CIE of photosynthesis is essential but not the sole reason for isotopic variations of photosynthesizing organism biomass. The role of CO_2 assimilation/photorespiration ratio in formation of carbon isotope composition of biomass has been considered above. It appears that photorespiration is followed by CIF, which exerts an additional influence on isotopic composition of biomass and some other isotopic characteristics of plants and other photosynthesizing organisms. CIE of photorespiration, the mechanism of its emergence, and the influence on carbon isotopic characteristics of photosynthesizing organisms are discussed below.

CIE of Photorespiration

General Background

All known models describing CIF in photosynthesis can explain either ^{12}C enrichment of biomass versus assimilated CO_2 or at least its isotopic identity. It follows from the kinetic nature of CIE in RuBP carboxylation, which is assumed to be responsible for the observed ^{13}C discrimination in photosynthesis. Experimental approval of ^{13}C enrichment of biomass in CO_2 assimilation (131–135) puzzled many researchers. The following experimental facts (not numerous but quite reliable) indicate that sometimes CIF in CO_2 photoassimilation is followed by the isotopic shifts with opposite sign.

In the experiments with leaves of some C_3 and C_4 plants (kidney bean, poplar, maize) carried out in a closed chamber with the use of CO_2 enriched in ^{13}C showed a gradual decline of $^{13}C/^{12}C$ ratio of the residual CO_2 (131–133). The effect was more pronounced in plants exhibiting a higher compensatory point, i.e., a more intense photorespiration. It means that the plants under experimental conditions of CO_2 assimilation have accumulated ^{13}C in their biomass and discriminate ^{12}C.

Similar results were obtained by Voznesenski et al. (134) who used $^{14}CO_2$ in chamber experiments. A 4-day-long growth period of the photosynthesizing alga *Chlorella vulgaris* Beirger exposed to $^{14}CO_2$ resulted even on the 2nd day of the experiment in a much higher biomass-specific radioactivity than that of CO_2 assimilated.*

The results obtained by Ivanov et al. were even more striking (135). They used ^{13}C enriched bicarbonate to study photosynthesis in purple sulfuric bacteria *Ectothiorhodospira shaposhnikovii*. The extent and even the sign of isotope enrichment of bacteria biomass depended on the $^{13}C/^{12}C$ ratio in the initial substrate. When the ratio was 0.59, the biomass ^{13}C enrichment amounted to 752‰. When the ratio declined to 0.03, i.e., approached the natural range of isotopic variations, the sign of the effect changed to the opposite and biomass got enriched in a light isotope. It became equal to −26‰ when the ratio was 0.011, which corresponded to the level of ^{12}C enrichment in natural plants and photosynthesizing organisms.

There are only two possibilities that explain any isotopic discrepancies between CO_2 and biomass arising in photosynthesis: 1) preferential selectivity towards one of CO_2 isotopic species in the course of assimilation, and 2) selective

*In a chemical sense the behavior of isotopic species of CO_2 ($^{12}CO_2$, $^{13}CO_2$, $^{14}CO_2$) is undistinguishable and isotope separation laws in chemical reactions are the same for different isotopic pairs. The differences are in the effect values, which are proportional to isotopic mass differences.

MARCEL DEKKER, INC.
270 Madison Avenue, New York, New York 10016

oxidation of one of isotopic species of organic substrate during photorespiration. Analysis of the literature showed that CO_2 assimilation is accompanied by preferential selection of light carbon isotope (^{13}C discrimination) that resulted in ^{12}C enrichment of organism biomass. Because ^{13}C enrichment of biomass cannot occur in CO_2 assimilation, the isotopically selective oxidation in photorespiration is the most probable reason to explain the above facts.

The biophysical interpretation of the hypothesis requires identification of the key metabolic point in photorespiration (similar to RuBP-carboxylating reaction in CO_2 assimilation) where CIF could occur. To propose a reasonable biophysical mechanism of photorespiration one needs to estimate the isotopic peculiarities of photosynthesizing organisms, which are expected to be the result of the supposed CIE of photorespiration and to compare them with the real facts. Following this scheme and analyzing photorespiration metabolism, we have supposed that the most plausible point of CIF was decarboxylation reaction of glycine in glycolate chain (39).

Hypothesis on CIF Point in Photorespiration

The results of experiments in vitro showed that enzymatic decarboxylations were always followed by CIF because of different rates of C—C cleavage for isotopic species (136–139). An important role of pyruvate decarboxylation in ^{13}C distribution in plant and animal biomass was experimentally confirmed (40,41,140,141). Hence, the conjecture of the role of glycine decarboxylation in supposed photorespiration, CIE was sufficiently justified. The following consideration makes this hypothesis more reasonable.

It was shown by inhibitory analysis that isonicotinylhydrozide (INH) (enzyme inhibiting transformation of glycine into serine in photorespiratory chain of photosynthesizing organisms) strongly affected the carbon isotope ratio of marine alga *Chlorella stigmatophora* (142).

The experimental study of enzymatic glycine decarboxylation in vitro showed considerable isotopic distinctions between carboxylic carbon of glycine and CO_2 (143,144). Some of the results of this series of experiments, which were carried out with mitochondria isolated from leaves of different plants, are shown in Table 1.

The data of Table 1 show that CIF in glycine decarboxylation really takes place but in most cases the sign of isotope effects is abnormal, i.e., CO_2 evolved is enriched in ^{13}C. It was supposed to be the result of strong influence of medium conditions that could remove the limiting stage from C—C bond cleavage to enzyme-substrate binding (139,145). It was found earlier (139) that in cases when the rate of enzymic decarboxylation was limited by enzyme-substrate binding, CO_2 formed in the reaction was enriched in ^{13}C. On the contrary, when the rate

Marcel Dekker, Inc.
270 Madison Avenue, New York, New York 10016

Table 1. Changes in Carbon Isotope Composition of CO_2 Evolved during Glycine Decarboxylation by Mitochondria From Different Plants. All Data are Given in PDB Units and Expressed in $\Delta^{13}C = \delta^{13}CO_2 - \delta^{13}C_{1(glycine)}$. $\delta^{13}C_{1(glycine)} = -26.8‰$ (143)

Object	Presence of THF, ADP, and NAD	Time of Exposition	
		0–2 h	3–14 h
Hordeum	+	15.4	16.0
Triticum	+	5.1	9.4
	−	5.5	3.6
Spinacia	+	16.2	15.2
	−	8.6	3.6
Brassica	+	7.8	4.8
Wolffia	+	7.6	0.1
Medicago	+	10.4	9.9
Pisum	+	0.4	−7.8
	−	−0.6	−1.6

was limited by C—C-bond cleavage, CO_2 was enriched in ^{12}C. The assumption is supported by the considerable differences in CO_2 carbon isotope ratio in short-term and long-term experiments (see Table 1), which can be caused by the increase of pH in the course of glycine deamination due to NH_3 evolution.

The strong influence of reaction conditions was confirmed in the detailed examination of enzymatic glycine decarboxylation carried out with mitochondria isolated from the leaves of pea (*Pisum sativum* L.) and spinach (*Spinacia oleracea* L.) (144) in the in vitro experiments under variable reaction conditions (pH, temperature, cofactors). Figure 7 shows the influence of pH in the range of 6.8 to 8.0 (close to conditions in vivo). As seen, carbon isotope ratio changes smoothly with pH achieving a maximum at pH 7.0. As also seen from Fig. 7, the curves follow the same pattern regardless of mitochondria source.

The impact of different cofactors on carbon isotope ratio of CO_2 evolved in the enzymatic decarboxylation of glycine in vitro by using mitochondria isolated from leaves of spinach (*Spinacia oleracea* L.) and pea (*Pisum sativum* L.) is shown in Table 2 (144). Cofactors are the substances of a protein and nonprotein nature that activate some enzymes (e.g., multienzymic glycine dehydrogenase complex in the present case). Determining the rate-limiting stage of the reaction, they can influence the reaction rate and the kinetic isotope effect. The cofactors used in experiments are as follows: PLP, pyridoxal phosphate; ADP, adenine diphosphate; and NAD, nicotinamidadenine nucleotide. This series of two independent experiments (I and II in Table 2) was carried out under the following conditions: pH = 7.2 and T = 25°C. In Table 2, $\Delta^{13}C = \delta^{13}C\hat{I}_2 -$

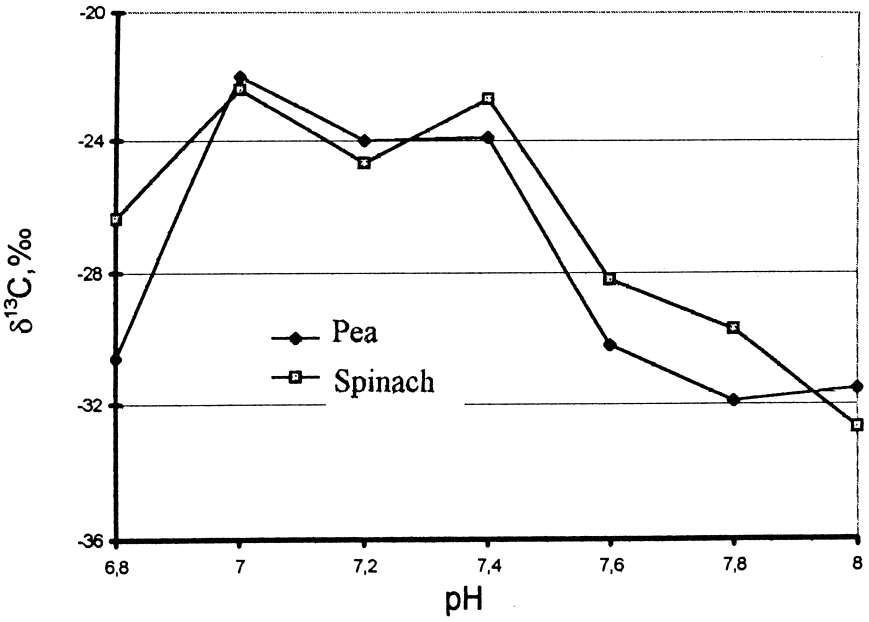

Figure 7. Dependence of CO_2 carbon isotope ratio on pH obtained in in vitro experiments on enzymatic decarboxylation of glycine by using mitochondria isolated from pea (filled circles) and spinach (open squares) leaves (144).

$\delta^{13}C$, where $\delta^{13}C = -32.4 \pm 0.8‰$ is the carbon isotope ratio of carboxyl group of glycine and $\delta^{13}C\hat{I}_2$ is the carbon isotope ratio of CO_2 evolved. The values of $\delta^{13}C$ collected in Table 2 are given in PDB units. The values in the last column correspond to the absence of cofactors in the system. As seen from Table 2, the impact of NAD^+ is the strongest one resulting in the change of the isotope effect sign.

Two main conclusions follow from the results of in vitro experiments shown in Table 2: 1) glycine decarboxylation can be accompanied by considerable CIF, and 2) isotope effect of this reaction depends on the reaction conditions so that the effect sign can be changed. These conclusions confirm the assumption about the role of glycine decarboxylation CIE in photorespiration. However, the results obtained in in vitro experiments cannot be directly transferred to the living organisms since the rate-limiting stage, depending on the reaction conditions and on other metabolic processes in a cell, cannot be exactly reproduced under in vitro conditions. Nevertheless the existence of CIE in glycine decarboxylation and its sign can be identified by examination of isotopic composition of metabolites formed in the photosynthesis.

Modeling of CIF in Photorespiration

To model CIF in photorespiration one needs to know the sign of CIE in glycine decarboxylation. As it follows from the previous section, this effect can be either "normal" (CO_2 evolved is enriched in ^{12}C) or "abnormal" (CO_2 is enriched in ^{13}C). We assume that in photosynthesizing cells the effect is normal. This assumption is based on the data on carbon isotope ratio of metabolites formed in glycolate chain in the course of photorespiration, such as for example, oxalates from C_3 and CAM plants (146–148), proline and labile sugars from alga *C. stigmatophora* (142,149), which are enriched in ^{13}C. A possible reason for ^{13}C enrichment in this case is the removal of ^{12}C species with CO_2 in glycine decarboxylation reaction.

As it follows from the discrete model (38,114), during the carboxylating phase of Rubisco function, a batch of "light" (enriched in ^{12}C) carbon enters the cell and fills via the Calvin cycle the carbohydrate pools such as starch and labile sugars. When the regulatory mechanism (see above) reswitches the enzyme to oxygenation function, labile sugars feed the glycolate chain. The CIF occurs at the point of glycine decarboxylation in glycolate chain (see Fig. 8) resulting in ^{13}C enrichment of the remaining substrates and in ^{12}C enrichment of CO_2 evolved (as

Table 2. Impact of Cofactors* on Carbon Isotope Ratio of CO_2 Evolved in Enzymatic Decarboxylation of Glycine in vitro by using Mitochondria Isolated From Leaves of Spinach (*Spinacia oleracea* L.) and Pea (*Pisum sativum* L.) (144). Reaction Conditions: pH = 7.2, T = 25°C. $\Delta^{13}C = \delta^{13}CO_2 - \delta^{13}C_1$, where $\delta^{13}C_1$ is Carbon Isotope Ratio of Carboxyl Group of Glycine and $\delta^{13}CO_2$ is Carbon Isotope Ratio of CO_2 Evolved. $\delta^{13}C_1 = -32.4 \pm 0.8‰$. Results of Two Independent Experiments (I) and (II) are Given. $\delta^{13}C$ Values are Given in PDB Units. The Values in the Last Column Correspond to the Case When Cofactors are Absent

Objects	Exp. No.	Param.	PLP	PLP + ADP	PLP + NAD^+	ADP	NAD^-	ADP NAD^+	Cofactor Abs.
Spinach	I	$\delta^{13}CO_2$	−25.9	−26.2	−29.6	−30.9	−42.2		−26.3
		$\Delta^{13}C$	+7.8	+7.5	+4.1	+2.7	−8.5		+7.4
	II	$\delta^{13}CO_2$		−25.6		−30.4			−25.4
		$\Delta^{13}C$		+8.0		+3.2			+8.2
Pea	I	$\delta^{13}CO_2$	−31.2	−28.2	−30.6	−35.6	−40.1	−35.3	−28.5
		$\Delta^{13}C$	+2.5	+5.5	+3.1	−2.2	−6.4	−1.6	+5.4
	II	$\delta^{13}CO_2$	−33.9			−40.2			
		$\Delta^{13}C$	−0.3			−6.5			

* Cofactors are substances of a protein and non-protein nature, which activate some enzymes (e.g., multienzymic glycine dehydrogenase complex in this case). They determine the rate-limiting stage of reaction and can influence the reaction rate and the kinetic isotope effect. The following cofactors were used in this series of experiments: PLP = pyridoxal phosphate, ADP = adenine diphosphate, and NAD = nicotinamidadenine nucleotide.

MARCEL DEKKER, INC.
270 Madison Avenue, New York, New York 10016

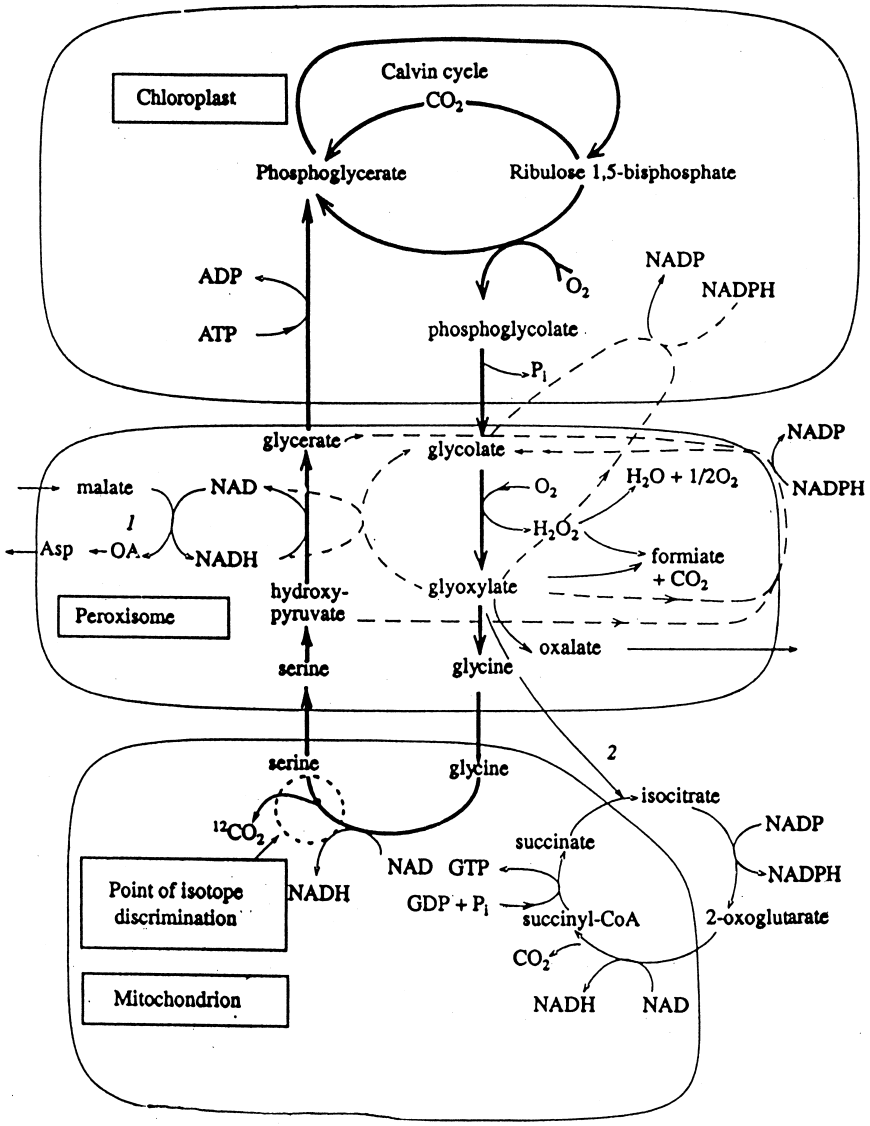

Figure 8. Schematic representation of carbon isotope discrimination during oxygenase phase of Rubisco functioning. Calvin cycle and part of photorespiratory pathway responsible for metabolite pool exhaustion leading to ^{13}C enrichment are marked by a thick solid line. Points of isotope discrimination due to kinetic isotope effect are denoted by a dotted line. 1, malate-aspartate shuttle; 2, synthase reaction brought about by cytosolic isocytrate lyase; OA, oxaloacetate; Asp, aspartate. Scheme of photorespiration is adapted from Igamberdiev (129).

normal CIE supposes). As the Calvin cycle and the glycolate chain form a closed loop, the substrates spinning in the loop may be regarded as belonging to the same carbon pool and hence, they are subjected to the isotope enrichment in ^{13}C. The ^{13}C enrichment of photorespiration metabolites causes, in turn, the enrichment of biomass in a heavy isotope. In general, this means that CIF in photorespiration brings about the isotopic discrepancies between biomass and nutrient CO_2, which appear to be of the opposite signs compared with those emerging due to isotope fractionation in CO_2 photoassimilation. The extent of ^{13}C enrichment is strengthened by the Releigh effect and depends on the degree of carbon pool depletion, i.e., on the intensity of photorespiration.

In parallel with ^{13}C enrichment of substrates remaining in the photorespiration chain, ^{12}C-enriched CO_2 formed in glycine decarboxylation enters cytoplasm and mixes there with the ^{13}C-enriched residual CO_2 left after RuBP carboxylation in the previous phase. The final carbon isotope composition of the total CO_2 removed from the cell is determined by the mixing of CO_2 flows formed in both phases. When CO_2 concentration inside of the cell exceeds that of outside, the CO_2 flux from the cell into the boundary layer and then to the atmosphere in the course of photorespiration provides respective isotopic shifts between biomass and environmental CO_2.

The proposed mechanism assumes (39) that carbon flows of substrates arising in carboxylation and oxygenation phases of Rubisco functioning are different by carbon isotope ratio. The latter is enriched in ^{13}C versus the former. Both carbon flows are isolated in time and space. The key element of CIF in photorespiration is the kinetic isotope effect of enzymatic glycine decarboxylation reaction multiplied by the Releigh effect. The latter arises due to the periodic exhaustion of the substrate pool and removal of light carbon isotope with CO_2 in the course of photorespiration.

CIF in glycolate chain is coupled with isotope fractionation in RuBP carboxylation via dual function of Rubisco (see above). Isotopic discrepancies of biomass and environmental CO_2 depend on both isotope effects. The influence of cell and environmental factors affecting both CO_2 photoassimilation and photorespiration results in isotopic shifts of biomass. For some factors such as salt stress, CO_2 and O_2 concentrations, light intensity, and some others, the shifts are the same for both processes. A strong effect of the enrichment of nutrient CO_2 in a heavy carbon isotope, which sometimes can result in ^{13}C enrichment of biomass (relative to CO_2) must be emphasized (131–135). It corresponds to the case when CIE of photorespiration exceeds that of CO_2 photoassimilation.

Among the factors determining the level of ^{13}C enrichment of biomass, the partitioning of carbon flow in photorespiration should be noted. One part of it is used for biosynthetic needs whereas the other is oxidized to CO_2. The bigger part of the carbon flow passes decarboxylation reaction (i.e., the more intense photorespiration occurs) the more photorespiration metabolites and the whole

MARCEL DEKKER, INC.
270 Madison Avenue, New York, New York 10016

biomass appear to be enriched in ^{13}C. On the contrary, the bigger part of photorespiration carbon flow is used for biosynthesis, the lesser part of it is subjected to decarboxylation reaction. It increases the photorespiration substrate pool and hence diminishes ^{13}C enrichment of biomass.

Experimental Confirmation of Photorespiration CIE and for Its Coupling with Effect of CO_2 Photoassimilation

All arguments in favor of the proposed concept can be divided into three groups. The first group includes the facts supporting the existence of photorespiration CIE (PRCIE) itself. The second one provides support to the conclusion following from the fact of its existence. As it has been predicted in (39), it is based on assumption of presence in the photosynthesizing cell of two isotopically different carbon flows resulting from CO_2 photoassimilation/photorespiration coupling. The third group comprises the facts indirectly confirming existence of PRCIE.

Let us consider arguments of the first group. The proposed model of PRCIE explains observed ^{12}C enrichment of ambient CO_2 in the gas exchange experiments and respective isotope depletion of biomass (131–135) through prevalence of PRCIE over that of CO_2 assimilation. According to the model, it takes place when some factors stimulating intense photorespiration result in the considerable exhaustion of photorespiratory carbon flow and in ^{13}C enrichment of photorespiratory metabolites. This metabolic shift in combination with a certain contribution of photorespiratory carbon flow to biomass synthesis can even reverse the sign of carbon isotope discrimination in photosynthesis, or, in other words, the ^{13}C enrichment of biomass versus assimilated CO_2. This is illustrated by drastic ^{13}C enrichment of alga biomass, which has been observed during its exposition in CO_2 enriched in ^{13}C (134,135). An additional confirmation of the impact of ^{13}C enrichment of ambient CO_2 on *Triticum aestivum* and *Phaseolus vulgaris* biomass was obtained in recently published work (150). The increase of ^{13}C carbon isotope ratio in ambient CO_2 caused respective decrease in ^{13}C discrimination, which the authors explained by activation of photorespiration.

In the same work, the authors investigated the impact of increased partial oxygen pressure (pO_2) on carbon isotope ratio of *T. aestivum* and *P. vulgaris* biomass. They found a distinct decrease in ^{13}C discrimination, i.e., ^{13}C enrichment of biomass at the same pCO_2 that was interpreted as the impact of photorespiration. This agrees with the results of a kinetic study of ^{14}C incorporation in glycine and serine (151), which shows that glycolate pathway is inhibited at low O_2 concentrations. The increase of the intracellular CO_2/O_2 ratio and the Rubisco affinity to CO_2 along with O_2 concentration decline was considered as a reason for photorespiration inhibition (152,153). Similar effects were also observed by Evans et

MARCEL DEKKER, INC.
270 Madison Avenue, New York, New York 10016

al. (88) in *Xantontium strumarum* leaves and by Smith et al. (154) in legume plants who found a 2‰ shift of ^{12}C enrichment in plant biomass when O_2 concentration increased from 4 to 21%. Ozone seems to have a similar influence on carbon isotope ratio of plant biomass (155).

However, some data showed the shift of the opposite sign in carbon isotope ratio of some C_3 plants under the same range of O_2 concentration (84). The proposed mechanism of photoassimilation/photorespiration coupling gives a possible explanation for this effect. The isotopic shift of biomass carbon caused by any factor is an integrated result of its impact both on CO_2 photoassimilation and photorespiration. Indeed, the growth of O_2 concentration makes the carboxylase phase of Rubisco function shorter and decreases depletion of cytoplasmic CO_2 pool. Hence, according to the CIF mechanism, this must result in ^{12}C enrichment of substrates. On the other hand, intensification of photorespiration due to the factor action should enhance its impact on biomass carbon isotope ratio via substrate pool depletion and must result in ^{13}C enrichment of photorespiratory products. The higher contribution to biomass isotopic balance determines the relative isotopic shift. This conclusion underlines the complexity of isotopic relations in photosynthesis. But in a common case because of an insignificant contribution of photorespiratory products to biomass versus that of the other metabolic pathways, the factors intensifying photorespiration bring about ^{13}C enrichment of biomass.

Similar results were obtained by studying the impact of water salinity on isotope composition of plant biomass. It is known that salinity stress stimulates photorespiration (156,157). In leguminous plants *Dolichos biflorus* L. and *Cicer arientinum*, salinity stress caused a sharp increase in the activity of glycolate oxidase, the key enzyme of glycolate chain (158). The increase of NaCl concentration in soil up to 50 mM enhanced oxygenase activity of Rubisco in wheat species *Triticum durum* and *T. aestivum* (159).

Guy et al. (87) found a close relationship between carbon isotope ratio and salinity of irrigation water for two C_3 halophytes *Salicornia europeae* subsp. *rubra* and *Puccinella nutaliana* (see Fig. 4, a and b). The changes in salinity presented by the corresponding changes of osmotic potential Ψ_s were followed by the proportional shifts in carbon isotope ratio. The same effect was observed for CAM halophyte *Disphina clavellatum* (Haw) Chinnock (Aisoaceae) (160). The isotopic shift of biomass carbon caused by salinity change was from -20.0 to -26.1‰. In *Plantago maritima* L. (121), salt stress caused 4‰ ^{13}C enrichment of leaf carbon even at elevated CO_2 concentration (up to 5%). In natural conditions, the salinity effect becomes apparent in the well-known ^{13}C enrichment of alga and plants growing in marine and saline marsh environments compared with those in fresh water reservoirs (161).

The above facts indicate the dominant contribution of photorespiration isotope effect to the observed isotopic shifts. But in some cases the shifts of the opposite sign with salinity were also found. The ^{12}C enrichment of marine alga *C.*

MARCEL DEKKER, INC.
270 Madison Avenue, New York, New York 10016

stigmatophora, which was about 3‰, observed an increase of NaCl concentration in the media from 0 to 595 mM/L (149). In wheat, the growth of salinity was not followed by proportional changes in carbon isotope ratio of biomass, but by shifts of the opposite sign depending on the type of wheat organ and ontogenetic stage (162,163). Such dependencies indicate that contribution of CO_2 assimilation CIE becomes comparable with that of photorespiration CIE. The possible mechanism of salinity impact on CIE of CO_2 photoassimilation is via reduction of cytoplasmic CO_2 pool because of the decrease in CO_2 solubility at higher salt concentrations causing the increase of exhaustion effect. The impact of salinity on CIE of CO_2 photoassimilation and photorespiration is of the same sign that can explain considerable isotopic shifts, which sometimes are observed although the variations of their contributions to the total isotopic shift may cause the interruption of the proportionality between salinity and isotopic shifts.

The well-known influence of water availability on carbon isotope ratio of plant biomass is also the result of its impact both on CO_2 photoassimilation and photorespiration CIEs. It was shown (120) that water deficiency was followed by the same metabolic shifts as those caused by the salt stress. It results in ^{13}C accumulation in biomass (164,165). When decreasing CO_2 access into the cell in CO_2 assimilation phase, water stress intensifies exhaustion of the cytoplasmic CO_2 pool and hence, increases ^{13}C enrichment of biomass. At the same time, water stress also intensifies photorespiration thus causing the additional ^{13}C enrichment of biomass. It might be the reason for considerable isotopic changes of plant biomass under drought conditions often observed in nature (166,167).

The second group (see above) comprises the facts supporting the crucial assumption of the model on the existence of two carbon flows differing from each other by carbon isotope ratio and the coupling mechanism. According to the latter, the flow arising in carboxylation phase of Rubisco function is enriched in ^{12}C and used to feed glycolytic chain during the dark period of photosynthesis, whereas the flow arising in oxygenation phase is enriched in ^{13}C. Both flows are separated in time and divided by cell compartments.

While summarizing the data on carbon isotope ratio of metabolites of different photosynthesizing organisms, it was noticed that metabolites, which might be referred to the assimilatory carbon flow, were enriched in ^{12}C, whereas those associated with the photorespiratory carbon flow are enriched in ^{13}C (39). In most of oxalate-accumulating plants, oxalate formed in glycolate chain is much more enriched in ^{13}C relative to biomass carbon (see Table 3) (146–148). The same effect was observed in CAM plants, including cacti (see Table 4), but the difference between carbon isotope ratio of leaf biomass and oxalates was less than in the previous case, which is likely due to the lower intensity of photorespiration in CAM plants.

In this context it is interesting to note that about thirty years ago geologists found a rare mineral in clay sedimentary rocks supposed to be of biogenic origin,

Table 3. Carbon Isotope Ratio of Leaf Biomasses and Oxalates of Some Oxalate-accumulating C_3 Plants (147). Values of $\delta^{13}C$ ‰ are Given in PDB Units

Plant Species	Whole Leaf	Oxalate
Spinacea oleracea	−27.5	−11.9
*Spinacea oleracea**	−25.7	−19.5
Pelagronium	−31.0	−12.4
Mereurialis perennis	−27.9	−13.7

* Data are taken from Rivera and Smith (146).

which had the chemical composition corresponding to $CaC_2O_4 \cdot H_2O$ (168). Its carbon isotope ratio ($\delta^{13}C$ was from +0.7 to +8.6‰) was dramatically different from that of all known organic matter, including an attendant organic matter ($\delta^{13}C = -23.2$‰). This fact was intensively discussed, but no explanation was found at that time. Basing on the proposed model, one can assume that the mineral consisted of oxalates derived from ancient oxalate-accumulating plants having intense photorespiration. After burial they transformed into this mineral.

Some of amino acids from the protein fraction of photosynthesizing microorganisms (92), such as glycine, serine, and alanine, in most cases were found to be enriched in ^{13}C compared with the other amino acids (Table 5) due to a high content of ^{13}C in their radical carbon. The observed ^{13}C enrichment of radical carbon in these amino acids could not be previously explained. The proposed mechanism and known metabolic pathways of their synthesis permits the supposition that the pools of these amino acids are (at least partially) supplied from the photorespiration chain. The mixing of carbon atoms in substrates due to transketolase and transaldolase reactions in Calvin cycle let the heavy isotope approach every site of the molecules causing finally the observed ^{13}C enrichment of radical carbon of the above amino acids.

Chlorophyll is known to be enriched in ^{13}C compared with the other cell components in plant leaves (79). It was also found that phorbin nucleus is the

Table 4. Carbon Isotope Ratio of Leaf Biomasses and Oxalates in Cacti (146). Values of $\delta^{13}C$ ‰ are Given in PDB Units

Plant Species	Whole Leaf	Oxalates
Echinomastus intertextus	−13.4	−7.3
Echinomastus horizonthalomus	−13.0	−7.8
Escobaria ruberoulosa	−12.3	−8.3
Opuntia euglemannii	−13.3	−8.5
Opuntia imbricata	−14.1	−8.7

Table 5. Carbon Isotope Distribution in Amino Acids of Protein Fraction Extracted From Biomass of Some Photosynthesizing Microorganisms (92). Isotopic Shifts are Given Relative to Nutrient CO_2 having $\delta^{13}C = 0‰$. Data adapted from Abelson and Hoering (92)

	Microorganism					
	Chlorella		*Chromatium*		*Euglena*	
Amino Acid	Carboxyl Carbon	Radical Carbon	Carboxyl Carbon	Radical Carbon	Carboxyl Carbon	Radical Carbon
Serine	−9.9	+2.5	−8.4	−2.8	−9.5	−6.1
Glycine	−23.3	−5.3	—	—	−14.9	−11.6
Alanine	−11.8	−7.3	—	—	−14.6	−13.8
Aspartic acid	−15.6	+2.2	−27.6	−15.9	−20.3	+1.0
Glutamic acid	−21.1	−8.8	−20.1	+2.2	−21.5	−0.2
Leucine	−26.0	−16.3	−23.7	−22.5	−25.6	−13.6
Lysine	−20.9	+2.5	—	—	−22.4	−24.8

heaviest part of the molecule (169). Considering that in a number of plants the phorbin nuclei are synthesized with the use of glycine formed in photorespiration (129,170), it is reasonable to explain the observed ^{13}C enrichment of chlorophyll by glycine participation in chlorophyll synthesis. The ^{13}C enrichment of oil and bitumen porphyrins discovered by geochemists (171,172) can only be inherited from chlorophyll, which is supposed to be the source of fossil porphyrins.

The results obtained by Kalinkina and Udelnova (142,149) are of special interest. The authors examined carbon isotope ratio of some fractions and metabolites in marine alga *C. stigmatophora* presenting simultaneously both assimilatory and photorespiratory pathways under salt stress and inhibitor action (see Table 6). It was proved (173) that proline and labile sugars related to the glycolate chain of photorespiratory pathway. On the contrary, proteins and lipids represent assimilatory pathways since their synthesis mostly occurs with the use of substrates of the carbon flow, which feeds glycolytic chain coupled with fatty acid synthesis and Krebs cycle in the dark period of photosynthesis (174,175).

As it follows from Table 6, under any conditions dried biomass of marine alga *C. stigmatophora* ($\delta^{13}C = 61.6‰$) and its proteins ($\delta^{13}C = 42.1‰$) are considerably enriched in ^{12}C compared with proline ($\delta^{13}C = -29.0‰$) and labile sugars ($\delta^{13}C = 30.0‰$) (142,149). A high content of ^{12}C in biomass agrees with the fact that alga biomass is rich in lipids having the lowest $^{13}C/^{12}C$ ratio (79,93). The synthesis of fatty acids and amino acids composing most of the lipid and protein fractions occurs in glycolytic phase of a cell cycle and is associated with glycolytic chain and Krebs cycle (92,175), whereas proline and labile sugars are formed in the glycolate chain in photorespiration (142,149). For this reason the discovered isotopic discrepancies may be regarded as confirmation of the exis-

Table 6. Effect of Salt Stress (NaCl) and Photorespiratory Inhibitors on Carbon Isotope Composition of Marine Alga *C. stigmatophora* Biomass and Some of its Components (149). $\delta^{13}C$ of Ambient CO_2 is −21‰. $\delta^{13}C$‰ Values are Given in PDB Units

	NaCl Content in Media, mM			
	0		595	
Identified Parameter	Without Inhibitors	HPMS* + INH**, mM	Without Inhibitors	HPMS + INH, mM
Biomass growth, mgM	3.5	1.7	2.4	1.4
Proline content	2.7	1.8	13.0	7.0
$\delta^{13}C$ of dried biomass	−61.6	−61.5	−64.5	−53.8
$\delta^{13}C$ of proteins	−42.1	−42.8	−47.3	−43.7
$\delta^{13}C$ of labile sugars	−30.0	−32.6	−30.5	−29.3
$\delta^{13}C$ of proline	−29.0	−29.4	−31.5	−30.5

Photorespiratory inhibitors: * HPMS (α-hydroxy-2-pyridinemethanesulfonate) and ** INH (isonicotinylhydrozide).

tence of two isotopically different and independent carbon flows emerging in photosynthesis. The closeness of carbon isotope ratio of proline and of labile sugars indicates that they belong to the same carbon flow, which passes Calvin cycle and glycolate chain.

The same results were obtained by studying quite different terrestrial plants of intermediate C_3-CAM type (176). Tables 7 and 8 show the data on carbon isotope ratio of some biochemical fractions isolated from leaves of *Clusia minor* L., which has been collected at dawn and dusk during wet and dry seasons. Accord-

Table 7. Carbon Isotope Ratio of Biochemical Fractions of Leaves of *Clusia minor* L. Collected During Wet Season. Naturally Exposed and Shaded Leaves were Collected at Dawn and Dusk (176). $\delta^{13}C$ Values are Given in PDB Units

		Exposed Leaves		Shaded Leaves	
n	Fractions	Dawn	Dusk	Dawn	Dusk
1	Dried biomass	−25.7		−30.3	
2	Structural components	−26.1	−27.2	−31.2	−31.8
3	Lipids, pigments	−28.2	−28.7	−33.3	−32.2
4	Amino acids	−30.2	−31.7	−32.0	−32.6
5	Soluble sugars	−23.6	−21.2	−30.5	−29.2
6	Organic acids	−20.6	−22.3	−27.6	−27.7
7	Glucans	−22.6	−22.3	−27.2	−27.6
8	Starch	−22.1	−22.3	−27.2	−27.8

MARCEL DEKKER, INC.
270 Madison Avenue, New York, New York 10016

Table 8. Carbon Isotope Ratio of Biochemical Fractions of Leaves of *Clusia minor* L. Collected During Dry Season. Naturally Exposed and Shaded Leaves were Collected at Dawn and Dusk (176). $\delta^{13}C$ Values are Given in PDB Units

		Exposed Leaves		Shaded Leaves	
n	Fractions	Dawn	Dusk	Dawn	Dusk
1	Dried biomass	−24.6		−29.1	
2	Structural components	−27.1	−27.5	−31.8	−31.0
3	Lipids, pigments	−27.1	−27.7	−30.8	−30.8
4	Amino acids	−31.2	−31.1	−32.4	−32.7
5	Soluble sugars	−20.4	−17.9	−24.3	−21.9
6	Organic acids	−17.6	−21.1	−21.8	−24.5
7	Glucans	−23.4	−21.6	−26.8	−23.6
8	Starch	−23.6	−23.1	−27.9	−26.6

ing to carbon isotope ratio values, two different groups of compounds can be distinguished. The first group includes amino acids and lipids, as in the case of *C. stigmatophora*, and structural components, whose synthesis is associated with glycolytic pathway substrates (177). Hence, the first group is composed of the components bound to the assimilatory carbon flow, and their carbon is enriched in ^{12}C in comparison with other components.

The rest of the components, including organic acids, glucans, starch, and soluble sugars, in accordance with their carbon isotope ratio and with possible ways of biosynthesis form the second group and belong to the photorespiratory chain. Indeed, in oxygenation phase of Rubisco function when glycolate chain and Calvin cycle form the common loop, carbohydrate components derived may be regarded as the products of photorespiration and must be enriched in ^{13}C. In the above case of *C. stigmatophora*, labile sugars exemplify these kinds of carbohydrates. Organic acids including C_4-dicarboxylic acids can be produced in glycolate pathway. They were extracted from vacuolar sap which gives the additional confirmation of their relation with photorespiration, since vacuoles are known to accumulate the products of photorespiration (170).

The difference in carbon isotope ratio found between biochemical fractions extracted from leaves of *Bryophyllum diagremontiana* Berger (145) can similarly be interpreted as an indication of the existence of two isotopically different carbon flows emerged in coupling of photoassimilation and photorespiration.

The results of the *Chlorella* cultivation experiments with the use of $^{14}CO_2$ lead to the same conclusion (134). Specific radioactivity (SR) of alga biomass was found to be higher than that of ambient CO_2 whereas SR of lipids, cellulose, and sucrose during the experiment remained far lower. SR of CO_2 expired in dark pe-

MARCEL DEKKER, INC.
270 Madison Avenue, New York, New York 10016

riod was two times less than SR of biomass. The decrease of starch content in the biomass during the dark period was followed by distinctive increase of its SR. Considering that the use of "heavy" CO_2 in photoassimilation can induce photorespiration and cause the inversion of the sign of carbon isotope discrimination, the above facts can be interpreted as follows. The enrichment of biomass in ^{14}C relative to the ambient CO_2 is an indicator of intense photorespiration, which results in CIE inversion. It means the existence of heavy carbon flow of photorespiration while depletion of lipids, cellulose, and sucrose in ^{14}C, low SR of CO_2 respired in dark, and changes of the starch content and of its SR during the night show that light carbon flow passes glycolytic chain and hence, is associated with assimilatory chain.

The following facts and phenomena can be included in the third group (see above). It was found that nitrogen assimilation (namely, the type of assimilating forms and their availability to organisms) influenced carbon isotope ratio of plant biomass (14,15). According to the proposed mechanism, the intensity of photorespiration directly depends on the malate-aspartate shuttle functioning in photorespiration chain (39) (see Fig. 8). The latter is determined by the availability of amino groups. The lack of amino groups in amination of oxaloacetate reduces shuttle rate and decreases photorespiration. As a result, the pool of photorespiration substrates increases to a larger extent thus decreasing the exhaustion of photorespiratory substrate pool and hence, diminishing Releigh effect and ^{13}C enrichment. It is clear that amino group availability depends on nitrogen assimilation.

Many researchers have found a strong positive correlation between bioproductivity of wheat and ^{13}C discrimination when plants were irrigated well (8,67,68,163,178). Although grown under identical conditions, more productive wheat was enriched in ^{12}C (see Fig. 9). But in drought conditions, the proportionality was sometimes interrupted or the sign of correlation changed to the opposite (8,68). The above correlation dependence on water availability is difficult to explain by isotope effect of CO_2 assimilation as the sole reason of CIF, but it is possible to connect it with photorespiration.

Indeed, if water availability is high and leaf stomata are entirely open, CIE of CO_2 photoassimilation is maximal and the difference in carbon isotope ratio of plant biomass is conditioned by CIE of photorespiration. The plants with higher photorespiration must have ^{13}C-enriched carbon isotope composition and less grain gain, which corresponds to positive correlation. At low water availability when stomata are nearly closed the grain gain will be limited by availability of CO_2 entering the cells. By taking the same enzymatic fixation rate (179), the degree of cytoplasmic CO_2 pool depletion in the carboxylating phase of RuBP activity must be higher resulting in ^{13}C enrichment of the assimilated carbon (biomass). The higher the pool depletion degree, the more grain gain must be observed and hence, a negative correlation between carbon isotope ratio of wheat biomass and grain gain must occur.

MARCEL DEKKER, INC.
270 Madison Avenue, New York, New York 10016

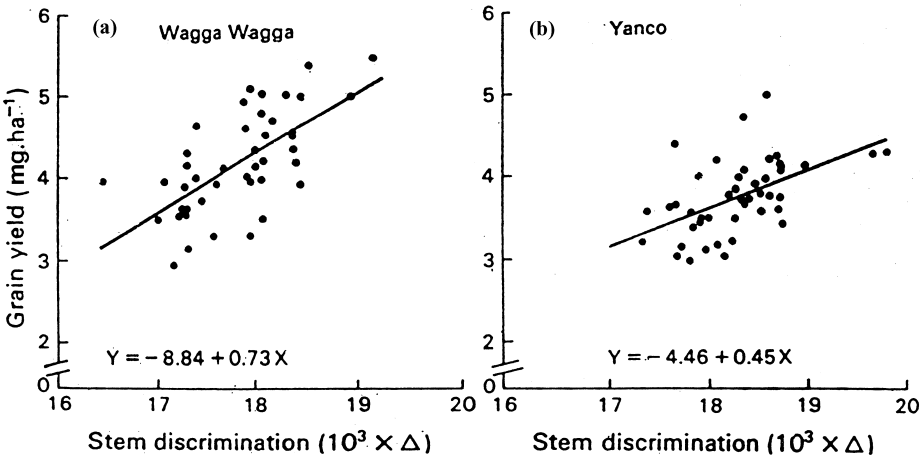

Figure 9. Relationships between grain yield (mg ha^{-1}) and carbon isotope discrimination (Δ) of stem material determined by results of 1984 field trials at Wagga Wagga (a) and Yanco (b). Reproduced from Condon et al. (68) with permission.

It was also noted (66,164), that spring wheats are usually enriched with ^{12}C (about 1 −2‰) compared with winter wheats (see Table 9). Considering that the latter have a more intense photorespiration to maintain their metabolism at low temperatures (170), it may be the reason for the observed isotopic discrepancies. This hypothesis is supported by the temperature effect of carbon isotope ratio of

Table 9. Dependence of Leaf Isotopic Composition on Watering and Temperature Conditions During Growth of Spring and Winter Wheat (65). δ^{13} C‰ Values are Given in PDB Units

	Continuous Watering		Night Watering
Culture	t = 25 − 20°C	t = 4 − 2°C	t = 25 − 20°C
Spring Wheat			
"Marquis"	−32.8	−31.6	
"Opal"	−32.7	−31.7	
"Kolibri"	−33.0	−29.7	−24.6
Winter Wheat			
"Kharkov"	−31.9	−30.2	−20.2
"Frederik"	−31.3	−29.0	
"Norstar"	−31.7	−29.9	

plants. Barley shoots grown at 18/10°C (light/dark) or 29/21°C had isotopic compositions of −28.2 and −28.8‰, respectively (155). The $\delta^{13}C$ values of tomato plants when grown at 17°C appeared to be by 3‰ less negative than at 32°C (164).

It is known that the mature leaves of plants are enriched in ^{13}C compared with the young ones (180–182). This fact is in agreement with intensification of oxygenase activity of Rubisco and hence, photorespiration in leaves with age (170). The contribution of photorespiration products to biomass increases accordingly. This fact is supported by the regular ^{13}C enrichment of stem and flag leaf biomass at the later ontogenetic stages and by typical isotopic differences of leaf, stem, and seeds (163). The latter are a result of the differences in the contribution of CO_2 photoassimilation and photorespiration to biomass synthesis at the stages when corresponding organs are formed. Seeds are mostly enriched in ^{13}C compared with stems and leaves because the ripening stage is the late one.

The ^{13}C gradient along the stem, which has been found in wheat at different conditions (see Table 10), is more evidence of correlation between isotopic changes and photorespiration contribution to metabolism in ontogenesis. Since the growth of the wheat stem proceeds from the bottom, the newly formed biomass is mostly accumulated in the lower part of the stem whereas previously formed biomass is concentrated in the upper one. Such distribution of biomass along with its relation to photorespiration changes in ontogenesis determines the observed gradient of ^{13}C.

Therefore, numerous facts, both direct and indirect, are in a good agreement with the hypothesis on CIE of photorespiration and with the proposed mechanism of its coupling with CO_2 photoassimilation. This permits us to formulate the following assertions. Two contours of carbon flows emerging in photosynthesis are coupled via double Rubisco function. When the enzyme works as carboxylase, CO_2 assimilation contour is in operation. Due to CIE in RuBP carboxylation, the carbon flow circulating in the contour is enriched in ^{12}C. When it works as oxygenase, the photorespiration contour is active. CIF in glycine decarboxylation results in ^{13}C enrichment of carbon flow circulating inside. The main feature of CIF in both cases is the combination of isotope effects with exhaustion effect (Releigh effect). This is the result of periodicity and of discreteness of carbon flows in the

Table 10. Gradient of Carbon Isotope Ratio ($\delta^{13}C$, ‰) Along Stem of Wheat "Zvezda" Under Different Irrigation Conditions (162,163)

Stem	Natural Irrigation	Artificial Irrigation, 0.2 M NaCl Solution	Artificial Irrigation, 0.5 M NaCl Solution
Bottom	−24.3	−24.7	−25.4
Middle	−24.4	−26.7	−26.0
Top	−25.2	−26.8	−27.5

contours caused by alternating functions of Rubisco. It also causes the dependence of isotopic discrepancies of metabolites on the degree of exhaustion and in some cases can provide their considerable increase.

Experimental data show that carbon flows in both contours are autonomous, i.e., no considerable mixing occurs. The switching over of the Rubisco functions is under the control of external and internal factors thus providing the adaptation of organism to the surroundings. The most probable way of this control is the impact of the above factors on CO_2/O_2 ratio in the cell. Carbon isotope discrimination in photosynthesis is an integrated result of CIE of CO_2 photoassimilation and that of photorespiration having the opposite signs. In cases when the combination of factors is most favorable for intense photorespiration, the ^{13}C discrimination in photosynthesis can change to ^{12}C discrimination.

According to the model and corresponding isotopic data, the coupling of photosynthesis (light phase) with respiration metabolism, which coincides with the dark phase, is realized through the carbohydrates (mostly starch) accumulated in assimilatory contour in carboxylation phase of Rubisco functioning. It leads to the ^{12}C enrichment of all metabolites synthesized in glycolysis including most of the lipids and amino acids whose isotopic composition thus reflects CIE of CO_2 assimilation.

On the Possibility of the Use of CIF Concept in Photosynthesis to Study Photosynthesis Physiology and to Solve Some Problems of Biochemical Adaptivity

Taking into consideration the close relationship between isotopic and metabolic shifts under action of environmental factors, the proposed mechanism of coupling of CO_2 photoassimilation and photorespiration can be used as a tool to study photosynthesis physiology and biochemical adaptation. In spite of the lack of the data available, some examples illustrating the approach can be presented after some preliminary notes are done. Interpretation of the isotopic data of photosynthesis in the frame of the above concept requires accounting for the kinetic nature of CIE of RuBP carboxylation and glycine decarboxylation. This feature makes these effects dependent on the rate-limiting stage of the reactions and hence, on cell conditions (pH, ionic strength, presence of cofactors, etc.). Moreover, although the effects are very important points of isotope fractionation mechanism of photosynthesis, they are not the sole reason of isotopic discrepancies of metabolites. The latter depends on the degree of substrate pool depletion, and hence, different factors controlling carbon flows in a cell via Rubisco activity can influence isotopic shifts of the metabolites. It is clear that because of the influence of numerous factors, the interpretation of isotopic data should be comprehensive and careful.

Marcel Dekker, Inc.
270 Madison Avenue, New York, New York 10016

The data extracted from Tables 7 and 8 and collected in Table 11 illustrate the close relationship of carbon isotope ratio of labile sugars and organic acids bound to photorespiratory flux. Labile sugars synthesized mainly in photorespiration are considered to be the source of organic acids formed in dark, including C_4 acids derived from PEP by C_4 fixation of CO_2. Their close relationship is confirmed not only by the closeness of their isotope composition, but also by parallel isotopic shifts in diurnal cycles. It becomes particularly clear when carbon isotope ratio of labile sugars at dusk and that of organic acid at dawn are compared. Small differences in their isotope ratios observed at a certain time of wet season is explained by the night fixation of exogenous CO_2, which is more enriched in ^{13}C versus CO_2 acceptor, phosphoenolpyruvate derived from labile sugars. The absence of such differences during dry season means that as a form of adaptation to drought conditions, the plants re-assimilate at night CO_2 evolved in dark respiration having the same isotopic ratio as acceptor.

The data presented in Table 11 also show that during wet season in the shaded leaves, the role of photorespiration and CAM metabolism is minimal and, on the contrary, C_3 assimilation is preferential. It leads to considerable ^{12}C enrichment of both labile sugars and organic acids in exposed and shaded leaves. At the same time, the decrease of photorespiration is manifested in small differences of carbon isotopic ratio of labile sugars at dawn and dusk. The presence of CAM metabolism in all other cases can be illustrated by notable ^{13}C enrichment of organic acids at night (from dusk to dawn)

In the experiments with marine alga *C. stigmatophora* (149) (see Table 6), the use of photorespiration inhibitors (HPMS + ING) in fresh water did not exert any distinct impact on carbon isotope ratio of metabolites, whereas under salt stress they caused a considerable ^{13}C enrichment of biomass. It drew the authors to the conclusion that photorespiration CIE was of the same sign as CO_2 assimilation effect. However, the data on carbon isotope composition of metabolites be-

Table 11. Diurnal (daily) Isotopic Variations of Organic Acids and Soluble Sugars Isolated from Leaves of *Clusia Minor* Taken at Different Exposition Under Wet and Dry Conditions (176). All $\delta^{13}C$ Values are Given in PDB Units

	Exposed Leaves		Shaded leaves	
	Dawn	Dusk	Dawn	Dusk
Wet season				
Soluble sugars	−23.6	−21.2	−30.5	−29.2
Organic acids	−20.6	−22.3	−27.6	−27.7
Dry season				
Soluble sugars	−20.4	−17.9	−24.3	−21.9
Organic acids	−17.6	−21.1	−21.8	−24.5

MARCEL DEKKER, INC.
270 Madison Avenue, New York, New York 10016

longing to assimilatory and photorespiratory carbon flows led to another explanation for the above fact. As seen from Table 6, the observed ^{13}C enrichment of biomass is associated with the ^{13}C enrichment of proteins and probably lipids, which belong to assimilatory flow but not to the photorespiratory one. It means that isotope fractionation in assimilatory contour is reduced. The reason for that is the increase of the CO_2 cytoplasmic pool depletion as the result of action of inhibitors that leads to the prolongation of carboxylase phase of Rubisco function. Carbon isotope ratio of photorespiration products remained at the same level, since photorespiration was reduced and no essential contribution of newly formed compounds to biomass occurred.

The data presented in Tables 7 and 8 illustrate the relationship of the metabolic and isotopic shifts in response to the environmental factors, which are known to induce photorespiration including intensity of impinging light. The growth of light intensity leads to an increase of CO_2 assimilation and is followed by pH growth in chloroplasts (183). It facilitates the oxygenase activity of Rubisco and glycolate accumulation to compensate pH change. At the same time the carboxylase activity is suppressed. The data given in Tables 7 and 8 show that regardless of wet or dry season conditions, ^{13}C enrichment of *Clusia minor* biomass occurs. For the plant having intermediate C_3-CAM assimilation, two possible reasons for the observed enrichment can be distinguished: 1) induction of C_4 assimilation and 2) induction of photorespiration. To understand the role of each of these factors one needs to consider the isotopic shifts of components related to assimilatory and to photorespiratory fluxes. As has been shown (176), under wet season conditions only C_3 assimilation in shaded leaves is active. This means that the isotopic differences between components of both fluxes under those conditions can be ascribed only to photorespiration and are about 4–5‰. For the light-exposed leaves under the same conditions, the biomass carbon is more enriched in ^{13}C than that of the shaded leaves (see Table 7). It is followed by simultaneous enrichment in heavy carbon isotope of both fluxes and by the growth of difference between them of 7–8‰. The first fact confirms the contribution of C_4 assimilation pathway to biomass synthesis, while the second one indicates an increase of photorespiration.

The situation observed during dry season is close to the previous one. The light exposition causes ^{13}C enrichment of both carbon fluxes circulating in photoassimilatory and photorespiratory contours. This enrichment reflects the contribution of both photorespiration and C_4 assimilation. An even more pronounced difference between components of assimilatory and photorespiratory fluxes (in comparison with the previous case) shows that the role of photorespiration increases. In this regard, it must be emphasized that the well-known midday decline of photosynthetic activity (184) followed by reduction of ^{13}C discrimination (185) can be explained by enhancement of photorespiration caused by a more intense light flux in the afternoon.

The salinity of irrigating water is known to intensify photorespiration (159). Different authors (158,186) reported the activation of glycolate pathway enzymes under salt stress conditions. Although most of the researchers who studied the impact of salinity on CIF found ^{13}C enrichment of biomass with increase of salt concentration (87,160), the opposite sign of isotopic shifts was also reported (142,163). The data of Table 6 illustrate the isotopic response of marine alga *C. stigmatophora* to salinity stress comparing carbon isotope ratio of compounds from assimilatory and photorespiratory fluxes. This comparison shows that the observed ^{12}C enrichment of biomass is equal to $\sim 3‰$. It is mainly conditioned by the corresponding shifts of metabolites from assimilatory flux, whereas the isotope ratio of photorespiration metabolites remains unchanged. Moreover, the isotopic shift of biomass is of the same sign and its value is close to that of the isotopic shift of proteins. Because synthesis of amino acids is mainly bound to Krebs cycle, one can assume that Krebs cycle actively participates in adaptation of *C. stigmatophora* to salt stress.

Water availability is another environmental factor that strongly influences the carbon isotope ratio of plant biomass [15,19,187]. The lack of water causes ^{13}C enrichment of biomass carbon. The role of CO_2 assimilation and photorespiration in the observed shifts is still unclear but some authors report enhancement of photorespiration and decline of carboxylase activity of Rubisco under drought conditions (19,188,189). The data of Tables 7 and 8 confirm these observations. They show that both in cases of exposed and shaded leaves, the lack of moisture is followed by considerable ^{13}C enrichment of photorespiration metabolites whereas the carbon isotope ratio of components of assimilatory flux remains the same. This indicates that photorespiration intensifies.

The above examples show that isotopic discrepancies emerging in photosynthesis along with proposed biophysical mechanism of CIF in photosynthesis can be used as a delicate tool to study structure of photosynthesis process, its regulations and physiology, and also the problems of biochemical adaptation. Carbon isotope analysis also provides useful information on dark respiration metabolism and its coupling with photosynthesis. These data are necessary to study CIF in respiration metabolism and related problems, which are considered below.

CIF IN RESPIRATION METABOLISM

General Background

In 1960, Park and Epstein (190) when studying the carbon isotope ratio of plant biomass discovered that lipids were distinctively enriched in ^{12}C compared with other biomass fractions. Later the same effect was observed by other authors not only in plants but in other organisms (191,192) including heterotrophic ones

MARCEL DEKKER, INC.
270 Madison Avenue, New York, New York 10016

(231,140,193). It was also found that individual metabolites are different by carbon isotope composition (194–197). Abelson and Hoering (92) established intramolecular carbon isotope heterogeneity of alga biomass. It was proved later (198–202) to be an essential and universal property of the living matter. Some general regularities in cellular and intramolecular carbon isotope distribution, which were found to be common both to photosynthesizing and heterotrophic organisms regardless of their positions on ontogenetic stairs (203,204) drew to the conclusion that the isotope fractionation responsible for it occurred in respiration* metabolism. The question was what was the probable mechanism providing such an isotopic pattern.

There was a hot and long discussion in the literature on the nature of isotope effects arising in respiration metabolism and on the points where isotope fractionation occurs. Galimov et al. (169,198,206,207) asserted that carbon isotope distribution was of a thermodynamic nature and the mechanism in a cell was isotope exchange in enzymatic reactions. However, most of the researchers considered the isotopic order of metabolites to be of a kinetic nature, i.e., to be dependent on reaction conditions in cell and metabolic pathways (141,182,208,209). The experimental data completely proved that thermodynamic conception was wrong. Its predictions fail to explain the real carbon isotopic order in most biological molecules (141,208,210) and recent works (33,148,211–213) give more evidence for this.

The supporters of the kinetic approach had different standpoints on the role of concrete cell reactions in the observed carbon isotope distribution in living matter. Since 1960, Park and Epstein (190) and many others (33,140,199–201) admitted a dominant role of pyruvate decarboxylation CIE in ^{12}C enrichment of lipids. To explain isotopic discrepancies of biochemical fractions and individual metabolites, some authors (93,161) assumed the existence of numerous CIF barriers in a cell associated with different metabolic pathways. Among them, CIF in mutual transformations of carbohydrates, proteins, and fatty acids, in respiration, associated with Krebs cycle, and in lipid-carbohydrate turnover were named. However, neither concrete points of isotope effects emergence nor possible mechanisms for that have been suggested. Having examined photosynthesizing microorganisms, Abelson and Hoering (92) have assumed that isotopic differences of metabolites are associated with different CO_2 assimilation pathways. Doubt is shed on this hypothesis by the observation of the isotopic differences in heterotrophic biomass.

*Respiration metabolism is considered to unite all the processes occurring in glycolysis phase of cell cycle as it has been formulated by Hayes and Monson (199), including glycolysis itself, pyruvate decarboxylation, fatty acid synthesis, Krebs cycle, and all attached syntheses.

MARCEL DEKKER, INC.
270 Madison Avenue, New York, New York 10016

The author has developed another approach (38,203,204) based on the assumption that the CIE of pyruvate decarboxylation is the ruling factor in respect to CIF in the whole cell. This effect influences the carbon isotope ratio of not only lipids but practically every metabolite throughout the cell. The suggested mechanism does not exclude from consideration the other points of possible isotope fractionation in the cell but ascribes to them a subordinate role. To simplify the analysis of such a complex system as a cell, we have tried to avoid additional conjectures if they are not necessary to explain the facts that the pyruvate decarboxylation hypothesis fails to explain. Following this reasoning, we found that CIE in pyruvate decarboxylation was enough to describe the principal features of ^{13}C distribution in a cell. Hence, this effect was considered to play the key role in CIF proceeding in a cell. We believe that future studies may help to refine this idea but not to revise. The following discussion supports this assertion.

Modeling of CIF in Respiration Metabolism. Main Postulates and Features

The model is based on three main postulates: 1) the isotopic distribution of metabolites is determined by the pathways of their biosynthesis; 2) the observed carbon isotope heterogeneity of biomass in most organisms is basically related to the isotope effect of pyruvate decarboxylation occurring in their cells; and 3) the fractionation of carbon isotopes in this reaction proceeds under conditions of the substrate pool depletion. The biophysical basis of the model is the cyclicity of metabolic processes. The full cell cycle consists of two alternating phases: glycolysis and gluconeogenesis. Such organization of cell cycle is necessary to regulate energy metabolism in a cell (214–217).

According to this hypothesis carbon flow in glycolytic phase decreases. Carbohydrate pool of the cell is depleted. Lipids and proteins are formed. In the gluconeogenetic phase, carbon flow increases. In plants and photosynthesizing organisms, carbohydrate pool is restored due to newly formed starch in Calvin cycle and partly because of degradation of lipid and protein pool into heterotrophs due to nutrient exogenous substrates coming in. Hence, in glycolytic chain of a cell, reciprocal vibrations of carbon flow take place. The cyclicity of metabolic processes is a necessary condition to stabilize regulation of the energy metabolism. The reswitch from glycolysis to gluconeogenesis and back is provided by the presence of fructose bisphosphate futile cycle in the glycolytic chain. The vibration period depends on many factors among which the sizes of carbohydrate and lipid pools are the most important. They control the switch of the futile cycle and hence, the direction of carbon flow (214,215). It is obvious that the full cell cycle consisting of the time of glycolysis and gluconeogenesis may be different for various types of cells. For most of the eucaryotic cells, the full cycle varies

MARCEL DEKKER, INC.
270 Madison Avenue, New York, New York 10016

from several to 24 h (215). Before considering the CIF mechanism in a cell, it needs to be emphasized that the mechanism can explain only the principal features of carbon isotope distribution in biomass, determined by CIE in pyruvate decarboxylation and by central metabolic pathways, but not the peculiarities of distribution depending on the metabolic pathways of the concrete organism. Taking the above into account, the mechanism of CIF can be described by the scheme shown in Fig. 10.

In the gluconeogenetic phase, the carbohydrate pool of photosynthesizing cells is filled with starch formed from the glucose synthesized in Calvin cycle. The carbohydrate pool of heterotrophic cells is filled with glycogen formed or taken from the nutrients. A part of carbohydrate pool is formed from glucose resynthesized in the course of lipid and protein-carbohydrate exchange. To simplify the examination of ^{13}C distribution caused by pyruvate decarboxylation CIE, the glucose from starch (glycogen) pool at the beginning of glycolysis is supposed to have even ^{12}C distribution, i.e., all glucose carbon atoms are of the same isotope ratio.

In the glycolytic phase the starch (glycogen) pool of cells stops to feed the glycolytic chain with substrates. An increase of glucose-6-phosphate and especially of fructose 1,6-bisphosphate concentrations makes fructose 1,6-bisphosphate a futile cycle to run in the direction of C_3 fragments (phosphoglyceric acid, phyosphoenolpyruvate, lactate, and pyruvate) formation. It strongly activates phosphofructokinase and inhibits fructose-biphosphatase (214,215). The above "events" are supposed to result first in the filling of the C_3 fragment pool. Then, in the course of pyruvate decarboxylation, the pool is depleted to provide substrates for biosynthetic and energetic needs of the cell. Taking into account a possible CIF in the reaction and its position at the crossing of the central metabolic pathways (see Fig. 10), the reaction is supposed to be the key element of the mechanism of carbon isotope distribution in the cell.

Hence, the periodic exhaustion of C_3 fragment pool combined with pyruvate decarboxylation CIE in the course of the reaction must lead to the formation of reaction products (CO_2, and acetyl-CoA including C_3 fragments) periodically changing their carbon isotope ratio. According to the theory of kinetic isotope effect (218), it occurs due to the change in carbon isotope ratio of particular atoms of the reaction products located at the breakage points of C—C bonds. Moreover the exhaustion of the substrate pool must be followed by the accumulation of ^{13}C in the above positions of residual C_3 fragments. This results in uneven ^{13}C intramolecular distribution of C_2 and C_3 fragments changing in the cell cycle. Hence, the metabolites formed from reaction products at different stages of pool depletion must have different carbon isotope ratio. The final isotope distribution in cell metabolites will be determined by the specificity of biochemical interactions and metabolic pathway pattern. Carbon fragments synphasically synthesized in exhaustion/refilling cycles of pyruvate pool must have close carbon isotope ra-

MARCEL DEKKER, INC.
270 Madison Avenue, New York, New York 10016

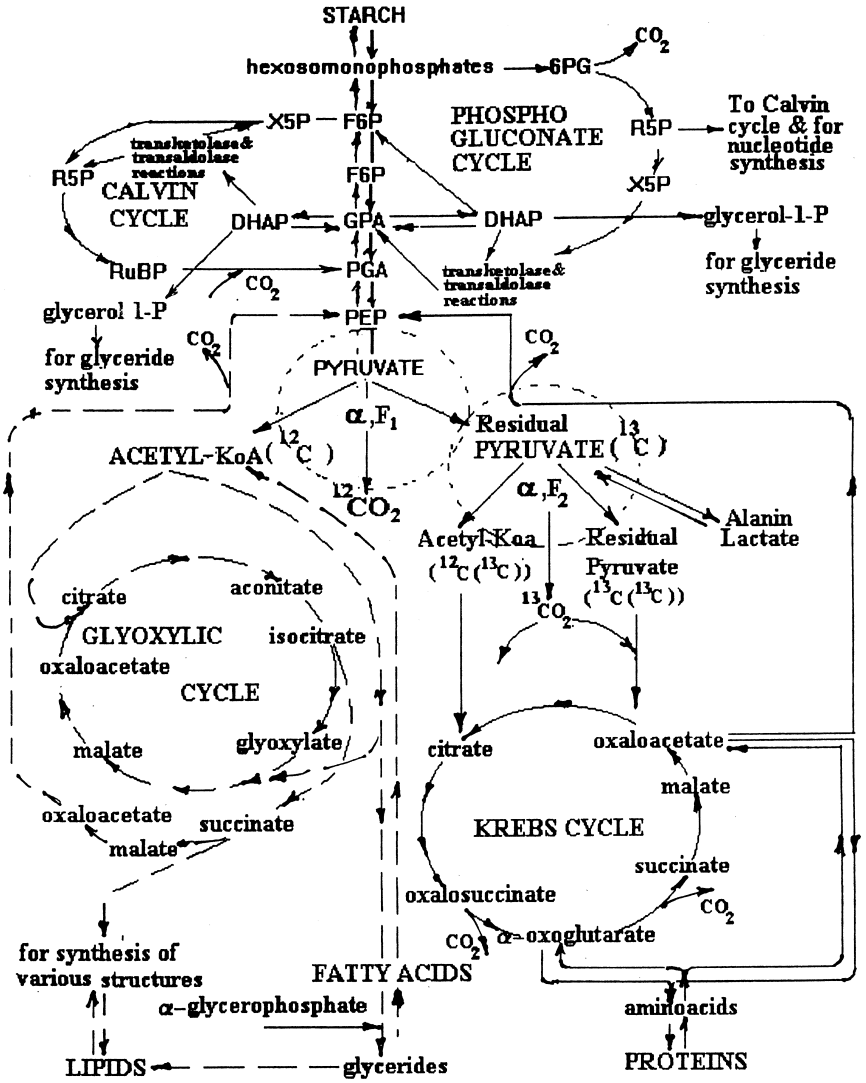

Figure 10. Schematic representation of carbon isotope distribution in secondary metabolism of photosynthesizing cell (for heterotrophic cell both Calvin and glyoxalate cycles must be excluded from consideration and starch must be substituted with glycogen). Carbon flows formed by C_3 (solid line) and C_2 (dashed line) fragments. The dotted line denoted point of carbon isotope fractionation in pyruvate decarboxylation (see text). X5P, xylulose-5-phosphate; R5P, ribose-5-phosphate; RuBP, ribulose 1,5-bisphosphate; 6PG, 6-phosphogluconate; F6P, fructose 6-phosphate; FBP, fructose 1,5-bisphosphate; PGA, phosphoglyceric acid; DHA-P, dihydroxyacetone phosphate; PEP, phosphoenolpyruvate.

MARCEL DEKKER, INC.
270 Madison Avenue, New York, New York 10016

tios and as being included in cell synthesis they determine observed constancy of metabolites carbon isotope ratios in respective functional states.

Experimental Data Supporting Proposed Model of CIF in Respiration Metabolism

Let us discuss now the postulates, which have been used to construct the model. The postulate asserting the link of carbon isotope distribution of metabolites with their synthesis pathway was formulated for the first time by Abelson and Hoering (92). This postulate seems to be obvious as it has been confirmed by many authors (33,40,41,141,148,211,213). We will begin our consideration from the second postulate: the pyruvate decarboxylation CIEs is the basic reason for the appearance of isotope heterogeneity in the cell. A principal possibility for the existence of CIEs in the reaction of enzymatic decarboxylation of pyruvate has been demonstrated by experiments in vitro (139,219,220). Results of one of them are presented in Table 12. The kinetic nature of the effect is confirmed by the observed isotopic shifts in the very positions predicted by the theory, namely at the cleavage point of C—C bonds (218,221), such as carbonyl carbon atom in acetyl-CoA (C_2 fragments), carboxyl and related carbonyl carbon atom in the residual substrate (C_3 fragments) of reaction products. The methyl carbon atoms of the C_2 and C_3 fragments save their isotope composition practically unchanged (see Table 12).

The pyruvate decarboxylation occurs at the crosspoint of the main metabolic pathways and C_2 and C_3 fragments are used as structural units in synthesis of nearly all cell metabolites. From the above mechanism of in vivo CIF, it

Table 12. Carbon Isotope Fractionation Observed in Enzymatic Pyruvate Decarboxylation with Enzyme Isolated from Yeast Under Different Reaction Conditions (140). $\delta^{13}C$ Values are Given in Per Mill Relative to PDB Standard

		$\delta^{13}C$ ‰		
No. Exp.	Experimental Conditions	Acetaldehyde		CO_2
1	100% reaction conversion	−20.6		−22.5
2	0.5% reaction conversion, 15°C	−26.5		−28.1
3	1.4% reaction conversion, 25°C	−28.5		−28.8
4	0.8% reaction conversion, 35°C	−30.2		−30.2
		methyl	carbonyl	
5	100% reaction conversion	−20.1	−19.9	−22.3
6	1.9% reaction conversion, 25°C	−21.1	−34.0	−28.8

Table 13. Carbon Isotope Composition of Lipids Formed by Fermentation of Different Substrates (140). $\delta^{13}C$ Values are Given in Per Mille Relative to PDB Standard

Substrate	Source Carbon $\delta^{13}C$	Lipids $\delta^{13}C$	Isotopic Shift $\Delta^{13}C$
Glucose	−9.5	−15.7	−6.2
		−16.3	−7.8
$CH_3COCOONa$	−20.5	−28.9	−8.4
CH_3COONa	−20.1	−21.5	−1.4
		−20.7	−0.6

$\Delta^{13}C = \delta^{13}C_{lip} - \delta^{13}C_{subs}$, where $\delta^{13}C_{lip}$ and $\delta^{13}C_{subs}$ are the isotope compositions of lipids and substrates, respectively.

is easy to predict the intramolecular heterogeneity of metabolites determining their isotopic differences as well as the differences of biochemical fractions. The analysis of isotope distributions in a series of metabolites (72,205) has shown a good agreement between theoretically expected and experimentally observed isotope distributions.

The direct experimental confirmation of the key role of CIE of pyruvate decarboxylation was first obtained for lipids (140). DeNiro and Epstein (140) proposed an original route to check the hypothesis: to block the entry of C_2 fragments from glycolytic chain by introducing them from outside of the cell when using exogenous acetate. In this way, the influence of the above effect on the carbon isotope composition of lipids (if it really exists) is eliminated. *Escherichia coli* bacterium was chosen for experimental examination because of its ability to grow both on glucose and pyruvate metabolized through the glycolytic chain, whereas in the presence of exogenous acetate it preferentially uses acetate formed in pyruvate decarboxylation.

By cultivation of *E. coli* in glucose and pyruvate media it was found (see Table 13) that isotopic composition of the lipids is enriched in ^{12}C versus carbon of the substrates by 6–9‰. By cultivation in the acetate medium the isotopic composition of the lipids was close to that of the substrate. Hence, the results are in an agreement with what might be expected from the model.

A somewhat different approach to prove the influence of pyruvate decarboxylation isotope effect on fatty acids (the main part of lipid fraction) was used by Monson and Hayes (141). They showed (see Table 14) that the intramolecular distribution of carbon isotopes in fatty acids isolated from *E. coli* lipid fraction was exactly the same as it is to be expected from the synthesis of fatty acids by condensation of C_2 fragments according to the "head-to-tail" principle. Bearing in mind the above mentioned uneven intramolecular isotope distribution of C_2 fragments having methyl atoms unchanged in CIE of pyruvate decarboxylation and carbonyl atoms subjected to isotopic shifts, one can expect that atoms in even po-

MARCEL DEKKER, INC.
270 Madison Avenue, New York, New York 10016

Table 14. Distribution of Carbon Isotopes in Fatty Acids of Lipid Fraction of *E. coli* Grown on Glucose of Known Isotope Composition ($\delta^{13}C_{gl} = -9.96‰$, N is Ordinal Number of Carbon Atoms) (141). $\delta^{13}C$ Values are Given in Per Mille Relative to PDB Standard

Fatty Acids		Total Carbon $\delta^{13}C$ ‰	Old Atoms		Even Atoms	
			N	$\delta^{13}C$ ‰	*N*	$\delta^{13}C$ ‰
Myristic	14 : 0*	−13.75	1	−27.1		
Palmitic	16 : 0	−12.23	1	−15.2		
Palmitoleic	16 : 1	−13.01	1	−19.2		
			9	−16.0	10	−9.5
9,10-Methylene-palmitic	17 : cycle	−13.71	1	−20.3		
Vaccenic	18 : 1	−12.58	1	−13.9		
			11	−15.8	12	−9.5

* Total number of carbon atoms : number of double bonds.

sitions of fatty acid skeletons must have a carbon isotope ratio close to that of ambient substrate whereas atoms in odd positions must change their carbon isotope ratio. Data of Table 8 are in full agreement with theoretical expectations and give strong evidence in favor of the concept under consideration.

However, some authors (140,141) considered that the action of pyruvate decarboxylation CIE is reduced to lipids. To prove the universal role of CIE we carried out experiments with *Corynebacterium* to investigate its influence on the distribution of carbon isotopes in some amino acids. The idea of this series of experiments was identical to that described above to block pyruvate decarboxylation by substituting carbohydrate substrates with acetate to check whether this resulted in shifts in isotopic patterns of amino acids. It should be underlined that in spite of completely different pathways of lipid and amino acids biosynthesis (222,223), they have the same source of the structural units. In the absence of an exogenous source of C_2 fragments, they are produced by pyruvate decarboxylation reaction metabolizing substrates coming from glycolytic chain and would undergo isotopic shift as compared with ^{13}C distribution of substrate. In case of partial or full substitution of carbohydrate substrate with acetate, the shifts are to be either less or must disappear at all. Hence, the observed shifts in the intramolecular isotope distribution of amino acids in the above experiments might confirm the influence of pyruvate decarboxylation CIE on isotopic composition of protein components.

As seen from Table 15, cultivation of *Brevibacterium flavum* E-531 on carbohydrate substrate (molasses) the carboxyl carbon in lysine produced by bacterium is enriched in ^{12}C versus total carbon of amino acids by 6.3‰. Cultivation on molasses with addition of acetate resulted in reduction of ^{12}C enrichment to 2.7‰. In the cultivation of *Corynebacterium glutamicum* 3144 on molasses, the

bacterium produced glutamic acid with the carboxyl group enriched in ^{13}C by 7.4‰. Complete substitution of molasses with acetate changed the sign of enrichment. Thus, carboxylic group of glutamic acid became enriched in ^{12}C by 2.7‰ as it was observed in experiment with *B. flavum* in the case of acetate addition to molasses. The total isotopic shift of carboxyl carbon of glutamic acid caused by the change of substrate was 10.1‰. Identical carbon isotope ratio of carboxyl carbon found in amino acids produced by bacteria on acetate substitution led to the conclusion that in both cases the carbon isotope distribution of amino acids was determined by the isotope distribution of acetate. Different signs of carboxyl carbon enrichment in ^{13}C for lysine and glutamic acid in cases when bacteria were grown on molasses confirms the first postulate (see above) on the relationship between carbon isotope distribution and metabolic pathways.

The results obtained support the hypothesis about dependence of isotopic composition of the protein fraction components and that of the lipid components on the isotope effect of pyruvate decarboxylation. Note that isotopic composition of carbohydrate components must also depend on this effect via lipid-carbohydrate and protein-carbohydrate exchange. Therefore, one can infer that pyruvate decarboxylation actually plays a key role in the cell distribution of carbon isotopes and hence, the validity of the second postulate of the model appears to be confirmed.

Let us consider the third postulate of the model: pyruvate decarboxylation in vivo proceeds by depletion of pyruvate pool. The assertion has a deep biophysical sense because it means that cell processes are non-steady ones. Depletion of pyruvate pool coupled with CIF in the reaction provides C_2 and C_3 fragments with carbon isotope ratio, which changes in the course of depletion. From the above, the following important biophysical conclusion can be derived: carbon isotope distribution of metabolites and their isotope ratios are the function of the sequence (time) of their syntheses in the cell cycle.

Table 15. Changes in Intramolecular Carbon Isotope Distribution in Amino Acids Produced by *Corynebacteria* Grown on Different Substrates (40,41). $\delta^{13}C$ Values are Given in Per Mille Relative to PDB Standard

Bacteria	Substrate	$\delta^{13}C$ ‰	Amino acids	$\delta^{13}C$ ‰	$\Delta^{13}C$ ‰
B. flavum E-531	Molasses	−23.6	Lysine	−24.8	−6.3
	Molasses +	−23.6	Lysine	−29.7	−2.7
	acetate*	−31.5			
C. glutamicum 3144	Molasses	−22.2	Glutamic acid	−28.0	+7.4
	Acetate	−32.2	Glutamic acid	−26.7	−2.7

Note: $\Delta^{13}C = \delta^{13}C_{carboxyl} - \delta^{13}C_{total}$, $\delta^{13}C_{carboxyl}$ and $\delta^{13}C_{total}$ are the isotope composition of carboxyl and total carbon of amino acid.

* Nutrition mixture: 80% molasses + 20% acetate.

MARCEL DEKKER, INC.
270 Madison Avenue, New York, New York 10016

Before considering experimental data confirming the above assertion, it seems reasonable to analyze the conclusions, which might be derived from the alternative approach. This approach can be formulated as follows: the processes are steady-state ones and hence, there is no depletion of the pyruvate pool in decarboxylation. Then, ^{12}C-enriched C_2 fragments with isotopically light carboxyl carbon are formed providing the same isotope distribution of carbon units for all to acetate-derived products, such as fatty acids, sterines, terpenes, carotenoids, etc., determining their similar carbon isotope ratio.

In parallel, C_3 fragments having carboxyl and the adjacent carbonyl carbon atoms enriched in ^{13}C, which are used in the syntheses of amino acids and other metabolites, provide corresponding isotope pattern and ^{13}C enrichment of these substances or those parts of their molecules where C_3 fragments are incorporated. Under given cell conditions, carbon isotope ratio of C_2 and C_3 fragments and their intramolecular isotope distribution must be constant. Hence, carbon isotope ratio of metabolites derived from these fragments should reflect their isotopic composition and remain unchangeable for the given conditions. Following this logic, carboxyl carbon of different fatty acids must have the same isotopic composition. Fatty acids, which are characterized by the methyl-C to carboxyl-C ratio of 1:1, compared to polyisoprenoids with the ratio of 3:2 must be proportionally enriched in ^{13}C (224). This approach leads to interpretational difficulties, which have been discussed by Blair et al. (201) and Hayes (224).

In purple photosynthetic bacterium, *Chromatium vinosum*, organic acids with 1:1 ratio of methyl-C and carboxyl-C appear to be enriched in ^{13}C versus carotenoids having 3:2 methyl:carboxyl ratio (225). Nevertheless, in most cases the opposite situation is observed. For example in cyanobacterium, zooplankton, vascular plant, and eucaryotic alga fatty acids were found to be depleted in ^{13}C by 1–2‰ in comparison with polyisoprenoids (226). Sharkey et al. (227) found that in oak tree leaves, isoprene and carotenoids were depleted in ^{13}C versus fatty acids by 2‰. 24-Ethylcholestanol having isoprenoic structure (whose origin was ascribed to terrestrial plants) was found to be enriched in ^{12}C versus relative to *n*-alkyl plant waxes of the same sediment with low methyl:carboxyl ratio (228,229). A similar distribution of ^{13}C was observed in methanotrophic bacteria, *Methylococcus capsulatus* and *Methylomonus methanica*, under different cell growth conditions (33). Fatty acids were enriched in ^{12}C compared with hopanoids and steroids by 5–7 ‰.

The steady-state approach fails to explain big differences between individual polyisoprenoid structures (33). Squalene forming carbon skeletons of many steroids and hopanoids is enriched in ^{13}C by 5–7‰ compared with these substances. Even substances with very close structures, such as hopane and 3β-methylhopane, methyl and dimethylsterol, or sterols differing from each other by one unsaturated C=C bond are characterized by the difference in carbon isotope ratio of 5–7‰. Removal of one methyl group or cleavage of one unsaturated car-

MARCEL DEKKER, INC.
270 Madison Avenue, New York, New York 10016

bon bond is unlikely to result in so drastic a change in carbon isotope ratio of large molecules.

The strongest arguments in favor of the non–steady-state nature of cell processes including pyruvate decarboxylation is provided by consideration of intramolecular ^{13}C distribution in metabolites. According to the steady-state approach, fatty acids must have carboxyl carbon enriched in ^{12}C and be of the same isotope ratio. As seen from Table 16, the real situation contradicts this conclusion.

Different fatty acids isolated from the lipid fraction of various organisms have carboxyl carbon with isotope ratio of ~20‰. In most cases, the carboxyl group of fatty acids is enriched in ^{12}C versus total carbon. In wheat seeds, the carboxyl carbon of vaccenic and linoleic acids is depleted in ^{12}C as compared with total one.

Blair et al. (201) examining *E. coli* metabolism found an even higher isotopic difference between carboxyl and total carbon of acetic acid (a metabolic product of C_2 fragment cell transformation) excreted by bacteria. The ^{13}C enrichment of carboxyl carbon was about 12‰. This kind of isotope distribution cannot

Table 16. ^{13}C Distribution in Fatty Acids Isolated from Lipid Fraction of Different Organisms. $\delta^{13}C$; Values are Given in Per Mille Relative to PDB Standard

Organism	Fatty Acids		$\delta^{13}C$ of Fatty Acid	
			Total Carbon	Carboxyl Carbon
E. coli (141)	Myristic	14:0*	−13.7	−27.1
	Palmitic	16:0	−12.2	−15.2
	Palmitoleic	16:1	−13.0	−19.2
	9,10-Methylenepalmitic	17:cycle	−13.7	−20.3
	Vaccenic	18:1	−12.5	−13.9
S. cereviseae (199)	Myristic	14:0		−5.1
		14:1		−0.7
	Palmitic	16:0		−3.1
	Palmitoleic	16:1		+1.1
	Stearic	18:0		−17.4
	Vaccenic	18:1		−5.1
Wheat seeds (230,231)	Palmitic	16:0	−18.1	−20.2
	Vaccenic	18:1	−16.0	−12.3
	Linoleic	18:2	−15.4	−6.5
Soybeans (230,231)	Palmitic	16:0	−30.3	−40.1
	Vaccenic	18:1	−29.4	−31.5
	Linoleic	18:2	−29.7	−28.5
Nutmeg (231)	Myristic	14:0	−29.9	−38.8

* Total number of carbon atoms : number of double bonds.

MARCEL DEKKER, INC.
270 Madison Avenue, New York, New York 10016

be achieved by the steady-state pyruvate decarboxylation but it can be easily explained by Releigh effect arising in the course of substrate pool depletion.

The analysis of the intramolecular carbon isotope distribution leads to the same conclusions. Amino acids belonging to the same acid family and inheriting carboxyl carbon from the same source, according to the steady-state concept must have carboxyl groups of identical carbon isotope ratio. This contradicts the data shown in Table 17. As seen, the isotope ratio of carboxyl carbon of amino acids differs dramatically from that of the total carbon (232), which is similar to what is observed for fatty acids (see Table 16). This confirms once again that cell processes are not steady-state processes.

Let us consider how the above results can be explained from the standpoint of the non-steady model. In accordance with the theory of kinetic isotope effect (218), the degree of ^{13}C enrichment of C_2 fragment carboxyl carbons as well as that of CO_2 formed in decarboxylation is determined by the degree of the pyruvate pool depletion. At low degrees ($0 < F < 0.5$) these carbon atoms

Table 17. ^{13}C Distribution in Amino Acids Isolated from Protein Fraction of Photosynthetic Microorganisms (92). $\delta^{13}C$ Values are Given in Per mille Relative to PDB Standard

		^{13}C Distribution		
Amino Acid Family	Amino Acid	*Chlorella*	*Euglena*	*Gracilaria*
α-Ketoglutaric acid family	Glutamic acid			
	Total carbon	−18.7	−17.3	−17.2
	Carboxyl carbon	−8.8	−0.2	−8.4
	Arginine			
	Total carbon	−19.2	−15.9	−13.8
	Carboxyl carbon	−2.6	+3.6	−3.6
Oxaloacetic acid family	Aspartic acid			
	Total carbon	−6.6	−9.6	−14.4
	Carboxyl carbon	+2.2	+1.0	−5.3
	Threonine			
	Total carbon	−14.5	−8.6	−14.5
	Carboxyl carbon	−0.5	+2.1	−8. 5
Triose family	Alanine			
	Total carbon	−10.3	−14.3	−15.3
	Carboxyl carbon	−7.3	−13.8	−11.5
	Serine			
	Total carbon	−5.5	−8.3	−14.1
	Carboxyl carbon	+2.5	−6.1	−8.8
	Glycine			
	Total carbon	−14.3	−12.8	−10.2
	Carboxyl carbon	−6.3	−11.6	−12.8

Table 18. Carbon Isotope Fractionation in *E. coli* Grown on Glucose of Known Carbon Isotope Composition ($\delta^{13}C_{glucose} = -9.0‰$) (201). $\delta^{13}C$ Values are Given in Per Mille Relative to PDB Standard

		^{13}C Distribution in Acetate		
Lipids	Fatty Acids	Total	Carboxyl	Methyl
−11.7	−12.1	+3.3	+15.0	−8.8

must be enriched in ^{12}C versus initial substrate. At higher F ($0.5 < F < 1$) the same atoms must be enriched in ^{13}C. Methyl carbon atoms of C_2 fragments are not involved in the C—C bond cleavage in pyruvate decarboxylation and retain their carbon isotope ratio inherited from initial substrate. Then the theory predicts that the carboxyl carbon of both fatty and amino acids can be enriched both in ^{12}C and in ^{13}C depending either on F value or the sequence (time) of their formation in the cell cycle. This explains thoroughly the data presented above. The isotopic differences of metabolites result from the intramolecular discrepancies. One more argument in favor of this assertion can be found in the work by Blair et al. (201).

By studying the CIF in *E. coli* in fermentation of glucose of known carbon isotope composition, the authors found that fatty acids were enriched in ^{12}C versus initial glucose whereas acetic acid produced by bacteria (though also synthesized from C_2 fragments) was sharply enriched in ^{13}C (see Table 18).

It is important to emphasize that the whole ^{13}C enrichment of acetic acid was entirely linked with its carboxyl atom, which inherited the carboxyl atom from C_2 fragments while the isotope composition of methyl carbon atom was close to that of carbon of the nutrient glucose. Although the data followed the same isotope distribution pattern as that reported by Monson and Hayes (141) for fatty acids, the sign of the isotopic differences was opposite. This directly confirms that C_2 fragments formed in decarboxylation of pyruvate may be enriched either in ^{12}C or in ^{13}C. This confirms, in turn, that pyruvate pool is depleted and metabolic processes are not the steady-state ones.

In this context, an abnormal ^{13}C enrichment of the guanido group of arginine ($\delta^{13}C = +7.1‰$) versus total carbon ($\delta^{13}C = -22.3‰$) found in photosynthetic alga *Chlorella pyrenoidosa* (34) must also be mentioned. It is known (232) that the guanido group is formed by interaction of CO_2 and NH_3 in ornithine cycle of the cell. Since the exogenous carbon dioxide ($\delta^{13}C = 0‰$) cannot be the source of heavy carbon isotope and among other possible sources only CO_2 derived in decarboxylation of pyruvate can provide heavy carbon for guanido synthesis, one has to conclude that it occurs at a high degree of pyruvate pool depletion. It also means that arginine is formed at a high degree of pool depletion. This conclusion is supported by high ^{13}C enrichment of arginine carboxyl group in

comparison with carboxyl groups of the other amino acids (34). The analysis of ^{13}C distribution in amino acids will be given below.

The conclusion about exhaustion of pyruvate pool following the analysis of isotopic data agrees with biophysical assumption of the model about existence of the reciprocal periodic vibrations in glycolytic chain of the cell. Though at present, no direct evidence in favor of these vibrations can be found, some data obtained by studying ^{13}C distribution in amino acids produced by *Corynebacteria* grown on substrates of known carbon isotope ratio (100), may be regarded as indirect confirmation of such vibrations.

It was found that in some lysine-producing bacteria an addition of acetate to the carbohydrate substrate sharply reduced the intramolecular isotopic differences (see Table 15). In other cases (see Table 19), even complete substitution of the substrate with acetate is not accompanied by such remarkable changes. The most logical explanation for this effect stems from the idea of existence of the reciprocal vibrations in the glycolytic chain. A decrease of the intramolecular isotope differences in lysine observed in the experiment with *B. flavum* E-531 after addition of acetate (see Table 15) was explained by the blocking of pyruvate decarboxylation by the flow of exogenous C_2 fragments (used for lysine synthesis) occurring in the glycolytic phase.

In the experiment with *C. glutamicum* E-95-10 (see Table 19), the addition of acetate results in a small change of the intramolecular isotope distribution. Even complete substitution of molasses by acetate does not result in a big change. A possible explanation of these results is either the absence of blocking in the case of partial substitution or incomplete blocking in the case of complete substitution of molasses by acetate. This can be explained, in turn, by consumption of exogenous C_2 fragments in *B. flavum* E-531 occurring in glycolytic phases of cell cycle when pyruvate decarboxylation must proceed and thus, they block the reaction. In

Table 19. Fractionation of Carbon Isotopes in Bacterium *C. glutamicum* E-95-10 Grown on Molasses and Acetate Media (40,41). $\delta^{13}C$ Values are Given in Per Mille Relative to PDB Standard

Substrate		Lysine	
Type	$\delta^{13}C$	$\delta^{13}C_{total}$	$\Delta^{13}C$
Molasses	−23.6	−24.4	−8.2
Molasses +	−23.6	−30.0	−7.8
Acetate*	−31.5		
Acetate	−31.5	−32.4	−5.5

Note: $\Delta^{13}C = \delta^{13}C_{carboxyl} - \delta^{13}C_{total}$, $\delta^{13}C_{carboxyl}$ and $\delta^{13}C_{total}$ are the isotope composition of carboxyl and total carbon of lysine.
* Nutrition mixture: 80% molasses + 20% acetate.

MARCEL DEKKER, INC.
270 Madison Avenue, New York, New York 10016

C. glutamicum E-95-10 cells the consumption of exogenous acetate occurs in gluconeogenetic phase where it is used for carbohydrate synthesis. In the glycolytic phase, the carbohydrates synthesized from exogenous acetate feed the glycolytic chain, the pyruvate decarboxylation, and Krebs cycle, and hence no blocking of the reaction occurs. The intramolecular isotope differences in lysine are determined by the isotope effect of pyruvate decarboxylation. From this the conclusion that substrate can be consumed either in gluconeogenetic phase when carbon flow increases or in glycolytic phase when it decreases may be regarded as indirect evidence in favor of the existence of periodic fluctuations in glycolytic chain.

^{13}C Distribution in Cell and Temporal Organization of Metabolic Processes: Preliminary Notes

The described model makes it possible to link ^{13}C distribution in a cell with temporal organization of metabolic processes. But the lack of currently available experimental data for different types of cells and organisms requires confining consideration by some examples and preliminary notes. The basic principles of such a consideration are formulated below.

All metabolites are mainly composed of C_2, $C_1(CO_2)$, and C_3 fragments, which are the products of pyruvate decarboxylation reaction. To analyze their isotope distribution one needs to know the isotopic pattern of the above units. The isotopic patterns of C_2 fragments and CO_2 are described above. In C_3 fragments the carboxyl and the adjacent carbonyl atoms in accordance with isotopic material balance of pyruvate decarboxylation reaction are always enriched in ^{13}C versus carbon of the initial substrate whereas their methyl carbon (as in C_2 fragments) retains its isotopic composition. Hence, all carbon atoms that are used in metabolite syntheses may be divided into 3 types: 1) carboxyl atoms of C_2 fragments and CO_2, which may be enriched either in ^{12}C at $F < 0.5$ or in ^{13}C at $F > 0.5$ relative to the initial substrate carbon; 2) carboxyl and adjacent carbonyl atoms of C_3 fragments, which at any level of pyruvate pool are always enriched in ^{13}C; and 3) methyl atoms of C_2 and C_3 fragments, which retain an unchanged carbon isotope ratio. Let us consider for simplicity that pyruvate atoms located at the ends of the broken C—C bonds undergo equal isotopic shifts in decarboxylation, and the atoms of the initial substrate are isotopically identical.

Another principle is based on the close link between ^{13}C distribution of metabolites and their synthetic pathways with the use of the above structural units. Following these principles and taking into account the known regularities in ^{13}C distribution and biochemistry of cell processes, let us try to find out some features of temporal organization of cell metabolism.

It is a well-known fact that lipids are always enriched in ^{12}C compared with proteins regardless of the organism type. Considering that lipids are mainly pre-

MARCEL DEKKER, INC.
270 Madison Avenue, New York, New York 10016

sented by fatty acids whereas synthesis of the most amino acids proceeds via Krebs cycle; based on the model, one can conclude that the synthesis of fatty acid occurs in a cell prior to Krebs cycle functioning. It seems to be a general principle of temporal organization of any cell.

The fatty acids of lipid fraction of methanotrophic bacterium, cyanobacterium, eucaryotic alga, zooplankton, and vascular plants were found to be depleted in ^{13}C by 2–5‰ versus steroids, carotenoids, terpenoids, and high molecular hydrocarbons (33,196,226–229). By following the above logic and noting that all the components are synthesized from C_2 fragments, in these organisms, polyisoprenoids and high molecular hydrocarbons are formed in cell cycle prior to fatty acids.

Since 1961 there is only one work by Abelson and Hoering (92) where ^{13}C distribution in protein fraction of photosynthetic microorganisms was comprehensively studied. Let us analyze their data shown in Table 20 in detail. By setting

Table 20. ^{13}C Distribution in Amino Acids Extracted from Protein Fraction of Photosynthetic Microorganisms (92). $\delta^{13}C$ Values are Given in Per Mille Relative to Nutrient CO_2. $\delta^{13}C$ of CO_2 is 0‰

Amino Acid	*Chlorella*	*Anacystis*	*Scenedes Mus*	*Chromatium*	*Euglena*	*Gracilaria*
Leu	−26.0	−17.8	−22.2	−23.7	−25.6	−22.1
	−16.3	−15	−17.8	−22.5	−13.6	−24.1
i-Leu	−22.0	−12.2	−17.7	—	—	−19.8
	−7.4	−1.5	−13.1	—	—	−14.0
Lys	−20.9	—	—	—	−22.4	—
	+2.5	—	—	—	−24.8	—
Ala	−11.8	−14.2	−20.5	—	−14.6	−17.2
	−7.4	+0.2	−13.5	—	−13.8	−11.5
Ser	−9.9	—	—	−8.4	−9.8	−16.8
	+2.5	—	—	−2.8	−6.1	−8.8
Gly	−23.3	−11.1	−17.5	—	−14.1	−17.7
	−5.3	−8.8	−11.8	—	−11.6	−12.8
Glu	−21.1	−16.7	−26.6	−20.1	−21.5	−19.3
	−8.8	+11.7	−5.6	+2.2	−0.2	−8.4
Arg	−22.6	—	—	—	−19.8	−15.9
	−2.6	—	—	—	+3.6	−3.6
Asp	−15.6	−22.1	−24.3	−27.6	−20.3	−18.4
	+2.2	−2.6	−0.8	−15.9	+1.0	−5.3
Thr	−19.2	—	—	—	−12.2	−16.4
	−0.5	—	—	—	+2.1	−8.5

Note: upper (underlined) and lower $\delta^{13}C$ values correspond to amino acid radicals and carboxyl carbons, respectively.

MARCEL DEKKER, INC.
270 Madison Avenue, New York, New York 10016

amino acids in the order of enrichment of their carboxyl carbon in ^{13}C, one can obtain the following sequences:

Gracilaria	Leu < i-Leu < Gly < Ala < Phe < Ser < Thr < Glu < Tyr < Asp < Arg
Euglena	Lys < Ala < Leu < Gly < Ser < Tyr < Phe < Glu < Asp < Thr < Arg
Chlorella	Leu < Gly < Ala < i-Leu < Glu <Thr < Asp < Ser < Lys < Tyr
Anacystis	Leu < Gly < i-Leu < Ala < Asp < Glu
Scenedesmus	Leu < Ala < i-Leu < Gly < Glu < Asp
Chromatium	Leu < Asp < Ser < Glu

The analysis of these sequences allows one to conclude that more often than others the branched amino acids such as leucine and i-leucine and then alanine and glycine are at the head of the rows. In accordance with the proposed model this means that they are the first among the protein components, which are formed in the cell cycle. Amino acids produced via Krebs cycle such as glutamic acid, arginine, aspartic acid, and threonine, as well as those formed in shikimate pathway, tyrosine and phenylalanine, are located closer to the end of sequences, and hence, they are synthesized later in the cell cycle. Some amino acids like lysine and aspartic acid can be found at the opposite ends of the sequences. This means that their synthesis in different microorganisms proceeds at different stages of the cell cycle. Different sequences of amino acid synthesis often corresponds to different metabolic pathways of their formation.

Lysine species in *Chlorella* and *Euglena* (see Table 20) are close in carbon isotope ratio of their radicals and differ by that of carboxyl carbon. Enrichment of carboxyl carbon of lysine in *Euglena* with light isotope compared with carboxyl carbon of amino acids associated with Krebs cycle allows for the conclusion that in this microorganism the synthesis of lysine precedes Krebs cycle activity. Unlike *Euglena*, enrichment of lysine carboxyl carbon in *Chlorella* with heavy isotope testifies that its synthesis proceeds via Krebs cycle. The following two pathways of lysine synthesis are known from the literature (232): via diaminopimelic acid (see Fig. 11a), and via α-aminoadipic acid (see Fig. 11b), which corresponds to the observed isotope distributions. The first one is associated with Krebs cycle, and the carboxyl group of lysine is inherited in this case from aspartic acid. Comparing carboxyl carbon of lysine and that of aspartic acid in *Chlorella* (see Table 20), one can see that they are really very close in ^{13}C content. The second pathway is associated with the use of C_2 fragments as a sole source of structural units, like in the synthesis of fatty acids. The "lightness" of the carboxyl group of lysine in this case testifies to the synthesis of lysine in *Euglena* by using C_2 fragments. Like synthesis of fatty acids, it precedes Krebs cycle operation.

MARCEL DEKKER, INC.
270 Madison Avenue, New York, New York 10016

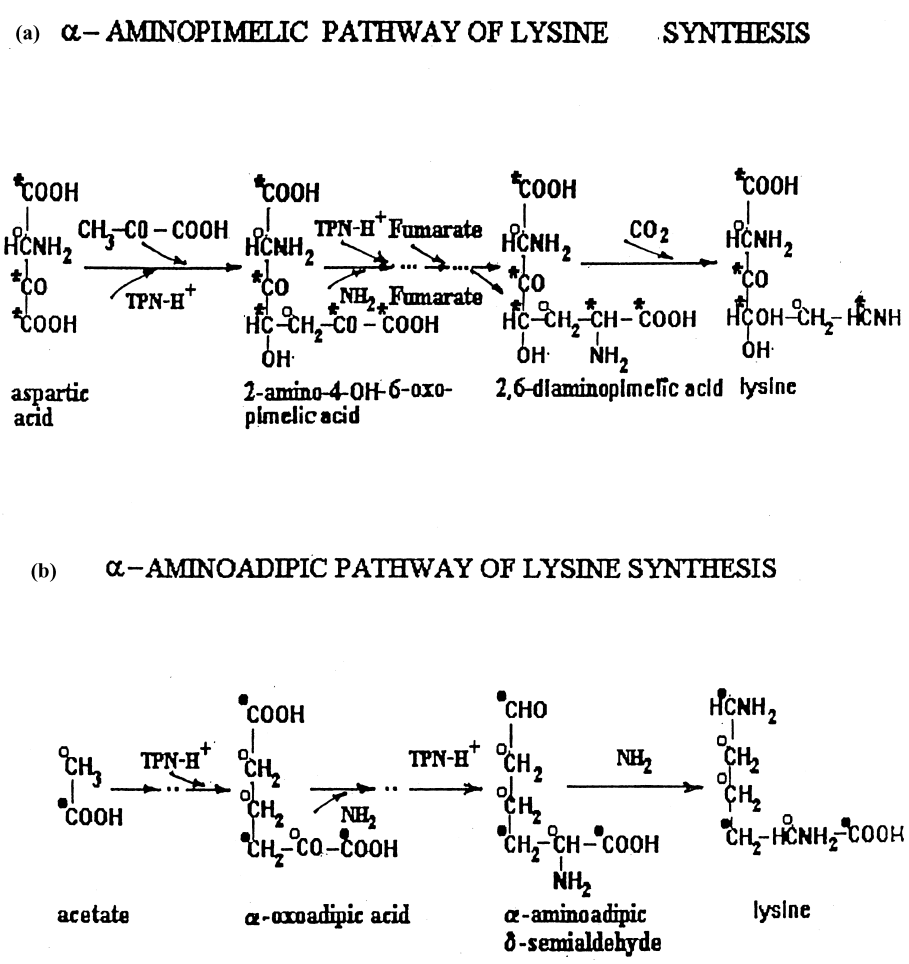

Figure 11. Distribution of carbon atoms in diaminopimelic acid (a) and α-aminoadipic acid (b) routes of lysine biosynthesis (232): methyl atoms originated from C_2 and C_3 fragments (asterisks); atoms originated from carbonyl atom of C_2 fragments (empty circles); carbonyl and carboxyl atoms originated from carbonyl atom of C_3 fragments (filled circles) (see text).

Comparing the isotope distributions of leucine and i-leucine one can see that carboxyl and radical carbon atoms in the former are more enriched in ^{12}C than those in the latter. In accordance with the known metabolic scheme of amino acid biosynthesis (232) (see Fig. 12), the carboxyl group of leucine is formed from C_2 fragments whereas the carboxyl group of i-leucine originates from C_3 fragments. This

agrees with the described ^{13}C distribution in the units used in their synthesis assuming that both amino acids are formed at the close levels of pyruvate pool depletion.

The C_2 fragments origin of the carboxyl group of leucine is also supported by the fact that isotope ratio of its carboxyl carbon can be enriched either in ^{12}C (*Gracilaria*) or in ^{13}C (other cases) (see Table 20). As it has been shown, both signs of isotopic shifts in intramolecular distribution are typical for C_2 fragments.

The lightness of leucine radical carbon compared with that of i-leucine stems from the difference in carbon atom distribution of their skeletons (see Fig. 12). The difference can be explained by incorporation of methyl carbon atoms from C_2 fragments into leucine skeleton instead of carbonyl carbon atoms in i-leucine skeleton. Carbonyl atoms of C_2 fragments are enriched in ^{13}C versus methyl atoms at $F > 0.5$ (see above).

The analysis of Table 20 shows that radical carbon of alanine, serine, and glycine in most of the studied microorganisms is characterized by high ^{13}C con-

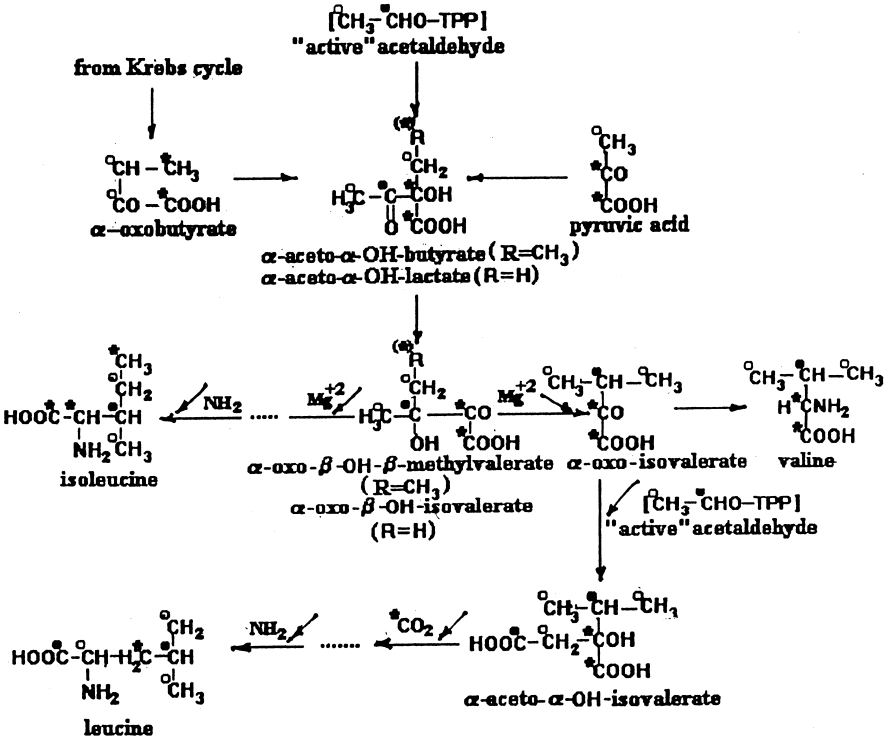

Figure 12. Distribution of carbon atoms corresponding to possible biosynthesis pathways of leucine and i-leucine formation (232).

tent compared with other amino acids. According to the known schemes of their biosynthesis (232), the amino acid precursors can be either phosphoglyceric acid formed in Calvin cycle or/and pyruvic acid derived in glycolysis. The logic of this consideration prompts to explain heavy isotopic composition of the amino acids with CIE of pyruvate decarboxylation. In this case, the proportionality between ^{13}C enrichment of radical and of carboxyl carbon must be observed, since heavy atoms are included both in radical and carboxylic group. However, as it follows from Table 20, a light carboxyl carbon of the aforementioned amino acids corresponds to a relatively heavy carbon of radical. Then it seems reasonable to assume that the observed ^{13}C enrichment of radical carbon emerges due to the contribution of the above amino acids synthesized by photorespiratory pathway. As it has been shown under *Modeling of CIF in Photorespiration*, the metabolites including amino acids synthesized in the photorespiratory chain are enriched in ^{13}C. Moreover randomization of atoms in transketolase and transaldolase reactions in the cycle ensures ^{13}C enrichment of any carbon atoms including those of radical. Thus, addition of alanine, serine, and glycine synthesized in this way to the total pools of these compounds can provide the described isotopic shift of their radical carbon.

As seen from Table 20, most amino acids produced via Krebs cycle, such as aspartic acid, threonine, glutamic acid, and arginine, are characterized by relatively light radical carbon and by carboxyl carbon, which is far more enriched in ^{13}C. To explain this, one needs to take into consideration that when amino acid synthesis occurs, the cycle is supplied both with C_2 and C_3 fragments. It has been shown (233) when intensity of Krebs cycle is low what corresponds to a low ratio of C_2 to C_3 fragments (N_{C2}/N_{C3}) entering the cycle, the radical carbon of Krebs cycle metabolites is more enriched in ^{13}C than at high intensity ($N_{C2}/N_{C3}>7$). This is the result of different randomization of light and heavy carbon atoms originated from structural units. At the same time a high content of ^{13}C in carboxyl carbon of amino acid indicates that Krebs cycle supplies amino acid synthesis with substrates at a high degree of pyruvate pool depletion. Hence, the observed ^{13}C distribution in amino acids derived via Krebs cycle testifies in favor of high intensity of the cycle in the majority of microorganisms studied. On the contrary, ^{13}C enrichment of radical and carboxyl carbon of threonine in *Euglena*, aspartic acid in *Chlorella*, and of glutamic acid in *Anacystis* indicates that sometimes the intensity of Krebs cycle is reduced.

The analysis of the above amino acid sequences permits the conclusion that amino acids of the triose family in most organisms are synthesized in cell cycle after the synthesis of branched amino acids and before Krebs cycle operation.

It must be emphasized that the chemical sequence of metabolites in their synthesis does not always coincide with their temporal sequence. The former reflects only the way of component synthesis while the latter corresponds to the real temporal sequence of their accumulation in a cell determined by the needs of en-

MARCEL DEKKER, INC.
270 Madison Avenue, New York, New York 10016

ergetic and structural metabolism of the organism under given conditions. For example, according to the chemical sequence, threonine synthesis must follow that of aspartic acid. If the temporal sequence were the same as the chemical one, the carboxyl carbon of threonine in *Chlorella* and in *Gracilaria* would be more enriched in ^{13}C than that of aspartic acid, because the latter is the precursor of threonine. In fact, as one can see from Table 20, an opposite situation is observed. This means that the pool of threonine is accumulated before that of aspartic acid. On the contrary, in *Euglena* the carboxyl carbon of threonine is isotopically heavier than that of aspartic acid, being the result of coincidence of chemical and temporal sequences in amino acid synthesis. Another reason for the difference in chemical and temporal sequences is the existence of the different ways of metabolite pool formation, which are active (as a rule) at different stages of cell cycle. The dramatic difference in ^{13}C distributions of glycine and serine in *Chlorella* from what it is expected to be if glycine is derived from serine (by removal of its methoxyl group) (232) gives proof of the existence of another pathway of serine synthesis. In particular, it might be the result of participation of photorespiratory carbon flow in amino acid synthesis as it has been indicated before. All above examples clearly demonstrate great possibilities of using metabolic CIEs in the examination of regulation and temporal organization of metabolism in organisms.

Other Points of CIF in Respiration Metabolism

All previous consideration of CIF in a cell was based on the key postulate that CIE of pyruvate decarboxylation is the sole reason for ^{13}C distribution in a cell. Though pyruvate decarboxylation isotope effect is very important and plays the ultimate role in cell carbon isotope distribution influencing the carbon isotope ratio of each cell component, this approach can give only a simplified picture of real isotope distribution. Nevertheless, it creates a necessary background to investigate mechanism of isotope fractionation more thoroughly by comparing isotope distribution in the frame of theoretical model with experimental isotope data. The discrepancy between the predicted isotopic distribution and the observed one can give information on the existence of some other isotope fractionation metabolic points. Some evidence for the existence of such points are given below and their role in cell isotope distribution is discussed. One of them is bound to fatty acid synthesis.

It is known that skeletons of fatty acids are built of C_2 fragments due to their condensation in accordance with head-to-tail principle (174). By following the suggested CIF model one must expect that even atoms of fatty acid skeletons should be of identical carbon isotope ratio. The isotope ratios of odd atoms (taking into account the duration of fatty acid synthesis) should reflect a trend to the gradual ^{13}C enrichment along the molecule skeleton starting from the carboxyl

MARCEL DEKKER, INC.
270 Madison Avenue, New York, New York 10016

carbon atom. The shift of the isotope ratio is determined by the depletion of pyruvate pool in the course of fatty acid synthesis. The longer time of synthesis, the higher isotopic shift must be observed. The data on carbon isotope ratio of individual atoms presented in Table 21 do not support the expected isotope distribution. Atoms C-9, C-10, C-11, C-12, and C-13 are considerably enriched in ^{12}C compared with C-1. The explanation for such a discrepancy is in the fact that all atoms examined are located at the ends of unsaturated C—C bonds. This enables us to suppose that isotope fractionation accompanies the formation of unsaturated bonds. The magnitude of this effect reaching 30‰ testifies in favor of carbonic ion mechanism of bond formation (234), but the lack of additional data does not permit us to make more definite conclusions.

Another point of CIF was reported by Welacher et al. (212). They investigated ^{13}C distribution in purine alkaloids extracted from black tea grown in different regions and found that carbon of methyl groups of caffeine (1,3,7-trimethyl-2,6-dioxopurine) is considerably enriched in ^{12}C versus total carbon of the caffeine molecule (see Table 22).

Good reproducibility of the results obtained for plants grown under different conditions shows that ^{12}C enrichment of C_1 fragments is not occasional and reflects CIF occurring in their formation. It is confirmed by the observed ^{12}C enrichment of methoxyl groups in some phenylpropanoic derivatives isolated from sugar cane and wheat (207). Weillacher et al. (212) considered the known way of C_1 fragment synthesis by splitting the methoxyl group of serine in glycine forma-

Table 21. Isotope Ratio of Carbon Atoms Located in Some Positions of Fatty Acid Skeletons. $\delta^{13}C$ Values are Given in Per Mille Relative to PDB Standard

Object		$\delta^{13}C$			
Organism	Fatty Acid	Odd Atoms		Even Atoms	
E. coli (141)	Palmitoleic 16:1*	C-1	−19.2		
		C-9	−16.0	C-10	−9.5
	Vaccenic 18:1	C-1	−13.9		
		C-11	−15.8	C-12	−9.5
S. cereviseae (199)	Palmitoleic 16:1	C-1	+1.1		
		C-9	−9.7	C-10	−13.8
	Vaccenic 18:1	C-1	−5.1		
		C-9	−18.0	C-10	−20.2
Soybeans (230,231)	Vaccenic 18:1	C-1	−31.5		
		C-9	−63.1	C-10	−41.4
	Linoleic 18:2	C-1	−28.5		
		C-9	−56.2		
		C-13	−30.8		

* Total number of carbon atoms : number of double bonds.

Table 22. Carbon Isotope Ratio of Certain Methyl Groups of Purine Alkaloids Extracted from Black Tea Leaves Grown in Different Regions (212). $\delta^{13}C$ Values are Given in Per Mille Relative to PDB Standard

	Caffeine of Black Tea	
Origin	Total Carbon	Methyl Carbon
Sri Lanka	−31.3	−34.7
Darjeeling	−30.2	−41.4
Assam	−29.4	−43.3
USSR	−29.2	−38.4
China	−41.4	−38.2
Mean values	−30.3	−39.2

tion. They assumed that the reduction of C_1 fragments in transfer to *S*-adenosylmethionine from tetrahydropholic acid pool is the point where the isotope effect emerged. It has been found that the carbon isotope ratio of C_1 fragments in different positions (even of the same molecule) is dramatically different (212). It allows us to suppose that in this process, like in the previously investigated, the isotope fractionation is followed by isotope effect of substrate pool depletion. Nevertheless, a thorough examination is needed to discuss this mechanism in more detail.

The above data show that the real distribution of carbon isotopes in a cell is more complex than that predicted by the proposed model. At the same time, it seems obvious that detailed study of ^{13}C distributions and their links with metabolic processes is impossible without knowing the principal features of distribution determined by isotope effect of pyruvate decarboxylation.

CARBON ISOTOPE CHARACTERISTICS OF HIGHLY ORGANIZED ANIMALS AND HUMANS

Preliminary Notes

How far the results obtained by CIF analysis in the simplest biological systems (mainly photosynthetic and heterotrophic microorganisms) can be transferred to highly organized biological systems (including humans) is the crucial point determining the applicability of isotopic data to investigate such systems. Because of the lack of experimental data, the problem is still far from being solved. Nevertheless, the following main reasons permit use of the results of the previous analysis to study highly organized animals and humans.

CIE in pyruvate decarboxylation was shown to be the principal element of CIF mechanism of any cell where the essential elements of metabolism are the

MARCEL DEKKER, INC.
270 Madison Avenue, New York, New York 10016

glycolytic chain, the Krebs cycle, and the chain of fatty acid synthesis. This assertion seems to be more reasonable because of the closeness of cell conditions (pH, temperature, ionic strength) regardless of the organism type and the level of its organization. Hence, there is no reason to suppose that the same processes under close conditions will result in different isotope fractionation in highly organized systems. This means that CIE in pyruvate decarboxylation is responsible for isotopic characteristics and their changes in organisms.

On the basis of this hypothesis, it is reasonable to extend the above conclusions obtained for the simplest systems to the complex ones. In particular, the most important finding that CIF in cells occurs in pyruvate pool depletion, i.e., metabolic processes are the non–steady-state ones, should be also valid for the complex organisms. Thus, a certain set of isotopic characteristics should correspond to each energetic state of organisms. They may be different for different organs of an organism consisting of different types of cells. The differences in carbon isotope ratio of individual components and tissue fractions, intramolecular isotope heterogeneity, and temporal cyclic variations of carbon isotope ratio of metabolic CO_2 evolved at different stages of cell cycle, typical of the simplest organisms and caused by dynamics of cell processes might be expected for highly organized animals as well.

Accounting for a high differentiation of tissue functions and compartmentalization of metabolic pathways, the dependence of isotopic characteristics on the parameters controlling nerve, hormone, and transport systems must also be expected. The ability of systems to self-regulate to maintain their internal medium in close limits allows one to expect a relative stability of the isotopic characteristics at particular functional states of the organism. At the same time, the differences of isotopic characteristics in different pathological and energetic states of the same organism may be predicted and will be shown below.

Let us consider now some peculiarities of studying the carbon isotope characteristics in highly organized animals and especially in humans. First of all, it should be emphasized that a low accessibility of the objects for a detailed study making to use for the investigations some integral isotope characteristics like isotope ratio of the breath CO_2 or those of the urine urea. The contributions of different tissues and organs of an organism to integral characteristics can be different for each energetic state and are the object of thorough consideration. In this situation it is reasonable to select for study such functional states of the organism when the contribution of individual organs are either dominant or specific.

Nevertheless, there are some difficulties connected with the lack of knowledge of temporal organization, regulation, and coupling of the processes in various tissues. In particular, the idea about the existence of reciprocal autovibrations in the glycolytic chain of cell based on purely chemical regulation in respect to highly organized animals becomes unclear. At the same time, periodic fluctuations of carbon metabolism under the control of endocrine, nerve, and transport

MARCEL DEKKER, INC.
270 Madison Avenue, New York, New York 10016

Table 23. Carbon Isotopic Composition of Different Organ Tissues of Rodents (236). $\delta^{13}C$ Values are Given in Per Mille Relative to PDB Standard

	$\delta^{13}C$ of Organ Tissues			
Organism	Liver	Fats	Spleen	Muscle of Legs
Dipoclomys				
Male	−15.6	−16.9	−14.1	−15.3
Female	−15.3	−18.2	−15.0	−14.6
Sigmodon hispidus				
Male	−23.2	−25.4	−22.4	−22.1
Female	−19.1	−19.6	−16.4	−13.4
Spermophilus Spilosoma				
Male	−22.2	−23.8	−20.8	−19.2
Female	−19.2	−22.4	−19.5	−19.8

systems are likely to exist. With the above ideas and doubts in mind and realizing the difficulties of the task, let us consider first the known factual material.

General Background

The heterotrophs including highly organized animals were considered at first to be incapable of fractionating carbon isotopes (78,235). This conclusion was based on the observed proximity of the carbon isotope ratio of biomass and that of the diet. Soon it was defeated by the discovery of the isotopic discrepancies between different organs of animals and humans (236–239). Data of Tables 23 and 24 clearly indicate the existence of CIF in tissue cells of animals. This conclusion more evidently follows from Tables 25 and 26 showing the results of comprehensive isotopic analysis of biomass fractions (123,238). As seen from these tables, the lipid fraction is enriched in ^{12}C versus biomass and other fractions. The

Table 24. Carbon Isotopic Composition of Human Organ Tissues (237). $\delta^{13}C$ Values are Given in Per Mille Relative to PDB Standard

Organ	Pancreas	Thyroid	Thymus	Kidney	Heart	Muscle
$\delta^{13}C$	−25.3	−22.7	−25.6	−24.0	−22.8	−23.6
Organ	Spleen	Liver	Brains	Blood	Blood Plasma	Lung
$\delta^{13}C$	−22.3	−22.7	−21.1	−18.2	−18.2	−22.4

MARCEL DEKKER, INC.
270 Madison Avenue, New York, New York 10016

Table 25. Carbon Isotopic Composition of Biomass and Lipid Fraction of Marine Animals (129). $\delta^{13}C$ Values are Given in Per Mille Relative to PDB Standard

	$\delta^{13}C$	
Object	Total Carbon	Lipids
Grass shrimp, *Palemonetes vulgaris*	−14.0	−19.0
Brown shrimp, *Penaeus aztecus*	−11.0	−14.0
Fiddler crab, *Uca pugilator*	−13.0	−18.0
Blue crab, *Callnectes sapides*	−17.0	−19.0
Killfish, *Cyprinodon variegutus*	−9.3	−11.5
Pinfish, *Lagadon rhomboides*	−13.0	−16.0
Spot, *Leiostomas xanthures*	−13.0	−13.0
Silver perch, *Baindiella chrysures*	−11.0	−13.0
Mullet, *Mugel cephales*	−12.0	−14.0

similarity in ^{13}C distribution with that found for microorganisms and plants confirms our conclusion on the principal proximity of CIF mechanism in respiration metabolism in organisms of different types and organization levels.

The results obtained by studying the carbon isotope ratio of breath CO_2 gave another confirmation of CIF in tissues of highly organized animals. In most cases, CO_2 respired by animals and humans was remarkably enriched in ^{12}C compared with their tissue carbon and diet (see Table 27) (238), although sometimes the isotope composition of carbon of breath CO_2 and that of the diet carbon were found to be nearly identical (239). Some authors observed variations in composition of CO_2 respired by different animals and even by separate organs (liver) reaching 5‰ (240). It was also noticed that carbonate fraction of bones of animals and humans was highly enriched in ^{13}C compared with metabolic CO_2 and organic carbon of tissues (237,238). Isotopic differences were found to

Table 26. Carbon Isotopic Composition of Biomass and its Fractions of Heterotrophs and Tropic Fly Species (238). $\delta^{13}C$ Values are Given in Per Mille Relative to PDB Standard

		Flies Grown on Horse-flesh			Flies Grown on Pork	
Object	Horse-flesh	*Caliphora*	*Musca*	Pork	*Caliphora*	*Musca*
Lipids	−28.5	−26.3	−25.3	−13.5	−13.0	−13.2
Glycogen	−24.1	−23.4	−23.0	−12.0	−14.1	−14.8
Soluble proteins	−23.7	−23.0	−22.2	−14.4	−15.0	−14.9
Biomass	−23.9	–	–	−13.5	−14.9	−13.8

MARCEL DEKKER, INC.
270 Madison Avenue, New York, New York 10016

Table 27. Carbon Isotope Fractionation in Animal Diet System (238). $\delta^{13}C$ Values are Given in Per Mille Relative to PDB Standard

Organism, Nutrient Substrate	$\delta^{13}C$ of the Objects			
	Breath CO_2	Feces	Biomass	Diet
Grasshopper, *Melanoplus sanguinipes*, Wheat seedlings	−39.0 to −42.0	−39.0 to −40.0	−36.2 to −38.5	−40.2
Grasshopper, *Melanoplus sanguinipes*, Corn seedlings	−23.0 to −26.5	−20.9 to −21.2	−20.6 to −20.9	−22.8
Milkweed bug, *Oncopeltus*, Branches, *latuca sativa*	−27.8 to −28.6	−26.3	−26.0 to −27.6	−26.8
Snail, *Helix aspersa*, Leaves, *latuca sativa*	−25.0 to −26.9	−25.2 to −27.3	−25.2 to −26.2	−26.7

be 10‰ and more. The change in carbon isotope ratio of the diet caused an adequate isotopic shift in carbon isotope ratio of bone carbonates (237). This confirms that metabolic CO_2 is the main source for carbonate carbon in bone tissue formation. If this is so, the drastic "heaviness" of bone carbonates in light of the suggested model may be regarded as evidence of the Releigh effect of substrate pool depletion in pyruvate decarboxylation occurring in animal tissue cells. In other words, CO_2, which is used for bone carbonate formation, is produced at the end stage of the glycolytic phase of cell cycle when heavy pyruvate is utilized (see above).

As previously mentioned, CO_2 respired by animals is an integral characteristic contributed by different metabolic processes and tissues. Hence, the complex character of the curves describing temporal changes in carbon isotope ratio of breath CO_2 is not surprising. But it is worthy to note the great difference in curves characterizing the variations of breath CO_2 isotope ratio for junior and aged rats under prolonged starvation observed by Mosora et al. (241) (see Fig. 13). Because of the obvious difference in energetic status of junior and aged rat organisms, this finding gives a confirmation of interconnection between isotopic characteristics and the functional state of the organism. The influence of hormones (desoxycorticosterone, glucagon, and insulin) and feeding substrates (glucose) on the discussed isotopic characteristic (241–243) gives more evidence in favor of this assertion.

CO_2 respired by rats and other animals (241–243) was found to be considerably enriched (up to 10‰) in ^{12}C versus nutrient substrate. As seen from Fig.

MARCEL DEKKER, INC.
270 Madison Avenue, New York, New York 10016

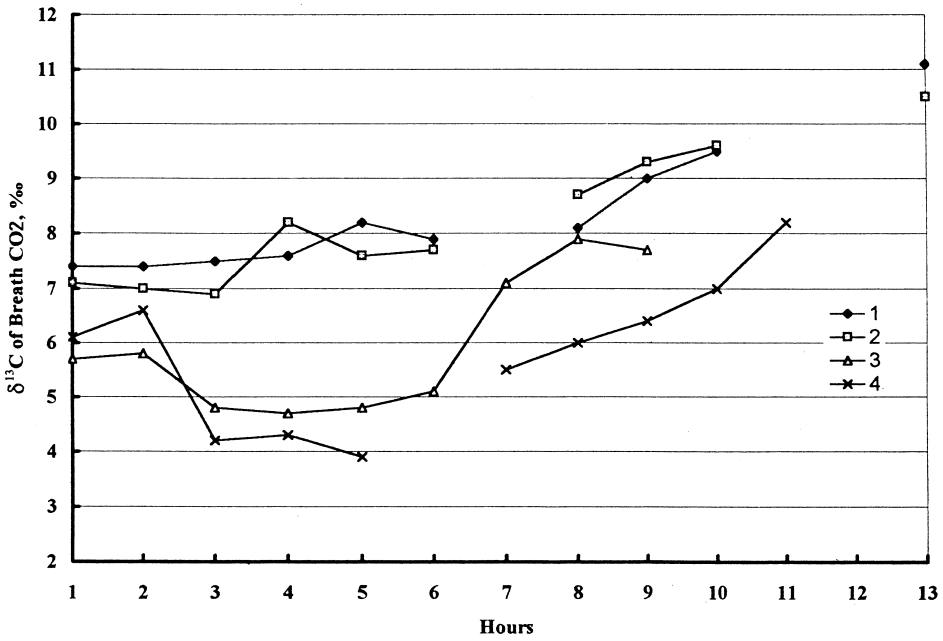

Figure 13. Variations of carbon isotope ratio of CO_2 respired by aged (1, 2) and junior (3, 4) rats under long-term starvation (241). $\delta^{13}C$ values are given relative to standard $\delta^{13}C = 28.5‰$, PDB units.

13, the curves describing variations of the above characteristics for junior and aged animals despite the isotopic shift observed for different animal groups have some common features. All the curves have an irregular pattern characterized by alternating the maxima and minima. It will be shown later that this pattern also is typical of the $\delta^{13}C$ of breath CO_2 variations of humans. $\delta^{13}C$ values of CO_2 vary from -17.5 to $-25.5‰$, and after 5 h of starvation, a distinctive trend to ^{13}C enrichment is observed.

Jacobson et al. (244) showed that feeding of rats with alloxan-containing nutrients caused diabetic shifts in their metabolism and resulted in ^{12}C enrichment of breath CO_2. The diabetic isotopic shifts of CO_2 were $\sim 2‰$, which agrees with intense metabolization of lipids observed and confirms the expected difference between the normal and pathological states.

Hence, all theoretical predictions based on the cell CIF model when applied to highly organized animals were either directly or indirectly supported by independent experimental data. This stimulates us to more thoroughly examine the human isotopic characteristics and attempting to apply them in the solution of certain physiological and medical problems.

Carbon Isotope Characteristics of Humans in Different Functional States

Isotopic characteristics of humans, such as carbon isotope ratio of hair, blood, nails, and respiratory CO_2, were studied recently (245,246). The results of long-term observations have shown that these characteristics are not constant. For example, systematic examination of human hair showed slow (with a 20–30 day period) variations of $\delta^{13}C$ values around a certain mean level with variable amplitude (see Fig. 14). The patterns of curves shown in Fig. 14 and the magnitude of amplitudes are different depending on the subject. In one case (see Fig. 14, curve 3), a sharp maximum (up to 20‰) corresponding to ^{13}C enrichment of hair carbon was detected for the patient who had recently undergone surgery for the removal of a tumor in the large intestine. The emergence of the peak coincides with

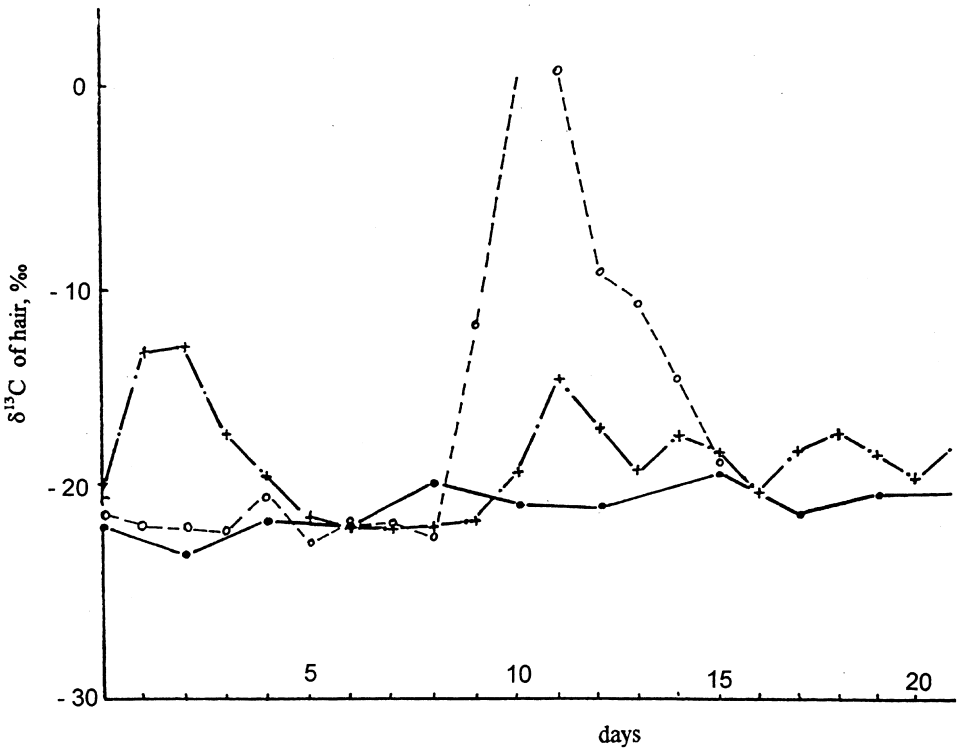

Figure 14. Time variations of $\delta^{13}C$ (PDB units) of facial hair for male subjects 29 (filled circles), 49 (crosses), and 79 (empty circles) years old. Time of subjects testing does not agree by date (246).

the worsening period of his state. In the further examination of this patient (1-month observation), this effect was not observed. The isotopic composition of nail, epidermis, and blood varied in time within the limits of 6‰ but the observations were not systematic.

Variations of carbon isotope ratio of blood plasma in different endocrine pathology states illustrate the relationship between isotopic characteristics and different hormone and energetic states of patients (247). Blood plasma samples of 48 patients suffering with diabetes mellitus, obesity, hypo- and hyperthyroidism, and Itzenko-Kushing syndrome were investigated. The entire interval $\delta^{13}C$ changes of blood plasma varied from -19.7 to -24.7‰. The distribution of blood plasma $\delta^{13}C$ values inside this interval was not random (see Fig. 15). As seen in Fig. 15, for patients suffering with diabetes mellitus $\delta^{13}C$ values are substantially higher than for those with obesity. This trend agrees with the traditional concept of the "polarity" of these types of dysmetabolism under consideration. The $\delta^{13}C$ values of blood plasma of patients suffering with Itzenko-Kushing syndrome tend to group in two intervals what can be explained by the heterogeneity

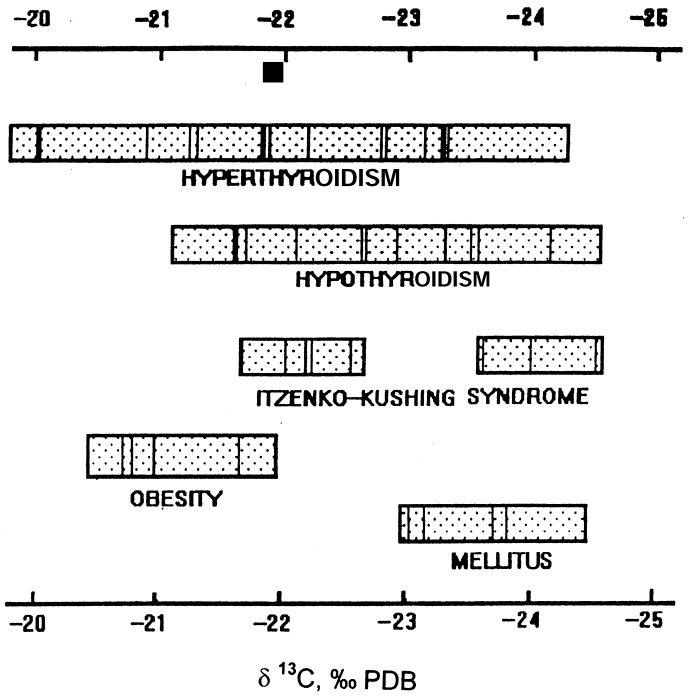

Figure 15. $\delta^{13}C$ (PDB units) of blood plasma of subjects with endocrine pathologies. Vertical dashes in bars correspond to different subjects (247).

MARCEL DEKKER, INC.
270 Madison Avenue, New York, New York 10016

Table 28. Carbon Isotope Composition of Respiratory CO_2 Collected During Physical Exercise of Constant Intensity (200 W, 60 rpm on Veloergometer) [245]. $\delta^{13}C$ Values are Given in Per Mille Relative to PDB Standard

τ_i, Min	Exp. No. 1	Exp. No. 2	Exp. No. 3	τ_i, Min	Exp. No. 3
0		−25.6	−29.6	8	−27.1
1	−30.6	−28.4	−25.6	9	−28.6
2		−27.3	−27.6	10	−31.6
3		−28.8	−28.0	11	−32.6
4	−27.0	−29.2		12	−30.8
5			−27.1	13	−29.7
6	−28.7	−26.8	−28.8	14	−22.9
7	−25.3		−29.7	15	−29.4

Note: each τ_i value corresponds to sampling for 1 min before τ_i . The subject under study was 29 years old.

of this pathology (248). Thus, it was found that in some cases the increase of cortisol in blood, which was typical to the syndrome, was followed by characteristic metabolic shifts of diabetes mellitus (according to sugar load curves). In other cases, it was followed by those of obesity. A broad interval of $\delta^{13}C$ variations in case of hypo- and hyperthyroidism are probably explained by high variability of energy metabolism observed in these pathologies (248). The distinctive ^{13}C enrichment of blood plasma of infants compared with adults agrees with the observed isotopic differences of respiratory CO_2 for junior and aged rats as described before. In both cases, the differences are likely bound to a different energetic status of the organism.

The observed fluctuations of the studied isotopic characteristics may be explained by regular variations of the energy needs of the organisms metabolism and finally of the cells corresponding to its functional state and environment. Indeed, the degree of the pyruvate pool depletion depends on the current energy demand of a cell causing corresponding shifts in ^{13}C distribution (see above). By analogy, the individual pattern of curves describing $\delta^{13}C$ variations in human hair (see Fig. 14) might be explained by the different energetic status of a particular subject. Unfortunately, at the moment, a more definite conclusion about relationships between variations of human isotopic characteristics and cell energy metabolism cannot be derived.

The variations of carbon isotope ratio of respiratory CO_2 under physical exercises were studied (245). The results of this study are presented in Table 28. The patient performed physical exercises at a constant stress of 200 W on a veloergometer for different time intervals. The power of the exercises was found to be less than that of the anaerobic exchange threshold, i.e., the exercises were per-

formed in a purely aerobic regime without an accumulation of oxygen deficit resulting in formation of lactic acid as a substrate. Thus, the experimental conditions provided the total utilization of glucose in cells during muscular contraction when the metabolic shifts in the organism were most remarkable compared with aerobic regimes.

During physical exercises of such intensity, the muscles consume over 90% oxygen to meet the energy requirements. The respiratory CO_2 in this case corresponds to ~90% of the macroergic substrate carbon spent to provide the energy supply work. In addition, the measurement of the respiratory quotient* (by using O_2/CO_2 gas analyzer) showed that starting from the 4th minute of the exercise, its value became close to unity. In the absence of progressive accumulation of the oxygen debt, it demonstrates practically 100% carbohydrate backing of muscular activity in the experiment.

Three experiments were conducted under the above conditions. In accordance with the above assumption, a fairly complex pattern of carbon isotope changes in respiratory CO_2 was found. As in the experiments with rats subjected to prolonged starvation (241), no smooth trend of the above characteristics in time was detected. Significant deviations from the mean were recorded with maximal amplitude of ~6‰. The $\delta^{13}C$ variations of respiratory CO_2 observed correspond to their maximal changes found for rats. They are also close to the isotopic differences between the lipid and carbohydrate-protein components of the diet. But it would be a mistake to assume that to ensure the energy needs of the muscles, whose energy consumption in physical exercises is dominant, the observed variations in $\delta^{13}C$ of respiratory CO_2 arise due to mobilization of different components of the diet. Indeed, simultaneous measurement of the respiratory quotient showed that its value was close to unity, i.e., almost a purely carbohydrate provision of muscular activity was provided. The last conclusion was reached by Aulik (249). It fully agrees with the results of direct measurements of non-esterified fatty acid level in blood (250). It seems reasonable to suppose that the only reason for the observed changes in $\delta^{13}C$ of respiratory CO_2 is the periodic filling/depletion of the pyruvate pool (taking into account the transitional firing process) in response to the varying energy needs of the organism. To obtain more detailed information, a comparison of respiratory CO_2 $\delta^{13}C$ variations determined under physical exercises at different power levels and with different time spans with those under the rest are needed.

Temporal variations of $\delta^{13}C$ of respiratory CO_2 were investigated in clinic for three metabolic states: norm, insulin-dependent diabetes mellitus, and obesity (71). The corresponding diurnal curves are shown on Figs. 16–18. The norm was presented by three females: no. 1 (14-years old), no. 2 (19-years old), no. 3 (21-

*The ratio of the volume of carbon dioxide expired to the volume of oxygen inspired during the same period.

MARCEL DEKKER, INC.
270 Madison Avenue, New York, New York 10016

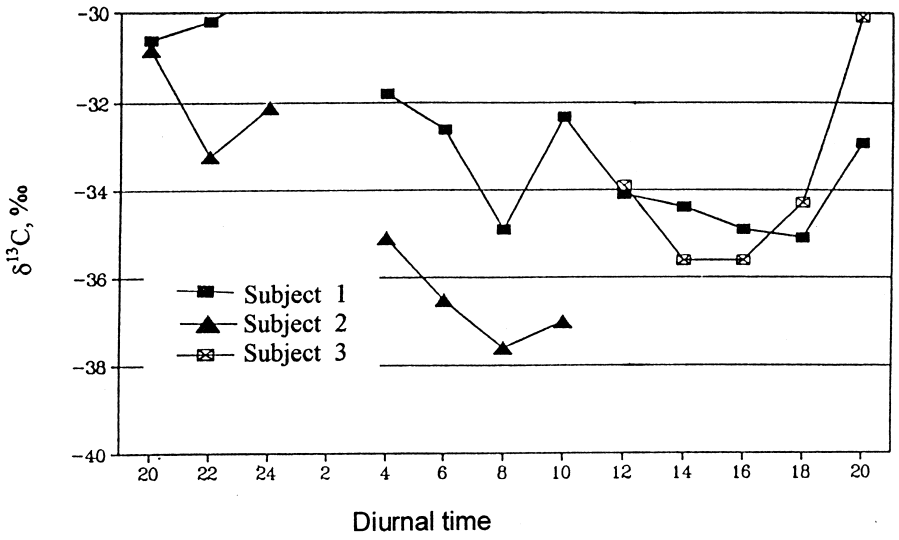

Figure 16. Variations of carbon isotope ratio of respiratory CO_2 in norm (71). $\delta^{13}C$ values are given in per mille relative to PDB standard.

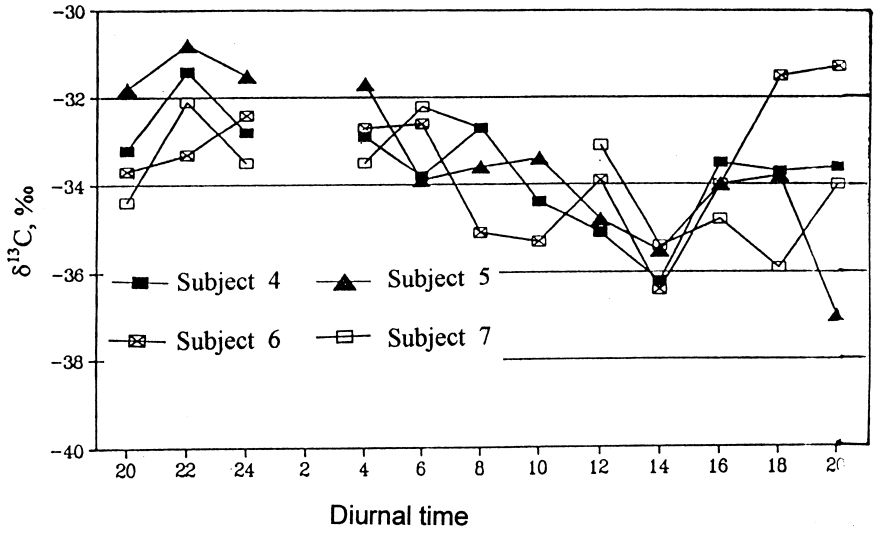

Figure 17. Variations of carbon isotope ratio of respiratory CO_2 in diabetes mellitus (71). $\delta^{13}C$ values are given in per mille relative to PDB standard.

MARCEL DEKKER, INC.
270 Madison Avenue, New York, New York 10016

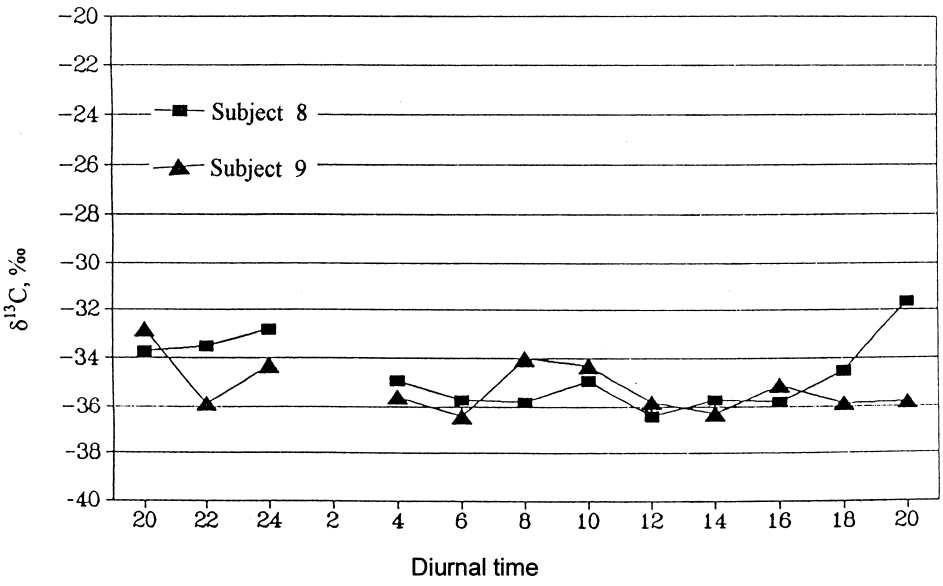

Figure 18. Variations of carbon isotope ratio of respiratory CO_2 in obesity (71). $\delta^{13}C$ values are given in per mille relative to PDB standard.

years old) (see Fig. 16). Diabetes mellitus was present in four females: no. 4 and no. 7 (both 14-years old) with type I in the decompensation phase, no. 5 (13-years old) with type I, and no. 6 (14-years old) with type I complicated in the decompensation phase (see Fig. 17). The obesity was presented by no. 8 (male, 11-years old) with hypogonadism and obesity of degree III, and no. 9 (female, 10-years old) with obesity of degree II (see Fig. 18). The patients from the diabetes mellitus group received insulin treatment for a period of 6–8 h, 20 min before the next uptake of food (six times per day according to the schedule). As seen in Figs. 17 and 18, the second (the insulin-dependent patients with diabetes mellitus in decompensation phase corresponding to acute metabolic stress), and the third group (obesity referring to the chronic dysmetabolism) are polar in their dysmetabolism. All experiments were carried out under identical conditions: diet, daytime regimes, time of food uptake, and administration of insulin (for diabetes mellitus patients). Drugs other than insulin (affecting metabolism) were not used. The analysis of the results allowed us to derive the following conclusions:

1. Carbon isotope ratio of respiratory CO_2 irrespective of functional state of the organism in all cases was found to be lighter (by 6–8‰) than that of the diet carbon. For all subjects, the patterns of diurnal curves (describing $\delta^{13}C$ variations of respiratory CO_2 in time) are complex. The

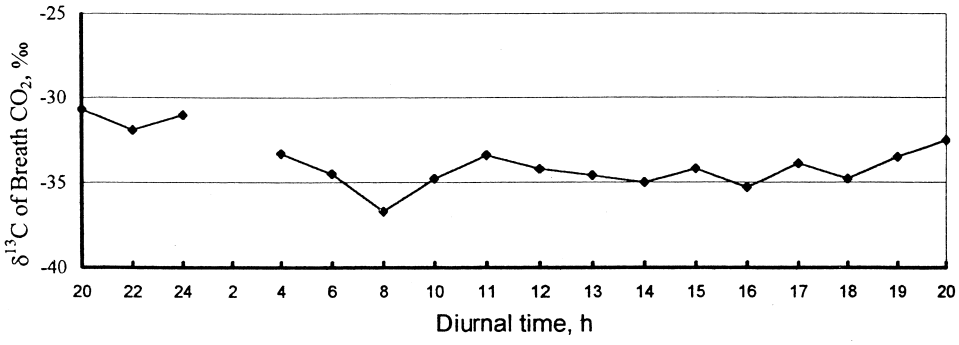

Figure 19. Averaged daily variations of carbon isotope composition of respiratory CO_2 in norm (71).

curves are characterized by alternating maxima and minima with variable amplitudes (see Figs. 16–18). The shape of the curves including the limits of their variations (6–8 vs. 4–6‰) strongly resembles analogous curves for rats (see Fig. 13). Hence, the $\delta^{13}C$ fluctuations can be considered to be regular and associated with the same reason.

2. To simplify the analysis of the particular features of the curves within the patient groups all individual curves were averaged (see Figs. 19 and 20). As seen from Fig. 20, respiratory CO_2 $\delta^{13}C$ values for the subjects

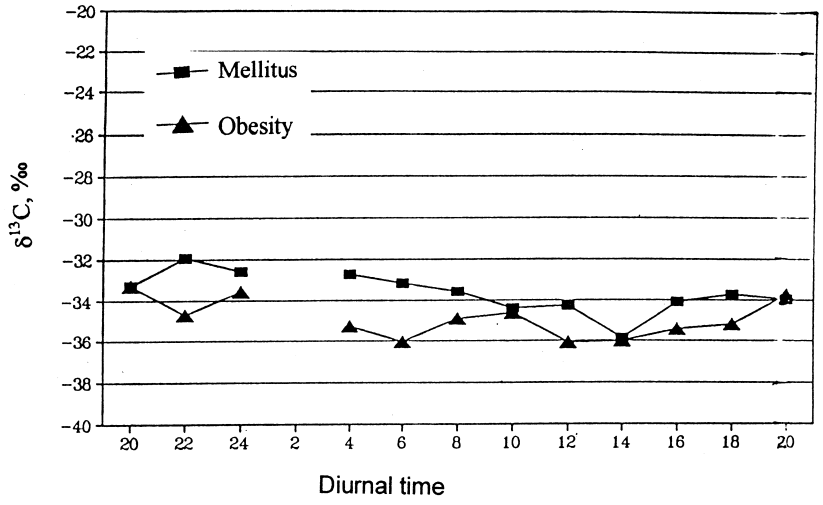

Figure 20. Averaged daily variations of carbon isotope composition of respiratory CO_2 in diabetes mellitus and obesity (71).

MARCEL DEKKER, INC.
270 Madison Avenue, New York, New York 10016

from the obesity group are shifted to the negative range relative to the corresponding values for the subjects from the diabetes mellitus group. Having an antibatic character, the curves for both groups approach each other at the moments of considerable uptake. Compared with the curves for diabetes mellitus subjects, which are flat in the nocturnal phase (between midnight and 6 A.M., see Fig. 17), the obesity subject curves are smooth having less amplitudes of variations all day long (see Fig. 18).

Let us see how the observed peculiarities of the above curves can be explained by using the cell CIF model. The alternation of the curve peaks can be ascribed to the changes in pyruvate pool level in the tissue cells in the course of pyruvate decarboxylation followed by its refilling. The CO_2 released is enriched either in ^{13}C when the level drops or in ^{12}C when it lifts. The pool level is controlled on one hand, by metabolism needs (both energetic and structural) of the organism, and by food consumption on the other. In respect to human metabolism, one can imagine it to be as follows.

Consumption of the food causes the increase of glucose content in the blood. It invokes insulin secretion by the pancreas providing glucose consumption by the cells of insulin-dependent tissues, such as liver, muscle, or fat tissues. Insulin activates glycolysis, lipogenesis, and glucogenesis, provides the carbon flow to fill pyruvate pool, and increases the fructose bisphosphate concentration. The latter is an allosteric regulator for pyruvate kinase. Activation of this enzyme results in the increase of the rate of pyruvate decarboxylation supplying with substrates first fatty acid and other lipid component synthesis, and then Krebs cycle, producing energy and amino acids. Therefore, after filling the pyruvate pool is exhausted.

Among different ways of regulation of carbon flow in glycolytic chain the coupling of pyruvate diffusion into mitochondria (it is known that pyruvate penetrates into mitochondria by diffusion (251)) with decarboxylation seems to be the main one. The possible regulatory role of this factor is associated with the difference in diffusion and chemical reaction rates as it was shown for photosynthesis (see *Modeling of CIF in Photosynthetic Assimilation of CO_2*), where the coupling of CO_2 diffusion into the cell with RuBP carboxylation is assumed to provide a discreteness of CO_2 carbon flow. Since the processes proceed under the control of hormone, nerve, and blood transport systems, their duration and intensity depend not only on the pool sizes (as in unicellular organisms) but on the energetic and biosynthetic needs at a particular functional state of the organism. Biosynthetic needs seem to play a secondary role compared with the energy consumption. The variations of pyruvate pool level in response to the change in the functional state of the organism should cause corresponding variations of the carbon isotope ratio of CO_2 evolved in both decarboxylation and Krebs cycle.

A decrease of glucose concentration in cells and then in the blood to a certain level causes the reswitch of ribulose bisphosphate futile cycle to gluconeogenesis and increases the glucose content in the blood. These changes result in elim-

ination of insulin and in secretion of somatotropin, glucagon and some other hormones (251), inducing lipolysis and protein catabolism and inhibiting enzymes responsible for the glycolysis. In the course of gluconeogenesis operation of the phosphogluconate cycle provides additional energy supply due to glucose oxidation. It is supposed that CO_2 produced in this cycle is of the same isotope composition as that formed from the oxidized glucose since there is no evidence of any CIF in gluconeogenesis. The gluconeogenesis causes the increase of glucose content in the blood again to the threshold when it induces excretion of insulin and other anabolic hormones and adequately eliminates catabolic hormones stimulating the opposite processes. Then cell cycle (consisting of glycolysis and gluconeogenesis) repeats again after a period determined by the organism resources (if they are not recovered by new food consumption).

Thus, in cells of insulin-dependent tissues, the carbon isotope ratio of CO_2 evolved in glycolytic phase of the cycles is determined by the value of kinetic isotope effect in pyruvate decarboxylation and by Releigh effect of pyruvate pool depletion corresponding to a particular functional state. The isotope ratio of CO_2 formed in gluconeogenetic phase is determined by that of substrates oxidized in the phosphogluconate cycle.

The normal functioning of cells of insulin-independent tissues (e.g., nerves or brain) requires a stationary flow of glucose without any sharp deviations of its content. Hence, a stable level of pyruvate pool maintains the stability of all isotopic characteristics of the tissue. Nevertheless, CO_2 formed in these tissues may vary by the carbon isotope ratio because of the various sources feeding glycolytic chain in glycolysis and in gluconeogenesis having glucose of different carbon isotope ratio.

The following data confirm this standpoint. For example, the absence of food consumption at night makes the lipids the main source of the energy substrate. The prevalence of lipid oxidation, which is known to have light isotope composition explains the observed ^{12}C enrichment of CO_2 respired in the nocturnal phase (between midnight and 8 A.M.) in norm (see Figs. 17–20).

Some peculiarities of carbon isotope variations of breath CO_2 related to diabetes mellitus subjects also correspond to the known metabolic shifts of this pathology. They primarily concern the insulin-dependent tissues. The insulin deficit (absolute or relative) in this state results in accumulation of glucose in the blood whereas the cells appear in glucose shortage. It is also observed that due to inhibition of glycolytic enzymes in cells, the gluconeogenetic processes are active (251,252). The role of phosphogluconate cycle coupled with gluconeogenetic processes for energy supply increases compared with that of the Krebs cycle. Because the functioning of phosphogluconate cycle is not accompanied by CIF (see above), CO_2 evolved in the cycle reactions must be of the same carbon isotope ratio as the oxidized substrates. Considering that the breath CO_2 is enriched in ^{12}C compared with diet carbon and the above assertion on CO_2 produced in phospho-

gluconate cycle, the increasing contribution of CO_2 evolved in phosphogluconate cycle to the total breath CO_2 of diabetes mellitus subjects explains the observed ^{13}C enrichment of the latter compared with the norm (see Table 29). Another specific feature of CO_2 respired by the diabetes mellitus patients is a more flat pattern of diurnal curves describing the variations of carbon isotope ratio of breath CO_2 compared with the norm that was particularly distinct at night (see Figs. 16 and 17). This testifies to the suppression of pyruvate decarboxylation reaction resulting in isotopic uniformity of oxidized substrates and for a higher role of the phosphogluconate cycle.

The metabolic shifts observed in obesity primarily affect the adipose cells. They are characterized by an increase of their mass, volume, and surface accompanied by simultaneous decrease of the number of insulin receptors at least by a factor of 2 (253). As a result, the sensitivity of cells to insulin diminishes, which causes an increase of secretion of this hormone by the organism. Insulin promotes conversion of glucose to lipids and inhibits lipolysis (252). This intensifies the lipogenesis at the expense of synthesis of other components. Lipids are the dominant source for energy production in obesity.

The above metabolic shifts determine the observed ^{12}C enrichment of CO_2 respired compared with norm (see Fig. 21) as lipids are lighter by their isotope composition relative to other components. The dominance of lipids as substrates under oxidation explains the lower amplitudes of $\delta^{13}C$ variations of CO_2 respired by the obesity subjects.

It is interesting to note that carbon isotope composition of CO_2 respired by obesity subjects is enriched in ^{12}C in comparison with that respired by diabetes mellitus subjects (see Fig. 20) whereas an opposite situation is observed for blood plasma (see Fig. 15). Such differences in ^{13}C distribution can be explained as follows. Unlike a high glycolytic conversion of substrates in obesity, a suppressed glycolysis in diabetes mellitus determines a lower ^{13}C enrichment of cell components in the first case than in the second. Regarding blood plasma as a part of biomass, one can explain the above difference. The more breath CO_2 is enriched in ^{12}C, the more residual carbon (i.e., a part of diet carbon transformed to biomass) must be enriched in ^{13}C.

A comparison of the mean daily carbon isotope ratio of respiratory CO_2 with that of the diet (see Fig. 21) for both types of dysmetabolism shows that distinctive metabolic shifts ($\Delta^{13}C$) of the opposite signs (compared with the norm) between different hormone-metabolic states are observed with a high level of confidence (P) (72): $\Delta^{13}C$(diabetes mellitus–obesity) $= +1.7‰$ ($P < 0.01$); $\Delta^{13}C$(diabetes mellitus–norm) $= +0.8‰$ ($P < 0.13$); $\Delta^{13}C$(obesity–norm) $= -0.9‰$ ($P < 0.11$).

It is important to emphasize that although the interval of daily variations of breath CO_2 $\delta^{13}C$ values is quite broad (from 5 to 7‰), the variations within hormone-functional groups are fairly small, i.e., by an order of magnitude less than the differences between functional states (see Table 29).

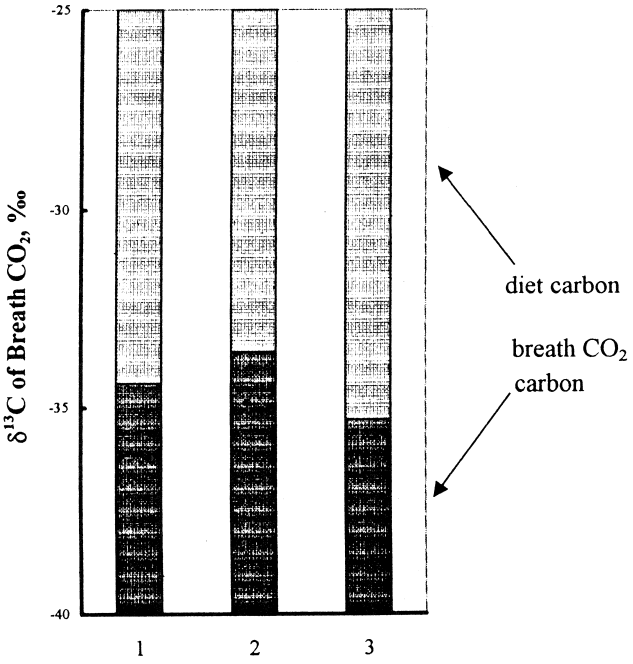

Figure 21. Comparison of daily averaged carbon isotope composition of CO_2 respired by humans in diabetes mellitus of type 1 (1), in norm (2), and in obesity (3) with carbon isotope composition of their diet (72).

More information can be obtained from the comparison of the daily averaged carbon isotope composition of the diet with those of respiratory CO_2 and urea urine for different functional states. The results of a corresponding experiment are given in Table 30 (73). Patients with the following functional states were used in this experiment: 1) norm with normal diet regime, subject 1 (male, 32-years old) and subject 2 (male, 23-years old); 2) norm under starvation, subject 3 (male, 54-years old); 3) obesity, subject 4 (female, 7-years old); 4) hypophysis cerebri nanism, subject 5 (male, 14-years old); 5) autoimmune thyroiditis, subject 6 (female, 14-years old); and 6) hypothyroidism, subject 7 (male, 6-years old).

As seen from Table 30, in all cases the CO_2 respired is markedly (~3–6‰) enriched in ^{12}C (as described above) whereas urea urine appears in some cases to be ^{13}C-enriched versus food carbon. Excluding non-assimilated part, the residual food is converted in breath CO_2, urea urine, and biomass growth representing the main parts of the system "food–body". Supposing proximity of the carbon isotope ratios of biomass and diet carbon and based on the material balance consideration, one must conclude that both isotopic characteristics are interrelated. The coupled

Table 29. Daily Averaged Values of Carbon Isotope Composition of Diet and CO_2 Respired by Humans in Different Hormone-Functional States (72). The Values of $\delta^{13}C‰$ Are Given in PDB Units

Object		Isotopic Characteristics of Diet							
Diet	Number of ingredients	6							
	Interval of $\delta^{13}C$ variations	From −25.2 to −27.4‰							
	Mean value	−26.7‰							
CO_2 from air respired by humans		$\delta^{13}C$ of CO_2 for different hormone - functional states							
		Norm		Mellitus Type I				Obesity	
Subject No.		1	2	3	4	5	6	7	8
Number of samples		7	10	12	12	12	12	12	12
Interval of $\delta^{13}C$ variations		−30.8 to −37.6	−31.5 to −35.6	−31.4 to −36.2	−30.8 to −37.9	−31.5 to −35.9	31.5 to −33.7	−32.0 to −36.4	−33.2 to −36.5
Mean value for a subject		−34.7	−34.1	−33.7	−33.5	−33.6	−33.7	−35.3	−35.3
Mean value for hormone-functional state group		−34.4		−33.6				−35.3	
$\Delta^{13}C = \delta^{13}CO_2 - \delta^{13}C_{diet}$		−7.7		−6.9				−8.6	

MARCEL DEKKER, INC.
270 Madison Avenue, New York, New York 10016

Table 30. Daily Averaged Values of Carbon Isotope Composition of Diet, Respiratory CO_2, and Urea Urine of Humans in Different Hormone-Functional States (74). The Values of $\delta^{13}C$% Are Given in PDB Units. The Numbers in Parentheses Denote Number of Subject. $\Delta^{13}C = \delta^{13}C_{CO2\ (diet)} - \delta^{13}C_{diet}$

Object		Isotopic Characteristics of Diet
Diet	Number of ingredients	11
	Interval of $\delta^{13}C$ variations	From −24.1 to −28.1‰
	Mean value	−26.7‰

$\delta^{13}C$ of respiratory CO_2 for different hormone-functional states

Products of metabolism		Norm			Endocrine Pathology			
		Normal Diet Regime (1)	Normal Diet Regime (2)	Starvation (3)	Obesity (4)	Nanism (5)	Thyroiditis (6)	Hypothyroidism (7)
Breath CO_2	Number of samples	22	23	23	22	23	23	18
	Interval of $\delta^{13}C$ variations	−26.9 to −32.9	−27.9 to −33.7	−30.8 to −34.3	−31.0 to −34.6	−29.3 to −34.2	−29.4 to −35.1	−25.7 to −32.6
	Mean value	−30.1	−30.8	−32.7	−32.2	−32.3	−32.4	−29.8
	$\Delta^{13}C$	−3.4	−4.1	−6.0	−5.5	−5.6	−5.7	−3.1
Urea urine	Number of samples	5	6	5	3	16	3	3
	Interval of $\delta^{13}C$ variations	−22.5 to −24.4	−21.2 to −25.3	−22.0 to −23.4	−21.8 to −22.7	−22.5 to −21.3	−23.0 to −23.5	−19.6 to −21.6
	Mean value	−23.6	−23.8	−22.7	−21.3	−22.3	−23.4	−21.3
	$\Delta^{13}C$	+3.1	+2.9	+4.0	+5.4	+3.2	+3.2	+5.1

MARCEL DEKKER, INC. 270 Madison Avenue, New York, New York 10016

isotopic shifts of both characteristics in norm under starvation and under normal diet regime give some evidence for this conclusion. The ^{12}C enrichment of breath CO_2 under starvation is followed by ^{13}C enrichment of the urea urine (see Table 30).

To explain these isotopic shifts relative to food carbon by using the cell CIF model, one must take into account that urine is formed in the ornithine cycle coupled with functioning of the Krebs cycle. Ornithine interacts with CO_2 derived in pyruvate decarboxylation and forms guanido groups, which are then transformed into urine (232). The observed isotopic shifts within the frame of the model permit one to assume that ornithine cycle coupled with Krebs cycle operates at the late stage of glycolytic phase and corresponds to a deep exhaustion of the pyruvate pool of cells (see *^{13}C Distribution in Cell and Temporal Organization of Metabolic Processes: Preliminary Notes*). Hence, CO_2 evolving at this stage determines ^{13}C enrichment of guanido and urine carbon. It is interesting to note that ^{13}C enrichment of guanido group was experimentally found by studying the carbon isotope composition of arginine extracted from protein fraction of microorganisms (92). The same conclusion on operation of the ornithine cycle at late stages of the glycolytic phase (see *^{13}C Distributuion in Cell and Temporal Organization of Metabolic Processes: Preliminary Notes*) also follows from the analysis of carbon isotope distribution in amino acids of microorganisms (92). One can suppose that such a sequence of metabolic processes is likely to be one of the common features of temporal organization of cell metabolism regardless of the level of subject organization. Though regular $\delta^{13}C$ variations of urine have not been systematically examined, high deviations observed for individual subjects (see Table 30) along with the interrelation between carbon isotope composition of urine and that of breath CO_2 support this assumption. Note that the observed range of $\delta^{13}C$ variations for urine (within 3% interval) appears to be narrower than that for CO_2.

Data given in Tables 29 and 30 confirm once again an interrelation between isotopic characteristics and metabolic peculiarities of the examined functional states. The polarity of isotopic shifts observed in diabetes mellitus and obesity in respect to the norm agrees with the known polarity of metabolic shifts. The ^{12}C enrichment of breath CO_2 in obesity and under starvation corresponds to the known preferential utilization of lipids in these states. The ^{13}C enrichment of urine carbon in these states testifies to the relationship between carbon isotope ratio of breath CO_2 and urea urine. In all endocrine pathologies under study (except hypothyroidism) and in norm under starvation, the breath CO_2 was found to be enriched in ^{12}C. This enables us to conclude that under stress conditions the organism prefers lipids as the main source of "fuel" substrates. A broad interval of breath CO_2 $\delta^{13}C$ variations observed in hypothyroidism corresponds to the previously noted abnormally wide interval of $\delta^{13}C$ variations for blood plasma (see *Carbon Isotope Characteristics of Highly Organized Animals and Humans: Preliminary Notes*).

In the above-described study of various functional states, an attempt to find out the nature of the discovered daily variations of carbon isotope ratio of the respiratory CO_2 has been undertaken. To obtain a more detailed pattern of diurnal curves, the intervals of sampling were decreased to 1 h (excluding nighttime from 12.00 P.M. to 8 A.M.) and in some cases to 30 min. The results obtained are presented in Figs. 22–25.

Lines 1 and 2 in Fig. 22 describe $\delta^{13}C$ variations of respiratory CO_2 at norm under normal diet regime. Line 3 describes the same variations under starvation. The variation patterns in all cases are similar. They are characterized by alternating peaks with periods of 2–3 h and variable amplitudes. Sometimes periods shorten to 1.5 h or increase to 4 h. The curve corresponding to the starvation state is shifted to a more negative range of $\delta^{13}C$ values with longer variation periods of 3–4 h. Although maxima and minima on curves 1 and 2 do not coincide, they develop an absolutely clear synchronic pattern.

The same behavior was observed for daily variations of $\delta^{13}C$ of respiratory CO_2 for endocrine pathology states shown in Fig. 23. As seen, the daily curve cor-

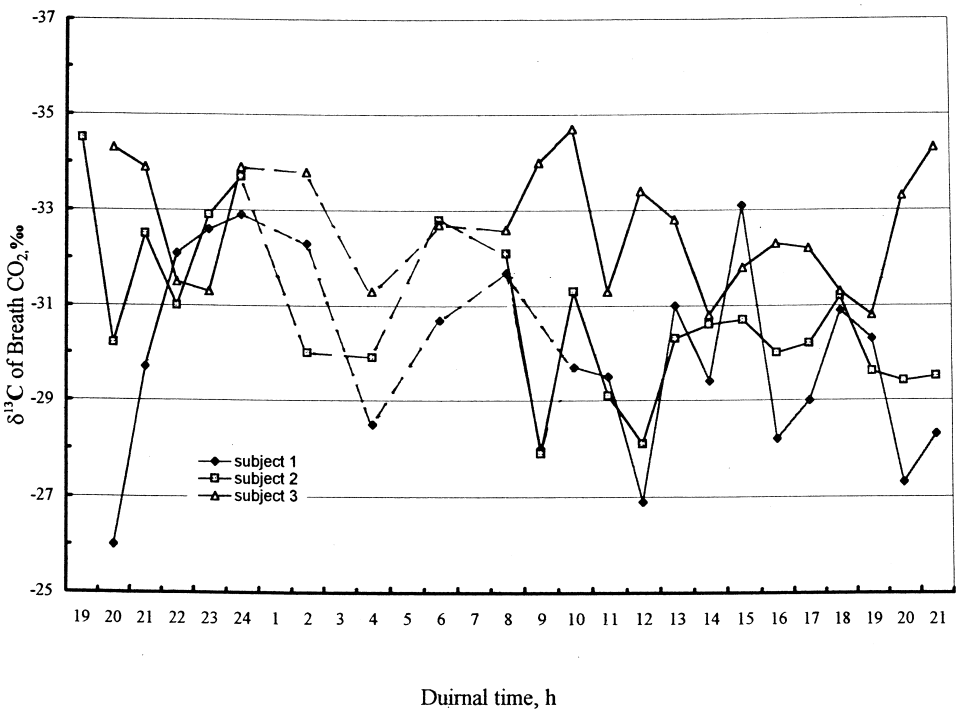

Figure 22. Daily variations of carbon isotope composition of respiratory CO_2 in norm under normal regime of diet (subjects 1 and 2) and under starvation (subject 3) (73).

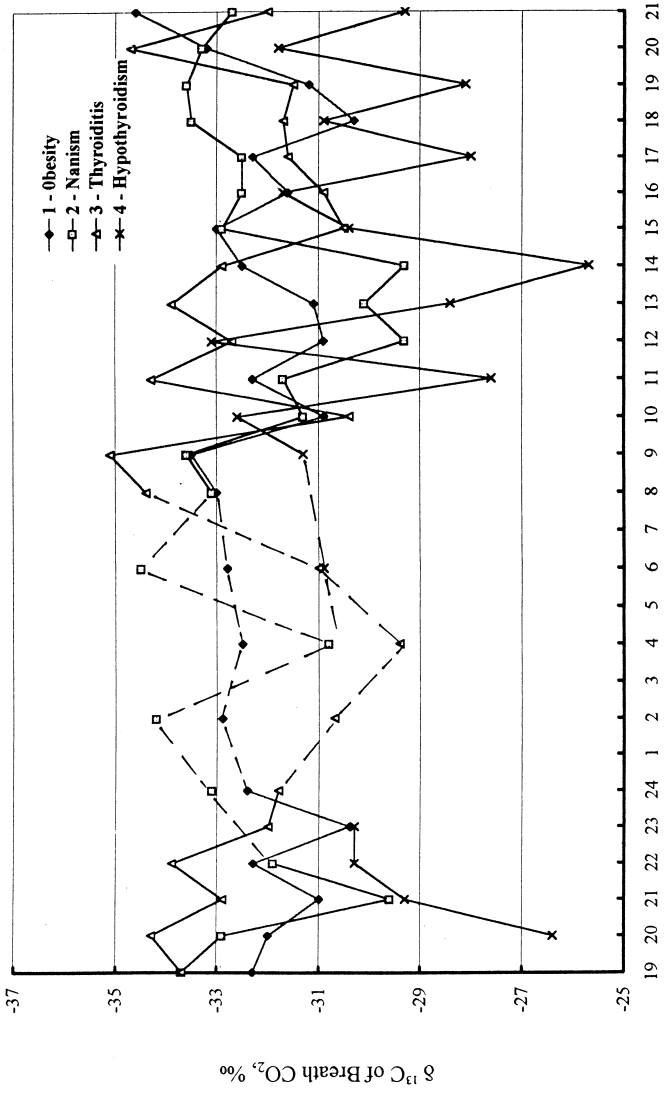

Figure 23. Daily variations of carbon isotope composition of respiratory CO_2 in endocrine pathological states: obesity (subject 4); nanism (subject 5); thyroiditis (subject 6), and hypothyroidism (subject 7) (73). Samples were collected every hour (see text).

MARCEL DEKKER, INC.
270 Madison Avenue, New York, New York 10016

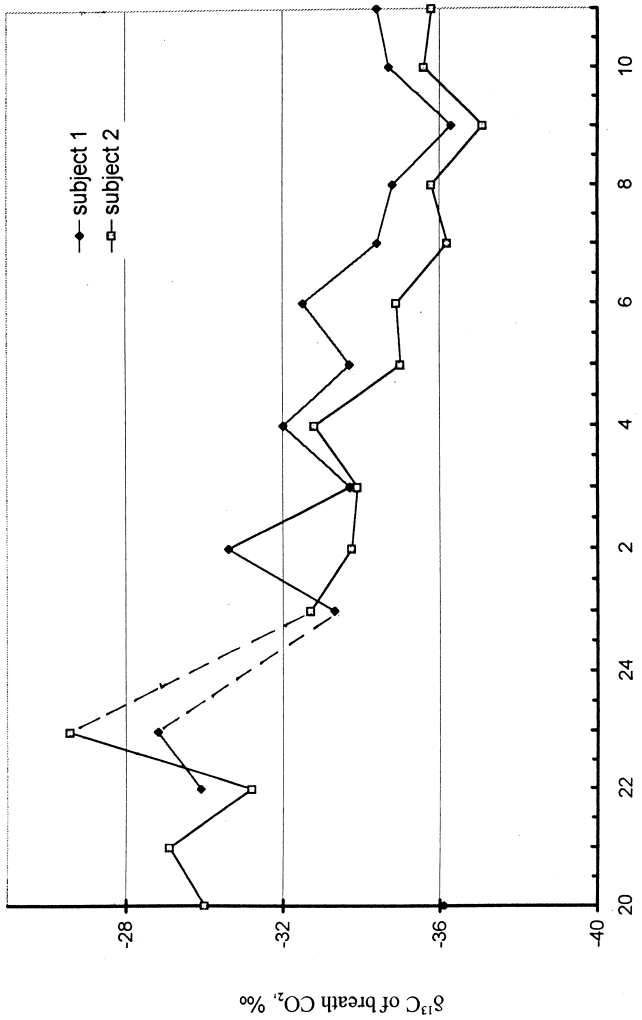

Figure 24. Variations of carbon isotope ratio of respiratory CO_2 in norm in nocturnal phase of experiment (73).

MARCEL DEKKER, INC.
270 Madison Avenue, New York, New York 10016

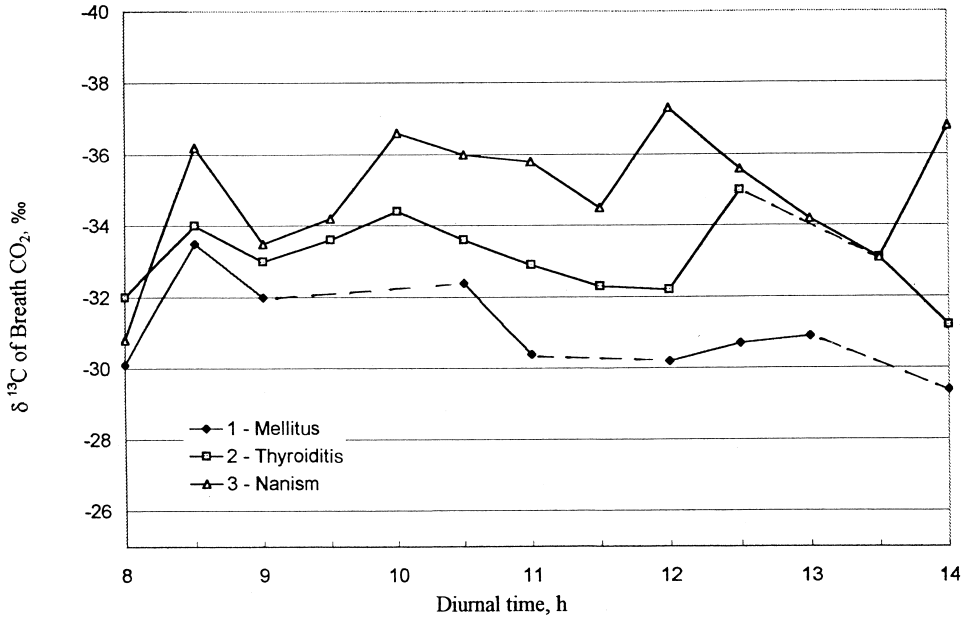

Figure 25. Variations of carbon isotope ratio of respiratory CO_2 in endocrine pathological states: diabetes mellitus type 1 (subject 4); thyroiditis (subject 6), and nanism (subject 5) (73). Samples were collected every 0.5 h (see text).

responding to hypothyroidism is characterized by higher amplitudes of variations. Sharp peaks with big amplitudes, typical to this functional state, indicate an unusual energy status of the organism (see above). On the contrary, the curve corresponding to obesity is characterized by less amplitudes, which agrees with the known character of the shifts indicated before. Comparison of diurnal curves corresponding to the normal and pathological states shows that they have one common maximum at 4 A.M. (see Figs. 22 and 23). Figures 24 and 25 show the nocturnal phase of daily curves for the norm with sampling intervals of 1 and 0.5 h, respectively. As seen from both Figs. 24 and 25 (showing a more detailed structure of variations), the same approximately 2-h synchronic variations of $\delta^{13}C$ values are observed for two different subjects.

It seems important to emphasize that variations of $\delta^{13}C$ values of respiratory CO_2 mainly reflect the changes in the pyruvate pool level. An indirect confirmation of this conclusion follows from cyclic variations of mitochondrial respiration and oxidative phosphorylation that have been observed by studying mitochondria

MARCEL DEKKER, INC.
270 Madison Avenue, New York, New York 10016

isolated from the rat liver tissues subjected to X-rays and neutron irradiation (253,254). Mitochondria are the cell organella where the pyruvate decarboxylation and the Krebs cycle operate. The period of variations of mitochondrial activity (~3 h) was found to be very close to the period of $\delta^{13}C$ changes of breath CO_2. This coincidence can be supposed to be due to the same nature of both variations.

The material presented here enables to make an important conclusion that the main principles of CIF mechanism in a cell found for microorganisms and for plants are applicable to highly organized animals including humans. These principles are the following:

1. The key point in the CIF mechanism is CIE in the pyruvate decarboxylation, which is responsible for the isotope heterogeneity of animal tissue. Although this effect arises in tissues where decarboxylation occurs, its influence spreads all over the organism due to the intertissue exchange of substrates.
2. The Releigh isotope effect associated with depletion of the pyruvate pool in the course of the reaction controlled by endocrine, nerve, and transport systems of the organism determines the specific isotopic characteristics, such as $\delta^{13}C$ of breath CO_2, the carbon isotope ratio of hair, urea urine, blood plasma, etc., at particular functional states.
3. Time-dependent character of the isotopic characteristics is caused by the change in energy and biosynthetic needs of the organism adapting to the changes in environmental conditions and (or) in its hormone functional status.

CONCLUSIONS

The following main conclusions can be derived from the results presented in this article: at least three metabolic reactions are known to be the points where CIF occurs: 1) isotope effect of RuBP carboxylation; 2) isotope effect of glycine decarboxylation; and 3) isotope effect of pyruvate decarboxylation. Since all these reactions proceed in the key metabolic points, which are common for cells of the great majority of organisms, CIE has a universal character.

The first effect accompanies photoassimilation of CO_2, which occurs in all photosynthesizing organisms including plants, alga, and bacteria. It results in the observed ^{12}C enrichment of plants and photosynthesizing microorganisms versus assimilated CO_2. As it follows from the proposed mechanism of CIF, assimilation of CO_2 is a discrete process, which may be described as a flow of CO_2 batches into a cell. This flow arises due to periodic alternating "reswitches" of Rubisco (the key enzyme of photosynthesis) capable of working as either carboxylase or oxygenase depending on CO_2/O_2 ratio in a cell. The discreteness of the flow provides the periodic filling/depletion of CO_2 cytoplasmic pool and determines the ap-

MARCEL DEKKER, INC.
270 Madison Avenue, New York, New York 10016

pearance of isotope Releigh effect. The degree of depletion determines the level of ^{12}C enrichment of cell biomass. The full consumption of CO_2 batches entering the cells is the main reason (besides the isotope effect of photorespiration) for the observed ^{13}C enrichment of C_4 plants compared with C_3 and CAM plants.

The second CIE is observed in glycine decarboxylation. It is the key point of isotope fractionation in photorespiration. The mechanism of CIF in this case is the same as that for CO_2 assimilation representing a combination of isotope effect of enzymatic reaction with Releigh effect of substrate pool depletion. The kinetic isotope effect of reaction is "normal", i.e., CO_2 evolved in the reaction is enriched in ^{12}C whereas substrates circulating in a closed loop comprising glycolate chain and Calvin cycle are enriched in ^{13}C. Their combination results in two main consequences. The first is a decrease of ^{13}C discrimination emerged in CO_2 photoassimilation. Some environmental factors, such as salinity, light intensity, water availability, and some others influencing photorespiration, cause considerable changes in the observed isotope discrimination in photosynthesis. In particular, when CO_2 assimilated is enriched in a heavy isotope (^{13}C or ^{14}C), the isotope effect of photorespiration can even prevail over that of photoassimilation, and the biomass carbon is enriched in ^{13}C versus initial CO_2. The second consequence is the emergence of two isotopically different carbon flows. One is enriched in ^{12}C and results in formation of light carbohydrate pools providing substrates for dark respiration metabolism, including glycolysis, fatty acid synthesis, Krebs cycle, and coupled amino acid synthesis. Another carbon flow is enriched in ^{13}C spinning in phoraspiratory chain and results in formation of heavy carbohydrates. This flow provides substrates for different synthesis of organic acids, amino acids, and some lipids, especially under stress conditions. Both carbon flows are independent from each other and are separated in time and in space. The coupling of these flows arises due to the double function of Rubisco thus providing discreteness of carbon flows. The light flow emerges in the carboxylation phase of Rubisco function, while the heavy flow arises in the oxygenation phase. Hence, the CIE of photosynthesis is in fact an integral result of two effects: CIE of CO_2 assimilation and that of photorespiration.

The third CIE in pyruvate decarboxylation is responsible for the appearance of carbon isotope heterogeneity in respiration metabolism (isotopic distinctions of fractions, metabolites, and uneven intramolecular distribution of ^{13}C in biomolecules). Since this reaction is the key crosspoint of the central metabolic pathways in the overwhelming majority of cells, the third isotope effect is typical of the most organisms including photosynthesizing and heterotrophic, protozoan, and humans. The mechanism of appearance of this isotope effect is the same as in the previous cases: a combination of CIE of the enzymatic reaction with Releigh effect of substrate pool depletion. Isotope effect of pyruvate decarboxylation occurs in the glycolytic phase of a cell cycle consisting of glycolysis and gluconeogenesis and supplies lipid and amino acid syntheses with structural units com-

MARCEL DEKKER, INC.
270 Madison Avenue, New York, New York 10016

prising C_2 and C_3 fragments. The kinetic nature of decarboxylation isotope effect generates intramolecular heterogeneity of structural units and finally of all cell components. Due to the Releigh effect accompanying pyruvate pool depletion, the carbon isotope ratio of units changes in parallel with pool depletion determining the differences in carbon isotope composition of metabolites whose synthesis occurs at different levels of the pyruvate pool. Therefore, ^{13}C distribution in the cell indicates temporal organization of cell processes. As it follows from the experimental data, in the majority of organisms the synthesis of fatty acid and other lipid components, which is coupled with amino acid synthesis cycle, precedes the functioning of Krebs cycle. It was also concluded that for a given energetic state of cells, corresponding to a particular energetic status of the organism, the synthesis of components occurs synphasically in the cell cycle, i.e., within the same interval of pyruvate pool depletion. This provides a relatively stable and definite isotopic pattern of metabolites and definite distribution of ^{13}C in a cell and in organism biomass as a whole.

To simplify understanding of the mechanism of CIF in respiration metabolism one can imagine a cell as a system consisting of a basin and valves. The pyruvate pool is regarded as a basin and metabolic pathways as valves. The basin is periodically depleted and filled with substrates. The opening of valves occurs within certain intervals of cell cycle in accordance with its needs. The leakage of substrates from the basin (their transformation into other cell metabolites) is under energy and biosynthetic control of the cell and is followed by the change in their isotope composition (isotope effect in pyruvate decarboxylation). Thus the opening and closing of valves in the course of cell cycle results in specific carbon isotope distribution between cell metabolites corresponding to a particular energy state of a cell and organism as a whole. The stereospecificity of enzymatic reactions and design of metabolic pathways determine the real intramolecular carbon isotope distribution in biomolecules.

Comparison of carbon isotope characteristics (carbon isotope ratio of breath CO_2, urea urine, blood plasma, etc.) of highly organized systems (animals and humans) permits one to conclude that basic principles of CIF established by studying respiration metabolism in plant cells and microorganisms are also valid for cells of such systems.

CIE of pyruvate decarboxylation was found to be the main reason for CIF in insulin-dependent tissues. It gives rise to temporal variations of isotopic characteristics. The periodic filling/depletion of pyruvate pool in cell cycles causes changes of biochemical and isotopic characteristics of the organism in time. These periodic variations are under the control of endocrine, nerve, and transport systems of the organism and reflect its energetic status, which is conditioned by the motor activity, the food regime, and the functional state.

The 2- to 3-h cyclic synphasic variations of isotopic characteristics observed for different subjects regardless of their functional state illustrate the influence of

MARCEL DEKKER, INC.
270 Madison Avenue, New York, New York 10016

some common external factors of an unknown nature. The daily averaged and dynamic carbon isotope characteristics (such as the carbon isotope ratio of breath CO_2 and urea urine) are found to correspond to the functional state of the organism. This opens new routes for application of these parameters in medical practice and scientific researches.

In conclusion, it is important to emphasize that there are still a lot of problems to be studied and solved in this particular area. Many theoretical suggestions must be better documented experimentally and confirmed. Nevertheless, theoretical analysis of currently available experimental data testifies to the validity of established principles of CIF in a cell, which can be used as a delicate instrument in studies of living processes and for application of metabolic carbon effects in various fields.

LIST OF SYMBOLS AND ABBREVIATIONS

GTP	guanosine triphosphate
GDP	guanosine diphosphate
PEP	phosphoenolpyruvate
RuBP	ribulose 1,5-bisphosphate
Rubisco	ribulose-1,5-bisphosphate carboxylase/oxygenase
THF	tetrahydrofolic acid
OA	oxaloacetate
PLP	pyridoxal phosphate
ADP	adenine diphosphate
ATP	adenine triphosphate
NAD	nicotinamidadenine dinucleotide
NADH	nicotinamidadenine dinucleotide reduced
NADP	nicotinamidadenine dinucleotide phosphate
NADPH	nicotinamidadenine dinucleotide phosphate reduced
HPMS	α-hydroxy-2-pyridinemethanesulfonate
INH	isonicotinylhydrozide
Leu	leucine
Gly	glycine
Ala	alanine
Phe	phenylalanine
Ser	serine
Thr	threonine
Glu	glutamic acid
Asp	aspartic acid
Arg	arginine
Lys	lysine

MARCEL DEKKER, INC.
270 Madison Avenue, New York, New York 10016

Tyr	tyrosine
TPN	tripyridine nucleotide
X5P	xylulose-5-phosphate
R5P	ribose-5-phosphate
6PG	6-phosphogluconate
F6P	fructose-6-phosphate
FBP	fructose-6-bisphosphate
PGA	phosphoglyceric acid
DHA-P	dihydroxyacetone phosphate
α	kinetic coefficient of isotope separation
Δ	^{13}C discrimination
F	degree of pool exhaustion

REFERENCES

1. Brenna, J.T. Acc. Chem. Res. **1994**, *27*, 340.
2. Meritt, D.A.; Hayes, J.M. Anal. Chem. **1994**, *66*, 2336.
3. Meritt, D.A.; Hayes, J.M. J. Am. Soc. Mass Spectrom. **1994**, *5*, 387.
4. Henderson, S.A.; Caemmerer, S.; Farquhar, G.D. Aust. J. Plant Physiol. **1992**, *19*, 263.
5. Evans, S.R.; Sharkey, T.D.; Berry, J.A.; Farquhar, G.D. Aust. J. Plant Physiol. **1986**, *13*, 281.
6. Guilluy, R.; Billion-Roy, F.; Pachiaudi, C.; Normand, S.; Riou, J.P.; Jumeau, E.J.; Brazier, J.L. Anal. Chim. Acta **1992**, *259*, 193.
7. Ismail, A.M.; Hall, A.E. Crop Sci. **1993**, *33*, 788.
8. Hall, A.E.; Mutters, R.G.; Hubick, K.T.; Farquhar, G.D. Crop.Sci. **1990**, *30*, 300.
9. Rafi, M.M.; Waines, J.G. Theor. Appl. Genetics **1994**, *88*, 1023.
10. Comstock, J.P.; Ehleringer, J.R. Proc. Natl. Acad. Sci. USA **1992**, *89*, 7747
11. Bond, W.J.; Stock, W.D. S. Afr. For. J. **1990**, *0*, 51.
12. Condon, A.G.; Richards, R.A. Aust. J. Agric. Res.**1992**, *43*, 921.
13. Maberly, S.C.; Raven, J.A.; Johnston, A.M. Oecologia **1992**, *9*, 481.
14. Raven, J.A.; Farquhar, G.D. New Phytol. **1990**, *113*, 505.
15. Condon, A.G.; Richards, R.A.; Farquhar, G.D. Aust. J. Agric. Res. **1992**, *43*, 935.
16. Kirchhoff, W.R.; Hall, E.A.; Thomson, W.W. Crop Sci. **1989**, *29*, 109.
17. Ehleringer, J.R.; Vogel, J.C. in *Stable Isotopes and Plant Carbon Water Relations;* Hall, A.E., Farquhar, G.D., Eds.; Academic Press: New York, 1993; 9.
18. O'Leary, M.H.; Madhaven, S.; Paneth, P. Plant Cell Environ. **1992**, *15,* 1099.

MARCEL DEKKER, INC.
270 Madison Avenue, New York, New York 10016

19. Kirda, C.A.R.; Mohamed, A.G.; Kumarasinghe, K.S.; Montenegro, A.; Zapata, F. Plant Soil **1992**, *147*, 217.
20. Ray, R.D.; Warne, P.G.; Reid, D.M. In *Stable Isotopes in Ecological Research. Ecological Studies*; Rundel, P.W., Ehleringer, J.R., Nagy, K.A., Eds.; Springer-Verlag: NewYork, 1988; Vol. 68, 55.
21. Macdowell, F.D.H.; Lowdon, J.A. Can. J. Bot. **1989**, *67*, 2828.
22. Toft, N.L.; Anderson, J.E.; Nowak, R.S. Oecologia (Berl.) **1989**, *80*, 11.
23. Borland, A.M.; Griffiths, H.; Maxwell, C.; Broadmeadow, M.S.J.; Griffiths, N.M.; Burnes, J.D. New Phytol. **1992**, *122*, 349.
24. Schidlowski, M. Ann. Rev. Earth Planet. Sci. **1987**, *15*, 47.
25. Villani, F.; Pigliucci, M.; Lauteri, M.; Cherubini M.; Sem, O. Genome **1992**, *35*, 251.
26. Aranus, J.L.; Buxo, R. Aust. J. Plant Physiol. **1993**, *20*, 117.
27. Ueno, O.; Samejima, M.; Koyama, T. Ann. Bot. **1989**, *64*, 425.
28. Polley, H.W.; Johnson, H.B.; Marino, B.D.; Mayeux, H.S. Nature, **1993**, *361*, 61.
29. Griffiths, H. Plant Cell Environ. **1992**, *15*, 1051.
30. Feng, X.; Epstein, S. Geochim. et Cosm. Acta **1995**, *89*, 2599.
31. Popp, B.N.; Takigiku, R.; Hayes, J.M.; Louda, J.W.; Baker, E.W. Am. J. Sci. **1989**, *289*, 436.
32. Freeman, K.H.; Hayes, J.M. Glob. Biogeochem. Cycles **1992**, *6*, 185.
33. Summons, R.E.; Jahnke, L.L.; Roksandic, Z. Geochim. et Cosm. Acta **1994**, *58*, 2853.
34. Ocampo, R.; Callot, J.; Albrecht, P.; Popp, B.N.; Horowitz, M.R.; Hayes, J.M. Naturwissenschaften **1989**, *76*, 419.
35. Kohnen, M.E.; Schouten, S.; Damste, J.S.S.; Leeuw, J.W.; Merrit, D.; Hayes, J.M. Adv. Org. Geochem. **1992**, *19*, 404.
36. Hayes, J.M. Marine Geol. **1993**, *113,* 11.
37. O'Leary, M.H. Plant Cell Environ. **1992**, *15*, **1099.**
38. Ivlev, A.A. Russ. J. Plant Physiol., **1992**, *39*, 825.
39. Ivlev, A.A. Russ. J. Plant Physiol., **1993**, *40*, 752.
40. Ivlev, A.A.; Knyazev, D.A.; Matyushenko I.N.; Esikov, A.D. Microbiologiya, **1990**, *59*, 373. (in Russian)
41. Ivlev, A.A.; Knyazev, D.A.; Matyushenko, I.N.; Esikov, A.D.; Balitskaya, R.M.; Kuznetsova, N.N. Biofizika, **1991**, *36*, 365. (in Russian)
42. Shearer, G.; Kohl, D.H. J. Biol. Chem. **1988**, *263*, 13231.
43. Zyakun, A.M.; Zakharchenko, V.N.; Sisoeva, V.A.; Shishkanova, N.V.; Bondar', V.A.; Vinokurova, N.G.; Ermakova, I.T. Mikrobiol. Zh. **1989**, *51*, 6. (in Russian)
44. Goldhaber, M.B.; Kaplan, I.R. Marine Chemistry. In *The Sea*; Goldberg, E.D., Ed., John Wiley & Sons: New York, 1974; Vol. 5, 569.
45. Gelwicks, J.T.; Risatti, B.; Hayes, J.M. Appl. Environ. Microbiology **1994**, *60*, 467.

46. Gelwicks, J.T.; Risatti, B.; Hayes, J.M. Org. Geochem. **1989**, *14*, 441.
47. Caplan, I.R. Proc. R. Soc. **1975**, *B189*, 183.
48. Marriotti, A.; Germon, J.C.; Hubert, P.; Kaizer, P.; Letolle, R.; Tardieux, A.; Tardieux, P. Plant Soil **1981**, *62*, 413.
49. Yoneyama, T.; Omata, T.; Nakata, S.; Yazaki, J. Plant Cell Physiol. **1991**, *32*, 1211.
50. Shearer, G.; Kohl, D.H. In *Stable Isotopes. Ecological Research. Ecological Studies*; Rundel, P.W., Ehleringer, J.R., Nagy, K.A., Eds.; Springer-Verlag: New York, 1988; Vol. 68, 342.
51. Torau, L.; Harris, K.F. Geochim. et Cosm. Acta **1989**, *53*, 2341.
52. Simple, K.M.; Westlake, D.W.; Krouse, H. Can. J. Microbiol. **1987**, *33*, 372.
53. Fry, B.; Gest, H.; Hayes, J.M. Appl. Environ. Microbiol. **1988**, *54*, 280.
54. Flanagan, L.B. In *Stable Isotopes and Plant Carbon Water Relations*; Hall, A.E., Farquhar, G.D., Eds.; Academic Press: New York, 1993; 71.
55. Smith, B.N.; Ziegler, H. Bot. Acta **1990**, *103*, 336.
56. Sternberg, L.S.L.; DeNiro, M.J.; Johnson, H.B. Plant Physiol. **1986**, *82*, 428.
57. Robinson, Sh.A.; Yakir, D.; Ribas-Carbo, M.; Giles, L.; Osmond, C.B.; Siedow, J.N.; Berry, J.A. Plant Physiol. **1992**, *100*, 1087.
58. Guy, R.D.; Fogel, M.L.; Berry, J.A. Plant Physiol. **1993**, *101*, 37.
59. Lane, G.A.; Dole, M. Science **1956**, *123*, 574.
60. Epstein, S.; Zeiri, L. Proc. Natl. Acad. Sci. USA **1988**, *85*, 1727.
61. Macko, S.A.; Hare, P.E.; Hoering, T.C. Chem. Geol. Isotope Geosci. Sect. **1987**, *65*, 79.
62. Yoneyama, T.; Kamachi, K.; Yamaya, T.; Mae, T. Plant Cell Physiol. **1993**, *34*, 489.
63. Yakir, D.; DeNiro, M.J. Plant Physiol. **1990**, *93*, 325.
64. De Niro, M.J.; Cooper, L.W. Geochim. et Cosm. Acta **1989**, *53*, 2573.
65. Johnson, D.A.; Asay, K.H.; Tieszen, L.L.; Ehleringer, J.R.; Jefferson, P.G. Crop Sci. **1990**, *30*, 338.
66. Read, J.J.; Johnson, D.A.; Asay, K.H.; Tieszen, L.L. Crop Sci. **1992**, *32*, 168.
67. Hubick, K.; Farquhar, G.D. Plant Cell Environ. **1989**, *12*, 795.
68. Condon, A.G.; Richards, R.A.; Farquhar, G.D. Crop Sci. **1987**, *27*, 996.
69. Donovan, L.A.; Ehleringer, J.R. Am. J. Bot. **1994**, *87*, 927.
70. Johnson, D.A.; Asay, K.H. J. Range Manage **1993**, *46*, 194.
71. Ivlev, A.A.; Yu.Panteleev, N.; Knyazev, Yu.A.; Logachev, M.F. Biofizika **1994**, *39*, 377. (in Russian)
72. Ivlev, A.A.; Knyazev, Yu.A.; Logachev, M.F. Biofizika **1996**, *41*, 499. (in Russian)
73. Ivlev, A.A.; Knyazev, Yu.A.; Logachev, M.F. Biofizika **1996**, *41*, 505. (in Russian)

MARCEL DEKKER, INC.
270 Madison Avenue, New York, New York 10016

74. Nier. A.O.; Gulbrunsen, E.A. J. Am. Chem. Soc. **1939**, *61*, 697.
75. Nier, A.O. Phys. Rev. **1950**, *77*, 789.
76. Craig, H. Geochim. et Cosm. Acta **1957**, *12*, 133.
77. Craig, H. Geochim. et Cosm. Acta **1953**, *3*, 53.
78. Craig, H. J. Geology **1954**, *62*, 115.
79. Park, R.; Epstein, S. Geochim. et Cosm. Acta **1960**, *21*, 110.
80. Smith, B.N.; Epstein, S. Plant Physiol. **1971**, *47*, 380.
81. Bender, M.M.; Rouhani, I.; Vines, H.M.; Black, C.C. Plant Physiol. **1973**, *52*, 427.
82. Osmond, C.B.; Allaway, N.G.; Sutton, B.G.; Troughton, J.H.; Queros, O.; Luttge, N.; Winter, K. Nature **1973**, *246*, 41.
83. Deleens, E.; Treichel, I.; O'Leary, M.H. Plant Physiol. **1985**, *79*, 202.
84. Troughton, J.H. In *Encyclopedia of Plant Physiology. New Series. Photosynthesis II: Photosynthetic Carbon Metabolism and Related Processes;* Gibbs, M., Latzko, E. Eds; Springer-Verlag: New York, 1979; Vol. 6, 140.
85. Smith, B.N.; Boutton, T.W. In *Photosynthesis VI. Photosynthesis and Productivity, Photosynthesis and Environment;* Akoyunoglou, G., Ed.; Balaben International Science Services: Philadelphia, PA, 1981; 255.
86. Farquhar, G.D.; Ball, M.C.; von Caemmerer, S.; Roksandic, Z. Oecologia **1982**, *52*, 121.
87. Guy, R.D.; Reid, D.M. Oecologia **1980**, *44*, 241.
88. Evans, J.R.; Sharkey, T.D.; Berry, J.A.; Farquhar, G.D. Aust. J. Plant Physiol. **1986**, *13*, 281.
89. Winter, K. Z. Pflanzenphysiol. **1981**, *101*, 421.
90. Guy, R.D.; Reid, D.M.; Krouse, H.R. Canad. J. Bot. **1986**, *64*, 2693.
91. Guy, R.D.; Reid, D.M.; Krouse, H.R. Canad. J. Bot. **1986**, *64*, 2700.
92. Abelson, P.H.; Hoering, T.C. Proc. Natl. Acad. Sci. USA **1961**, *47*, 623.
93. Degens, E.T.; Gullard, R.R.L.; Sackett, W.M.; Hellebust, J.A. Deep Sea Res. **1968**, *15*, 1.
94. Sackett, W.M.; Eckelmann, W.R.; Bender, M.L.; Be, A.W.H. Science **1965**, *148*, 235.
95. Van, T.K.; Haller, W.T.; Bowes, G. Plant Physiol. **1976**, *58*, 761.
96. Pardue, I.W.; Scalan, R.S.; Van Baalen, C.; Parker, P.L. Geochim. Cosm. Acta **1976**, *40*, 309.
97. Surif, M.B.; Raven, J.A. Oecologia **1990**, *82*, 68.
98. Saurer, M.; Fuhrer, J.; Siegenthalar, U. Plant Physiol. **1991**, *97*, 313.
99. Kumarasinghe, R.S.; Kirda, C.; Mohamed, A.R.; Zapata, F.; Danso, S.K. Plant Physiol. **1992**, *139*, 145.
100. Naidi, S.L.; Sullivan, J.H.; Teramuta, A.H.; Delucia, E.H. Tree Physiol. **1993**, *12*, 151.
101. Ivlev, A.A. Fiziologiya rastenii **1984**, *31*, 765. (in Russian)
102. Estep, M.L.F.; Tabita, F.R.; Parker, P.L.; Baalen, Ch.V. Plant Physiol. **1978**, *61*, 680.

103. Wong, W.W.; Benedict, C.R.; Kohel, R.J. Plant Physiol. **1979**, *63*, 852.
104. Roeske, C.A.; O'Leary, M.H. Biochemistry **1984**, *23*, 6275.
105. Whelan, T.W.; Sackett, W.M.; Benedict, C.R. Plant Physiol. **1973**, *51*, 1051.
106. Reibach, M.R.; Benedict, C.R. Plant Physiol. **1974**, *59*, 564.
107. O'Leary, M.H.; Reife, J.E.; Slater, J.D. Biochemistry **1981**, *20*, 7308.
108. Ivlev, A.A.; Knyazev, D.A.; Timiryazev, Izv. Selskokhoz. Akad. **1986**, *N 2*, 175. (in Russian)
109. Rubin, A.B.; Gavrilenko, V.Ph. Biokhimia & Fisiologia Fotosinteza Moscow State University, Moscow, 1977. (in Russian)
110. O'Leary, M.H.; Osmond, C.B. Plant Physiol. **1980**, *66*, 931.
111. O'Leary, M.H. Phytochemistry **1981**, *20*, 553.
112. Farquhar, G.D.; O'Leary, M.H.; Berry, J.A. Aust. J. Plant Physiol. **1982**, *9*, 121.
113. Peisker, M. Kulturpflanze **1984**, *32*, 35.
114. Ivlev, A.A. Biofizika **1989**, *34*, 887. (in Russian)
115. Peisker, M. Photosynthetica **1982**, *16*, 533.
116. Laisk, A. Kh. *Kinetics of Photosynthesis and Photorespiration in C-3 Plants;* Nauka: Moscow, 1977. (in Russian)
117. Berezin, I.V.; Varfolomiev, S.D. *Biokinetics;* Nauka: Moscow, 1979. (in Russian)
118. Farquhar, G.D. Aust J. Plant Physiol. **1983**, *10*, 205.
119. Ehleringer, J.R. In *Stable Isotopes and Plant Carbon Water Relations* Hall, A.E., Farquhar, G.D., Eds.; Academic Press: New York, 1993; 41.
120. Bowman, W.D.; Hubick, K.T.; Caemmerer, S.; Farquhar, G.D. Plant Physiol. **1989**, *90*, 102.
121. Flanagen, L.B.; Jefferies, R.L. Planta **1989**, *178*, 377.
122. Saurer, M.; Fuhrer, J.; Siegenthaler, U. Plant Physiol. **1991**, *97*, 313.
123. Parker, P.L. Geochim. Cosm. Acta **1964**, *28*, 1135.
124. Keeling, Ch.D. Geochim. Cosm. Acta **1961**, *24*, 277.
125. Guy, R.D.; Vanlerberghe, G.C.; Turpin, D.H. Plant Physiol. **1989**, *89*, 1150.
126. Semenenko, V.E. Fiziologiya rastenii **1964**, *11*, 216. (in Russian)
127. Badger, M.R.; Andrews, T.J. Biochem. Biophys. Res. Comm. **1974**, *60*, 204.
128. Laing, W.A.; Ogren, W.L.; Hageman, R.H. Plant Physiol. **1974**, *54*, 678.
129. Igamberdiev, A.U. Fiziologiya rastenii **1991**, *39*, 774. (in Russian)
130. Martin, B.; Thorstenson, Y.R. Plant Physiol. **1988**, *88*, 213.
131. Sanadze, G.A.; Tevzadze, I.T.; Tarkhnishvili, G.M. Fiziologiya rastenii **1977**, *24*, 646. (in Russian)
132. Tevzadze, I.T.; Tarkhnishvili, G.M.; Sanadze, G.A. Fiziologiya rastenii **1977**, *24*, 1073. (in Russian)
133. Sanadze, G.A.; Black, C.C.; Tevzadze, I.T.; Tarkhnishvili, G.M. Fiziologiya rastenii **1978**, *25*, 171. (in Russian)

MARCEL DEKKER, INC.
270 Madison Avenue, New York, New York 10016

134. Voznesenskii, V.L.; Glagoleva, T.A.; Zubkova, E.K.; Mamusina, N.S.; Filippova, L.A.; Chulanovskaya, N.V. Fiziologiya rastenii **1982**, *29*, 564. (in Russian)
135. Ivanov, M.V.; Zyakun, A.M.; Gogotova, G.I.; Bondar', V.A. Dokl. Akad. Nauk SSSR **1978**, *242*, 1417. (in Russian)
136. Seltzer, S.; Hamilton, G.A.; Westheimer, F.H. J. Am. Chem. Soc. **1979**, *81*, 4018.
137. O'Leary, M.H.; Richards, D.T.; Hendrickson, D.N. J. Am. Chem. Soc. **1970**, *92*, 4435.
138. O'Leary, M.H.; Piazz, G.G. Biochemistry **1981**, *20*, 2743.
139. Yordan, F.; Kuo, D.J.; Monse, E.U. J. Am. Chem. Soc. **1978**, *100*, 2872.
140. DeNiro, M.J.; Epstein, S. Science **1977**, *197*, 261.
141. Monson, K.D.; Hayes, J.M. Geochim. Cosm. Acta **1982**, *46*, 139.
142. Kalinkina, L.G.; Udelnova, T.M. Fiziologiya rastenii **1990**, *37*, 95. (in Russian)
143. Ivlev, A.A.; Bykova, N.V.; Igamberdiev, A.U. Russ. J. Plant Physiol. **1996**, *43*, 37.
144. Ivlev, A.A.; Igamberdiev, A.U.; Trelkeld, Ch.; Bykova, N.V. Russ. J. Plant Physiol. **1999**, *46*, 653.
145. Abell, L.M.; O'Leary, M.H. Biochemistry **1988**, *27*, 3325.
146. Rivera, E.R.; Smith, B.N. Plant Physiol. **1979**, *64*, 966.
147. Raven, J.A.; Griffiths, H.; Glidewell, S.M.; Preston, T. Proc.R.Soc. Ser.B **1982**, *216*, 87.
148. Gleixner, G.; Danier, H.J.; Werner, K.A.; Schmidt, H.-L. Plant Physiol. **1993**, *102*, 1287.
149. Kalinkina, L.G.; Udelnova, T.M. Fiziologiya rastenii **1991**, *38*, 947. (in Russian)
150. Gillon, J.S.; Griffiths, H. Plant Cell and Environment **1997**, *20*, 1217.
151. Morot-Gaudry, J.F.; Farineau, J.P.; Huet, J.C. Plant Physiol. **1980**, *66*, 1079.
152. Kennedy, R.A. Plant Physiol. **1976**, *58*, 573.
153. Osmond, C.B.; Bjorkman, O. Aust. J. Plant Physiol. **1987**, *13*, 281.
154. Smith, B.N.; Oliver, J.; McMillan, C. Bot. Gaz. **1976**, *437*, 99.
155. Saurer, M.; Siegenthalar, U. Plant Physiol. **1991**, *97*, 313.
156. Kalinkina, L.G.; Rusinova, N.G.; Stroganov, V.P. Fiziologiya rastenii **1981**, *28*, 5. (in Russian)
157. Ramazanov, Z.M.; Semenenko, V.E. Fiziologiya rastenii **1986**, *33*, 864. (in Russian)
158. Nigawekar, A.S.; Murumkar, C.V.; Chavan, P.D. Acta Agron. Hungarica **1991**, *40*, 333.
159. Passera, C.; Albuzio, A. Can. J. Bot. **1978**, *56*, 121.
160. Neales, T.F.; Frazer, M.S.; Roksandic, Z. Aust. J. Plant Physiol. **1983**, *10*, 437.

MARCEL DEKKER, INC.
270 Madison Avenue, New York, New York 10016

161. Degens, E.T. Ch.7. In *Organic Geochemistry;* Eglinton, G., Murphy, M.T.J., Eds.; Springer-Verlag: Berlin, 1969; 207.
162. Ivlev, A.A.; Pichouzhkin, V.I.; Knyazev, D.A. Russ. J. Plant Physiol. **1995**, *42*, 345.
163. Ivlev, A.A.; Pichouzhkin, V.I.; Knyazev, D.A. Russ. J. Plant Physiol. **1999**, *46*, 443.
164. O'Leary, M.H. Bioscience **1988**, *38*, 328.
165. Teery, J.A. Oecologia **1984**, *64*, 68.
166. Lauteri, M.; Brugnoli, E.; Spaccino, L. In *Stable Isotopes and Plant Cabon - Water Relations;* Ehleringer, J.R., Hall, A.E., Farquhar, G.D., Eds.; Academic Press: San Diego, 1993; 93.
167. Rundel, P.W.; Sharifi, M.R. In *Stable Isotopes and Plant Cabon - Water Relations;* Ehleringer, J.R., Hall, A.E., Farquhar, G.D., Eds.; Academic Press: San Diego, 1993; 173.
168. Hoefs, J. Nature **1969**, *223*, 397.
169. Galimov, E. *The Biological Fractionation of Isotopes;* Academic Press: Orlando, FL, 1985.
170. Igamberdiev, A.U. Uspekhi sovremennoi biologii **1988**, *105*, 488. (in Russian)
171. Park, R.S.; Danning, H. Geochim. et Cosm. Acta **1961**, *22*, 99.
172. Hayes, J.M.; Takigiku, R.; Ocampo, R.; Callot, H.J.; Albrecht, P. Nature **1987**, *329*, 48.
173. Kalinkina, L.G.; Naumova, T.G. Fiziologiya rastenii **1993**, *40*, 577. (in Russian)
174. Lehninger, A.L. *Biochemistry. The molecular basis of cell structure and function*; Worth Publishers: New York, 1972.
175. Musil, J.; Nováková, O.; Kunz, K. *Biochemistry in schematic perspective*; Avicenum Czechoslovak Medical Press: Prague, 1980.
176. Borland, A.M.; Griffiths, H.; Maxwell, C.; Broadmeadow, M.S.J. Fordham, M.C.; Maxwell, G. Oecologia **1993**, *95*, 444.
177. Nord, F.F.; Schubert, W.J. In *Biogenesis of Natural Compounds;* Bernfeld, P., Ed.; Pergamon Press: Oxford, 1963; 623.
178. Bjorn, M.; Thorstenson, V.M. Plant Physiol. **1988**, *88*, 213.
179. Ivlev, A.A. Dokl. AN SSSR **1986**, *291*, 1514. (in Russian)
180. Lerman, J.C.; Deleens, E.; Nato, A.; Moyse, A. Plant Physiol. **1974**, *53*, 581.
181. Deleens, E.; Qeiroz, O. Plant Cell Environ. **1984**, *7* (1), 23.
182. Deleens, E.; Qeiroz, O. Plant Cell Environ. **1984**, *7* (4), 279.
183. Servaites, T.J.; Ogren, W.L. Plant Physiol. **1977**, *60*, 693.
184. Demmig-Adams, B.; Adams, W.W. III.; Winter, K.; Meyer, A.; Schreiber, U.; Pereirs, J.; Krüger, A.; Czygan, F.Z.; Lange, O. Planta **1989**, *177*, 377.
185. Borland, A.M.; Griffiths, H.; Broadmeadow, M.S.J.; Fordham, M.C.; Maxwell, G. Oecologia **1993**, *95*, 444.

186. Kalinkina, L.G.; Rusinova, N.G.; Strogonov, B.P. Fiziologiya rastenii **1981**,*28*, 5. (in Russian)
187. Farquhar, G.D.; Hubick, K.T.; Condon, A.G.; Richards, R.A. In *Stable Isotopes in Ecological Research*, *Ecological Studies*; Rundel, P.W., Ehleringer, J.R., Nagy, K.A., Eds.; Springer-Verlag: NewYork, 1988; Vol. 68, 21.
188. Krampitz, M.J.; Klug, K.; Fock, H.P. Photosynthetica **1984**, *18*, 322.
189. Coudret, A.; Ferron, F. Photosynthetica **1982**, *19*, 217.
190. Park, R.; Epstein, S. Plant Physiol. **1961**, *36*, 133.
191. Degens, E.T.; Gullard, R.R.L.; Sackett, W.M.; Hullebust, J.A. Deep Sea Res. **1968**, *15*, 11.
192. Smith, B.N.; Epstein, S. Plant Physiol. **1970**, *46*, 738.
193. DeNiro, M.J.; Epstein, S. Geochim. et Cosm. Acta **1978**, *42*, 495.
194. Benedict, C.R.; Scott, J.R. Plant Physiol. **1970**, *57*, 876.
195. Calder, J.A.; Parker, P.L. Geochim. et Cosm. Acta **1973**, *37*, 133.
196. Whelan, T.W.; Sackett, W.M.; Benedict, C.R. Biochem. Biophys. Res. Comm. **1976**, *41*, 1205.
197. Deleens, E.; Garnier-Dardart, J. Planta **1977**, *135*, 241.
198. Galimov, E.M. In *Advances in Organic Geochemistry;* Technip: Paris, 1973; 439.
199. Hayes, J.M.; Monson, K.D. J. Biol. Chem. **1982**, *257*, 5568.
200. Meinschein, W.G.; Rinaldi, G.G.L.; Hayes, J.M.; Schoeller, D.A. Biomed. Mass-spectrometry **1974**, *1*, 172.
201. Blair, N.; Lea, A.; Munez, E.; Olsen, J.; Kwong, E.; Des-Marais, D. Appl. Environ. Microbial. **1985**, *50*, 996.
202. Ivlev, A.A.; Lapin, A.V.; Brizanova, L.Ya. Fiziologiya rastenii **1986**, *34*, 493. (in Russian)
203. Ivlev, A.A. Biofizika **1985**, *30*, 506. (in Russian)
204. Ivlev, A.A. Biophysics **1992**, *36*, 1078.
205. Ivlev, A.A. Biokhimiya **1985**, *50*, 1607. (in Russian)
206. Galimov, E.M.; Polyakov, B.V. Geokhimiya **1990**, *N9*, 1232. (in Russian)
207. Galimov, E.M.; Kodina, L.A.; Generalova, B.N. Geokhimiya **1976**, *N1*, 11. (in Russian)
208. O'Leary, M.H.; Yapp, C.J. Biochem. Biophys. Res. Comm. **1978**, *83*, 155.
209. Varshavsky, Ya.M. Biofizika **1988**, *33*, 351. (in Russian)
210. Ivlev, A.A. Biofizika **1987**, *31*, 181. (in Russian)
211. Rossmann, A.; Butzenlechnar, M.; Schmidt, H.-L. Plant Physiol. **1991**, *96*, 609.
212. Weillacher, T.; Gleixner, G.; Schmidt, H.-L. Phytochemistry **1995**, *41*, 1073.
213. Schmidt, H.-L.; Kexel, H.; Butzenlechner, M.; Schwarz, S.; Gleixner, G.; Thimet, S.; Werner, R.A.; Gensler, M. In *Stable Isotopes in the Biosphere;*

MARCEL DEKKER, INC.
270 Madison Avenue, New York, New York 10016

Wada, E., Yoneyama, T., Minagawa; Ando, M.; Fry, B.D. Eds.; Kyoto University Press: Kyoto, 1995; 17.
214. Kondrashova, M.N.; Mayevskii, Ye.I. In *Regulation of Energy Exchange and the Physiological State of the Organism;* Kondrashova, M.N., Ed.; Nauka: Moscow, 1978; 5. (in Russian)
215. Selkov, Ye.Ye. In *Regulation of Energy Exchange and the Physiological State of the Organism;* Kondrashova, M.N., Ed.; Nauka: Moscow, 1978; 15. (in Russian)
216. Selkov, Ye.Ye. ; Shevelev, E.A. Biofizika **1989**, *34*, 797. (in Russian)
217. Dilman, V.M. *Great Biological Clocks*; Znanie: Moscow, 1982 (in Russian)
218. Melander, L.; Saunders, W.H. *Reaction rates of isotopic molecules;* Wiley Interscience Publ.: New York, 1983.
219. Yordan, P.; Kuo, D.J.; Monse, E.U. J. Am. Chem. Soc. **1978**, *100*, 2872.
220. Melzer, E.; Schmidt, H.-L. J. Biol. Chem. **1987**, *262*, 8159.
221. Ivlev, A.A.; Knyazev, D.A.; Kaloshin, A.G. Biofizika **1982**, *27*, 762. (Russian)
222. Strickland, K.P. In *Biogenesis of Natural Compounds*; Bernfeld, P., Ed.; Pergamon Press: Oxford, 1963; 82.
223. Ryban, Ye.L. *Microbial Synthesis of Amino acids*; Zinantne: Riga, 1968. (in Russian)
224. Hayes, J.M. Mar. Geol. **1993**, *113*, 111.
225. Wong, H.G.; Sakket, W.M.; Benedict, C.R. Plant Physiol. **1975**, *55*, 475.
226. Galimov, E.M.; Shirinskiy, V.G. Geochem. Inter. **1975**, *12*, 157.
227. Sharkey, T.D.; Loreto, F.; Delwiche, C.F.; Treichel, I.W. Plant Physiol. **1991**, *97*, 463.
228. Jones, D.M.; Carger, J.F.; Eglinton, G. Biol. Mass Spectr. **1991**, *20*, 641.
229. Rieley, G.; Collier, R.J.; Jones, D.M.; Eglinton, G.; Eakin, P.A.; Fallick, A.E. Nature **1991**, *352*, 425.
230. Vogler, E.A.; Hayes, J.M. J. Org. Chem. **1979**, *44*, 3682.
231. Vogler, E.A.; Hayes, J.M. In *Advances in Organic Geochemistry;* Douglas, A.G., Maxwell, J.R. Eds.; Pergamon Press: New York, 1980; 697.
232. Metun, J. In *Biogenesis of Natural Compounds;* Bernfeld, P., Ed.; Pergamon Press: Oxford, 1963; 9.
233. Ivlev, A.A.; Knyazev, D.A.; Kaloshin, A.G.; Radyukin, Yu.N. Izv. Timiryazev. Selskokhoz. Akad. **1982**, *N 4*, 76. (in Russian)
234. Ivlev, A.A.; Knyazev, D.A. Izv. Timiryazev. Selskokhoz. Akad. **1983**, *N 4*, 105. (in Russian)
235. Sackett, W.M. Trans. Am. Geophys. Union **1963**, *47*, 221.
236. Fry, B.; Jeng, W.-L.; Scalan, R.S. Geochim.et Cosm. Acta **1978**, *42*, 1299.
237. Lyon, T.D.B.; Baxter, M.S. Nature **1978**, *273*, 750.
238. DeNiro, M.J.; Epstein, S. Geochim. et Cosm. Acta **1978**, *42*, 495.

MARCEL DEKKER, INC.
270 Madison Avenue, New York, New York 10016

239. Mosora, C.R.; Lacroix, M.H.; Duchesne, M.M.J. C. R. Acad. Sci., Ser.D **1971**, *273*, 1422.
240. Lacroix, M.H.; Badea, M.; Duchesne, M.M.J. C. R. Acad. Sci., Ser.D **1971**, *273*, 240.
241. Mosora, F.; Duchesne, M.M.J.; Lacroix, M. C. R. Acad. Sci., Ser.D **1974**, *278*, 1119.
242. Mosora, F.; Lacroix, M.; Pontus, M.M.; Duchesne, M.M.J. C. R. Acad. Sci., Ser.D **1972**, *274*, 2723.
243. Duchesne, M.M.J.; Mosora, C.R.; Lacroix, M.H.; Lefebvre, P.; Luycks, A.; Lopez-Habib, G. C. R. Acad. Sci., Ser.D **1973**, *277*, 2261.
244. Jacobson, B.J.; Smith, B.N.; Jacobson, A.V. Biochem. Biophys. Res. Comm. **1972**, *47*, 398.
245. Ivlev, A.A.; Panteleyev, Yu.N.; Glukhov, A.A. Biophysics **1992**, *37*, 989.
246. Ivlev, A.A. Biophysics **1992**, *37*, 985.
247. Ivlev, A.A.; Goncharov, N.P. Problemy Endocrin. **1993**, *N 1*, 71. (in Russian)
248. White, A.; Handler, S.; Smith, E.L.; Hill, R.L.; Lehman, I.R. *Principles of Biochemistry*, 6th Ed.; McGraw-Hill: New York, 1981.
249. Aulik, I.V. In *Determination of Physical Performance in the Clinic and in Sport;* Meditsina: Moscow, 1990; 35. (in Russian)
250. Kuel, J.; Doll, E.; Keppler, D. Pflug.Arch. **1968**, *301*, 198.
251. McMurray, W.C. *Essentials of Human Metabolism. The Relationship of Biochemistry to Human Physiology and Desease;* Publisher Hegerstown: New York, 1980.
252. Ostapova, V.V. *Metabolic Disturbances in Mellites;* Moskovskii rabochii: Moscow, 1990. (in Russian)
253. Kozireva, V.; Sirotkin, V.V.; Mityushin, V.M. In *Energy Exchange and Organism Stability;* Nauka: Moscow, 1978; 173. (Russian)
254. Kozireva, E.V. The Role of Mitochondria in Cell Reparation, Diss. Abstract., Institute of Biophysics, Moscow, 1994. (in Russian)

MARCEL DEKKER, INC.
270 Madison Avenue, New York, New York 10016

Request Permission or Order Reprints Instantly!